
[All ETDs from UAB](#)

[UAB Theses & Dissertations](#)

2015

A novel role for USP14 in regulating non-proteolytic ubiquitin signaling

Jada Hallengren Vaden
University of Alabama at Birmingham

Follow this and additional works at: <https://digitalcommons.library.uab.edu/etd-collection>

 Part of the [Medical Sciences Commons](#)

Recommended Citation

Vaden, Jada Hallengren, "A novel role for USP14 in regulating non-proteolytic ubiquitin signaling" (2015).
All ETDs from UAB. 3197.
<https://digitalcommons.library.uab.edu/etd-collection/3197>

This content has been accepted for inclusion by an authorized administrator of the UAB Digital Commons, and is provided as a free open access item. All inquiries regarding this item or the UAB Digital Commons should be directed to the [UAB Libraries Office of Scholarly Communication](#).

A NOVEL ROLE FOR USP14 IN REGULATING NON-PROTEOLYTIC
UBIQUITIN SIGNALING

by

JADA HALLENGREN VADEN

LUCAS POZZO-MILLER, COMMITTEE CHAIR
SCOTT WILSON, MENTOR
MICHAEL BRENNER
LORI MCMAHON
ERIK ROBERSON

A DISSERTATION

Submitted to the graduate faculty of The University of Alabama at Birmingham
in partial fulfillment of the requirements for the degree of
Doctor of Philosophy

BIRMINGHAM, ALABAMA

2015

A NOVEL ROLE FOR USP14 IN REGULATING NON-PROTEOLYTIC UBIQUITIN SIGNALING

JADA HALLENGREN VADEN

NEUROSCIENCE

ABSTRACT

Loss of the deubiquitinating enzyme (DUB) USP14 in the *ataxia* (*ax^J*) mice leads to altered neuromuscular junction (NMJ) structure, reduced synaptic transmission at the NMJ, and decreased mobility. However, the types of processes that USP14 regulates in the nervous system remain unclear. Because association with the proteasome stimulates USP14's ubiquitin hydrolase activity, it is thought to act primarily on proteasomal substrates. Therefore, one way for USP14 to support nervous system function is by modulating protein turnover. While a number of studies done in yeast and immortalized cell lines demonstrate that loss or inhibition of USP14 alters proteasome function, there is no consensus on whether inhibition of USP14 accelerates or delays protein degradation. A second possibility is that USP14's primary role is the maintenance of ubiquitin homeostasis. The proteasome-associated DUBs remove ubiquitin from substrates prior to their degradation and indeed, loss of USP14 leads to ubiquitin depletion in both yeast and the *ax^J* mice. These two suggestions assume that, in keeping with its association with the proteasome, USP14 acts on proteasome-targeting ubiquitin chains. However, in the following pages, we demonstrate that USP14 is required to disassemble proteasome-independent ubiquitin chains and regulate kinase activation in the nervous system. Specifically, USP14's ubiquitin hydrolase activity regulates the ubiquitination of mixed lineage kinase 3 (MLK3) to control the activation of its

downstream target c-Jun N-terminal kinase (JNK), and over-activation of JNK contributes to the alteration of NMJ structure and motor function observed in a transgenic mouse expressing a dominant-negative, catalytically-inactive USP14 species in the nervous system. Moreover, we show that increasing the amount of ubiquitin conjugates in the nervous system alters motor function and muscle development even when not accompanied by depletion of free ubiquitin pools. These studies underline the importance of tightly regulated ubiquitin signaling at the NMJ.

Keywords: ubiquitin-specific protease 14, ubiquitin, neuromuscular junction

ACKNOWLEDGEMENTS

To Scott Wilson: You have been the best mentor I could have asked for, and I can't thank you enough for everything you have done for me. You've always seen the best in me, both professionally and personally, which inspires me to be better. Thank you for all of your patience, your advice, and the love of discovery that you model every day. I am a better scientist and, I hope, a better person for having trained with you.

To Julie Wilson: I truly don't think that you realize the impact that you have on the students in the lab. You are one of the most hardworking and selfless people that I know, and my writing is immeasurably better because of your guidance. Thank you.

To the members of my thesis committee, Drs. Michael Brenner, Lori McMahon, Lucas Pozzo-Miller, and Erik Roberson: Thank you for the valuable guidance and critical input on my project. Lucas, you have been particularly generous with your time and expertise, and I appreciate it so much.

To Jennifer Watson: I would not have made it through this in one piece without you.

To Ryan: Thank you for making my life infinitely more interesting, for making me laugh when I am stressed, and for serving as my personal IT specialist.

TABLE OF CONTENTS

	<i>Page</i>
ABSTRACT	ii
ACKNOWLEDGEMENTS	iv
LIST OF TABLES	vii
LIST OF FIGURES	viii
LIST OF ABBREVIATIONS	x
INTRODUCTION	1
Ubiquitin Signaling	1
The Ubiquitin Proteasome System	5
USP14 in the Nervous System	8
<i>The ataxia Mice</i>	8
<i>Regulation of Protein Turnover by USP14</i>	9
<i>Maintenance of Ubiquitin Homeostasis by USP14</i>	12
<i>Regulation of Non-Proteolytic Ubiquitin</i>	
<i>Signaling by USP14</i>	14
USP14 as a Regulator of Protein Kinase Activation	17
UBIQUITIN-SPECIFIC PROTEASE 14 REGULATES C-JUN N-TERMINAL KINASE SIGNALING AT THE NEUROMUSCULAR JUNCTION	20
DISTINCT EFFECTS OF UBIQUITIN OVEREXPRESSION ON NMJ STRUCTURE AND MOTOR PERFORMANCE IN MICE EXPRESSING CATALYTICALLY INACTIVE USP14	67
DISCUSSION	105
Dissociating the Ubiquitin-Hydrolase-Dependent and –Independent Functions of USP14	106
USP14 Non-Catalytically Promotes Viability	107

	<i>Page</i>
USP14's Ubiquitin Hydrolase Activity Supports NMJ Structure and Synaptic Transmission.....	108
<i>USP14 Regulates NMJ Structure through pJNK Activation.....</i>	108
<i>USP14's Ubiquitin Hydrolase Activity Dynamically Regulates Synaptic Transmission.....</i>	112
USP14 Maintains Ubiquitin Homeostasis both Catalytically and Non-Catalytically	114
<i>Ubiquitin Complementation in the ax^J and TgCA Mice</i>	116
Trimming of Proteasome-Independent Ubiquitin Chains by USP14	117
<i>Evidence for Disassembly of K63-Linked Ubiquitin Chains by Proteasome-Bound USP14</i>	118
<i>Evidence for an Alternative Binding Partner of USP14.....</i>	121
Conclusion.....	122
LIST OF GENERAL REFERENCES	124
APPENDIX: INSTITUTIONAL ANIMAL CARE AND USE APPROVAL FORM	140

LIST OF TABLES

<i>Table</i>		<i>Page</i>
	INTRODUCTION	
1	Descriptions of mutant and transgenic mice	19

LIST OF FIGURES

<i>Figure</i>	<i>Page</i>
---------------	-------------

INTRODUCTION

1	Ubiquitin conjugation	2
2	Structurally distinct chains linked through ubiquitin's internal lysine residues	3
3	Structure of the proteasome	6

UBIQUITIN-SPECIFIC PROTEASE 14 REGULATES C-JUN N-TERMINAL KINASE SIGNALING AT THE NEUROMUSCULAR JUNCTION

1	Transgenic expression of USP14CA in the nervous system	27
S1	USP14CA is expressed specifically in the nervous system.....	29
2	Neuronal expression of USP14CA leads to decreased body weight, muscle weight, and motor performance	31
3	Expression of <i>TgUsp14CA</i> causes functional and structural deficits at the NMJ	33
S2	<i>TgUsp14CA</i> mice have abnormal NMJ structure starting at 2 weeks of age.....	35
4	Acute inhibition of USP14 causes synaptic transmission deficits at the adult NMJ	37
S3	Genetic inactivation and pharmacological inhibition of USP14's ubiquitin hydrolase activity lead to increased ubiquitin conjugates	41
5	Loss of USP14's ubiquitin hydrolase activity results in accumulation of non-proteasomal associated ubiquitin conjugates.....	42

<i>Figure</i>	<i>Page</i>
---------------	-------------

6	Inhibition of USP14's DUB activity leads to enhanced activation of the MLK3 signaling cascade	44
---	---	----

S4	No evidence of cell death in Tg <i>Usp14CA</i> spinal cord.....	46
7	Inhibition of pJNK improves the structural and functional deficits caused by inhibition of USP14's DUB activity	48

DISTINCT EFFECTS OF UBIQUITIN OVEREXPRESSION ON NMJ STRUCTURE AND FUNCTION IN MICE EXPRESSING CATALYTICALLY INACTIVE USP14

1	Analysis of USP14 mutations on neuronal ubiquitin pools	73
2	Ubiquitin complementation does not rescue muscle mass, or motor deficits in Tg <i>CA</i> mice	75
3	Effects of ubiquitin overexpression on AChR transcript levels in Tg <i>CA</i> mice.....	78
4	Dose-dependent effects of ubiquitin on muscle development and motor function.....	80
5	Ubiquitin complementation improves NMJ structure in Tg <i>CA</i> mice	83
6	Ubiquitin complementation reduces pJNK levels at the NMJs of Tg <i>CA</i> mice	86
7	Ubiquitin overexpression does not reduce pJNK abundance in Tg <i>CA</i> spinal cords.....	89
8	Relationship between the abundance of ubiquitin conjugates in the spinal cord and development of the gastrocnemius muscle	93

LIST OF ABBREVIATIONS

53BP1	p53-binding protein
AChR	acetylcholine receptor
AIP4	atrophin interacting protein 4
APF1	ATP-dependent proteolysis factor 1
<i>ax^J</i>	USP14-deficient <i>ataxia</i> mice
CP	20S core particle of the proteasome
CSP	cysteine string protein
CXCL12	(C-X-C motif) chemokine 12
CXCR4	chemokine (C-X-C motif) receptor 4
CYLD	cylindromatosis
DLK	dual lysine zipper-bearing kinase
DSB	double-strand break
DUB	deubiquitinating enzyme
Dvl2	Disheveled 2
EGFR	epidermal growth factor receptor
EJP	excitatory junction potential
EPC	endplate current
ERK	extracellular signal-related kinase
ESCRT	endosomal sorting complex required for transport
fEPSP	field excitatory postsynaptic potential
GABA _A R	GABA _A Receptor

HEK	human embryonic kidney
<i>hiw</i>	highwire
HRS	hepatocyte growth factor-regulated tyrosine kinase substrate
IAP	intracisternal-A particle
IKK	inhibitor of kappa B kinase
IL-2R	interleukin-2 receptor
ILV	intraluminal vesicle
IPSC	inhibitory post synaptic current
IU1	active-site directed USP14 inhibitor
JIP3	JNK-interacting protein 3
JNK	c-Jun N-terminal kinase
K	lysine
K48-linked	ubiquitin chain linked through lysine 48
K63-linked	ubiquitin chain linked through lysine 63
MAP1B	microtubule-associated protein 1B
MAP2	microtubule-associated protein 2
MAPKKK	mitogen activated protein kinase kinase kinase
MAPs	microtubule-associated proteins
MEF	murine embryonic fibroblast
MEPC	miniature endplate current
MKK4	mitogen activated protein kinase kinase 4
MLK3	mixed lineage kinase 3
MVB	multivesicular body

NF- κ B	nuclear factor kappa B
NGF	nerve growth factor
NMJ	neuromuscular junction
p38	p38 MAP kinase
PC	Purkinje cell
POH1	pad one homolog 1
PPF	paired pulse facilitation
PSMA7	proteasome subunit alpha type-7
Rab7	Ras-related protein 7
RNF168	ring finger protein 168
RNF8	ring finger protein 8
RP	19S regulatory particle of the proteasome
RPN1	regulatory particle non-ATPase 1
RPN10	regulatory particle non-ATPase 10
RPN13	regulatory particle non-ATPase 13
SCG10	superior cervical ganglion 10
SDF-1	stromal-derived factor-1
SP	SP600125; JNK inhibitor
STAM	signal transducing adaptor molecule
TA	tibialis anterior
TAK1	transforming growth factor β activated kinase 1
TgCA	transgene expressing USP14CA under <i>Thy1.2</i> promoter
TGF- β	transforming growth factor beta

Tg <i>Ub</i>	transgene expressing ubiquitin under <i>Thy1.2</i> promoter; moderate expression level
Tg <i>Ub</i> -High	transgene expressing ubiquitin under <i>Thy1.2</i> promoter; high expression level
Tg <i>Usp14</i>	transgene expressing USP14 under <i>Thy1.2</i> promoter
Tg <i>Usp14CA</i>	transgene expressing USP14CA under <i>Thy1.2</i> promoter
TRAF6	tumor necrosis factor receptor associated factor 6
TrkA	tropomyosin-related kinase A
Ub-VME	ubiquitin vinyl-methyl-ester
UBL	ubiquitin-like
Ubp6	ubiquitin-specific protease 6
Ubp6-C118A	Ubp6 mutant in which cysteine 118 is mutated to alanine
UCH37	ubiquitin carboxyl-terminal hydrolase 37
UCHL5	ubiquitin carboxyl-terminal hydrolase L5
USP14	ubiquitin-specific protease 14
USP14C114A	USP14 mutant in which cysteine 114 is mutated to alanine
USP14CA	USP14 mutant in which cysteine 114 is mutated to alanine
USP4	ubiquitin-specific protease 14
YFP	yellow fluorescent protein
α -BTX	alpha-bungarotoxin

INTRODUCTION

While the human genome includes 20,000-25,000 genes (International Human Genome Sequencing Consortium, 2004), the human proteome is much more vast, consisting of more than 1 million functionally distinct proteins (Jensen, 2004). The increased complexity of the proteome compared to the genome is due, in part, to posttranslational modifications. Posttranslational modifications, often reversibly, alter protein activity, localization, and stability. Ubiquitination is one such modification. The 76 amino acid ubiquitin protein was originally isolated in a search for hormones produced in the thymus (Goldstein et al., 1975), and was later discovered to be identical to ATP-dependent proteolysis factor 1 (APF1) (Ciechanover, Hod, & Hershko, 1978; Wilkinson, Urban, & Haas, 1980), which was known to stimulate ATP-dependent protein degradation (Hershko, Ciechanover, Heller, Haas, & Rose, 1980). However, although ubiquitin was first described in its role of targeting proteins to the proteasome for degradation (Ciechanover, Heller, Elias, Haas, & Hershko, 1980), it is now known to impact a wide range of cellular processes extending well beyond proteasome-mediated protein degradation (reviewed in Komander, 2009).

Ubiquitin Signaling

Ubiquitin's versatility as a posttranslational modification derives from its structure and the means by which it is conjugated onto other proteins (Komander, 2009).

Ubiquitin conjugation relies on the sequential action of a cascade of enzymes known as E1, E2, and E3 ligases (Figure 1; Hershko, Heller, Elias, & Ciechanover, 1983). Briefly, the E1 activating enzyme harnesses ATP hydrolysis to adenylylate ubiquitin's c-terminal glycine residue and then transfers the ubiquitin to its active site cysteine residue, forming a thioester bond (Ciechanover, Elias, Heller, & Hershko, 1982; Ciechanover, Heller, Katz-Etzion, & Hershko, 1981; Haas, Warms, Hershko, & Rose, 1982). Next, the E2 conjugating enzyme binds both ubiquitin and the E1 enzyme and ubiquitin is transferred to the E2's active site cysteine (Hershko et al., 1983). Following dissociation of the E1 enzyme (Eletr, Huang, Duda, Schulman, & Kuhlman, 2005), the E2 enzyme interacts with an E3 ubiquitin ligase that is associated with the protein to be ubiquitinated, resulting in an isopeptide bond between ubiquitin's c-terminal glycine and the ϵ -amino group of a lysine residue within the substrate protein.

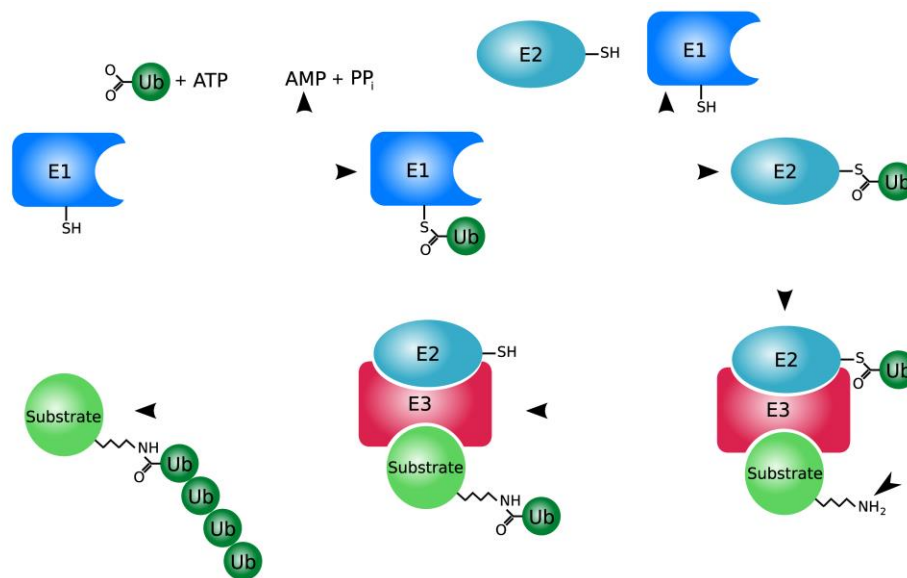


Figure 1. Ubiquitin conjugation. Schematic depiction of the sequential actions of the E1, E2, and E3 enzymes.

Note: Created by Roger B. Dodd for English Language Wikipedia. Copyright 2005 by rogerdodd. Reprinted under the terms of the GNU Free-Documentation License.

Ubiquitin chains are formed by the conjugation of additional ubiquitin monomers to lysine residues within ubiquitin itself. Because ubiquitin has 7 internal lysine (K) residues—K6, K11, K27, K29, K33, K48, and K63—a wide variety of chains can be formed (Figure 2). These chains have different topologies (Tenno et al., 2004), allowing them to be recognized by distinct binding partners (Komander et al., 2009) and to participate in a wide array of processes. Ubiquitin chains linked through K63 and K48, which are among the most well-studied linkages, illustrate the structural and functional diversity of ubiquitin linkages.

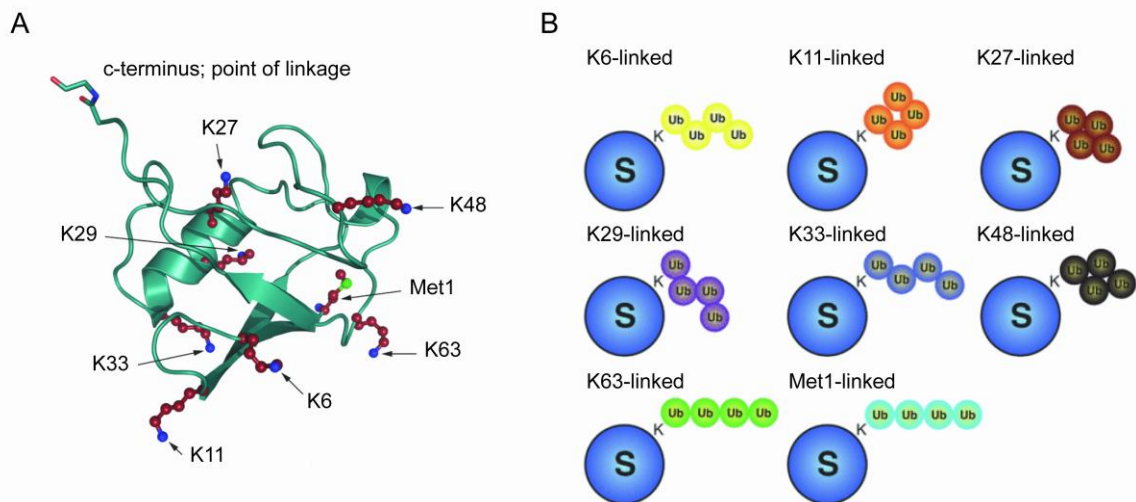


Figure 2. Structurally distinct chains linked through ubiquitin's internal lysine residues. (A) The structure of ubiquitin, demonstrating the locations of the 7 lysine residues. Chains can also be formed through methionine 1 (Met1). (B) The topology of ubiquitin chains depends on the lysine residue through which they are linked.

Note: Reproduced with permission from “The emerging complexity of protein ubiquitination” by David Komander, 2009, *Biochemical Society Transactions*, 37(5), p. 938-9. Copyright 2009 by Biochemical Society Transactions.

K63-linked ubiquitin chains have an open configuration, resembling beads on a string, which allows them to be distinguished from the more compact proteasome targeting K48-linked ubiquitin chains (Tenno et al., 2004; Varadan et al., 2004). As a

result, K63-linked chains promote proteasome-independent processes, including the endocytosis and trafficking of plasma membrane receptors (Lauwers, Jacob, & Andre, 2009; Marchese et al., 2003; Tanno & Komada, 2013), DNA-damage repair (Chiu et al., 2006; Langie et al., 2007; Yan & Jetten, 2008), and kinase activation.

The role of K63-linked ubiquitination in kinase activation came to light with the discovery of a 700 kD kinase complex in the nuclear factor kappa B (NF- κ B) pathway that was regulated by polyubiquitin in a degradation-independent manner (Z. J. Chen, Parent, & Maniatis, 1996). Further work showed that the activation of transforming growth factor β activated kinase 1 (TAK1) and the inhibitor of kappa B kinase (IKK) complex, both of which promote NF- κ B activation, depends on the assembly of K63-linked ubiquitin chains by the E3 ubiquitin ligase tumor necrosis factor receptor associated factor 6 (TRAF6; Deng et al., 2000; Wang et al., 2001). Since then, it has been demonstrated that K63-linked ubiquitination of AKT (also known as protein kinase B) is required for AKT to translocate to the plasma membrane and subsequent activation in response to growth factor stimulation (W. L. Yang et al., 2009; W. L. Yang, Wu, Wu, & Lin, 2010), and that K63-linked ubiquitination of mixed lineage kinase 3 (MLK3) promotes dimerization and autophosphorylation, which are required for MLK3 activation (Humphrey et al., 2013). Strikingly, TRAF6, also ubiquitinates AKT (W. L. Yang et al., 2009) and MLK3 (Humphrey et al., 2013), demonstrating that kinase activation is an important aspect of TRAF6 function.

The Ubiquitin Proteasome System

In contrast to K63-linked ubiquitin chains, K48-linked chains have a compact topology and are primarily involved in degradative pathways (Tenno et al., 2004). Cytosolic proteins that are modified by the addition of a polyubiquitin chain of at least 4 monomers linked through K48 (Deveraux, Ustrell, Pickart, & Rechsteiner, 1994; Piotrowski et al., 1997) are shuttled to the 26S proteasome for degradation, allowing for the removal of damaged or misfolded proteins. Proteins can also be degraded by the proteasome as a means to down-regulate activated signaling pathways (Collins, Wairkar, Johnson, & DiAntonio, 2006; Xiong et al., 2010). Briefly, the 26S proteasome is composed of a 20S core particle (CP), which catalyzes the degradation of proteins into small peptides, and two 19S regulatory particles (RPs), which recognize ubiquitinated proteins to ensure specificity and prevent ubiquitin from being degraded alongside the proteins it modifies (Figure 3; Kanayama et al., 1992; Lupas, Koster, & Baumeister, 1993; Yoshimura et al., 1993). The CP contains four stacked rings that create an open cylinder, with two identical β -rings in the center of the cylinder flanked by α -rings on either side (Puhler et al., 1992). The β -rings contain active sites with chymotrypsin-like, trypsin-like, and caspase-like protease activity (Seemuller et al., 1995). The RPs, which can be further subdivided into a base and lid, reside on either side of the CP.

The RP's base is composed of ATPases, which unfold substrate proteins to allow their translocation into the CP (Nickell et al., 2009), ubiquitin receptors, which recognize ubiquitinated proteins (Bennett et al., 2001; Deveraux et al., 1994; Husnjak et al., 2008), and docking sites for two of the three proteasome-associated deubiquitinating enzymes (DUBs): ubiquitin-specific protease 14 (USP14; Leggett et al., 2002) and ubiquitin-c-

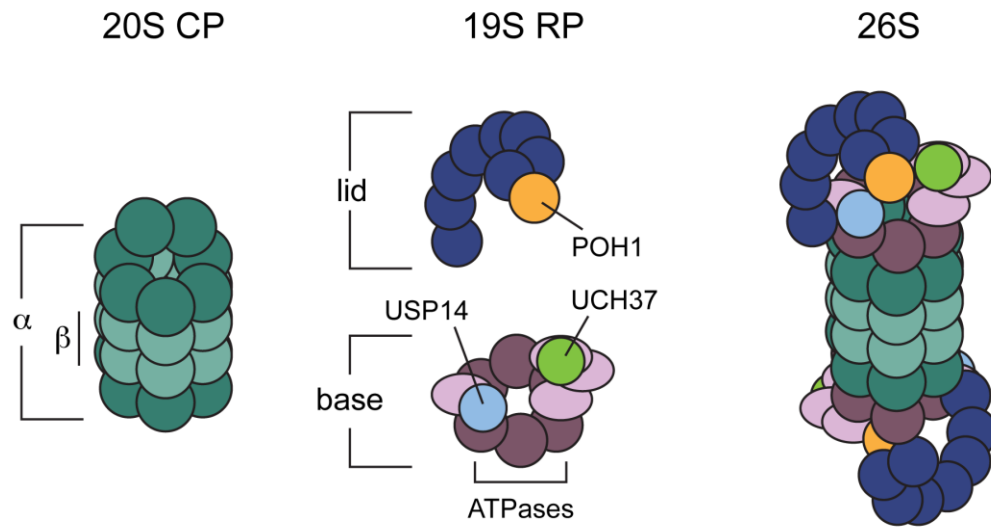


Figure 3. Structure of the proteasome. Schematic of the 20S CP, in which α -subunits are shown in dark green and β -subunits are shown in light green. The 19S RP is divided into the lid, which contains the DUB POH1 (orange), and the base. Within the base, ATPases are shown in dark purple and the DUBs USP14 and UCH37 are shown in blue and bright green, respectively. Light purple represents non-ATPase, non-DUB proteins of the base of the regulatory particle. The 26S proteasome is composed of a CP flanked by two RPs.

terminal hydrolase (UCH37; also known as UCHL5; Hamazaki et al., 2006; Stone et al., 2004). Recent structural studies have shown that the RP's "lid" is not a lid at all, but instead flanks the base and makes direct contact with the CP (Pathare et al., 2012). The lid houses pad one homolog 1 (POH1; Verma et al., 2002; Yao & Cohen, 2002), the third proteasome-associated DUB, and may assist in the assembly of the 26S proteasome (Vilchez et al., 2012).

The disassembly of ubiquitin chains by DUBs plays an important role in maintaining the levels of free ubiquitin, and proteasome-associated DUBs are especially important in this context because they prevent the degradation of ubiquitin by the proteasome. However, although all three proteasomal DUBs remove ubiquitin from

proteasomal substrates, their mechanisms of deubiquitination and relationship to protein degradation differ (reviewed in M. J. Lee, Lee, Hanna, King, & Finley, 2011). POH1, a metalloprotease, is the only DUB that is a permanent, stoichiometric proteasomal subunit (Yao & Cohen, 2002). The catalytic activity of this DUB is strongly coupled to protein degradation: POH1 appears to interact with ubiquitinated proteins only after they have been committed to degradation, perhaps due to partial unfolding by the ATPases of the regulatory particle (Verma et al., 2002; Yao & Cohen, 2002). POH1 cleaves at the base of the ubiquitin chain, removing it *en bloc* from the proteasomal substrate (Lam, Xu, DeMartino, & Cohen, 1997).

In contrast to POH1, both USP14 and UCH37, which associate with the proteasome reversibly, disassemble ubiquitin chains monomer by monomer, starting at the distal tip (Hu et al., 2005; Lam et al., 1997). Chain trimming by USP14 and UCH37 occurs before the substrate is committed to degradation and may weaken the interaction between the substrate and the proteasome, allowing the substrate to dissociate and escape degradation (Lam et al., 1997; Thrower, Hoffman, Rechsteiner, & Pickart, 2000). However, despite the similarities between USP14 and UCH37, deletion of either gene leads to embryonic lethality in mice (Al-Shami et al., 2010; Crimmins et al., 2009), demonstrating that the two proteins have unique, non-redundant functions. Resorption of *Uch37*^{-/-} embryos is observed as early as 8.5 days after conception, and a dramatic reduction in brain development is seen in embryos that survive to 13.5 days (Al-Shami et al., 2010); whereas the *Usp14*^{-/-} embryos die around 14 days after conception (Crimmins et al., 2009).

USP14 in the Nervous System

The ataxia Mice

Even though USP14 knockout mice are not viable (Crimmins et al., 2009) it has been possible to learn about USP14's *in vivo* role through studies of the *ataxia* (ax^J) mice. The ax^J mice have a spontaneously occurring intracisternal-A particle (IAP) insertion into intron 5 of the *Usp14* gene; the IAP is spliced to exon 5 and introduces a translational stop codon, which leads to reduced levels of *Usp14* mRNA (Wilson et al., 2002). As a result, homozygous ax^J mice have a 95% reduction in USP14 in the brain, but the remaining 5% of protein enables their survival for 8 to 10 weeks after birth (D'Amato & Hicks, 1965; Wilson et al., 2002). The ax^J mice, as their name implies, have a severe movement disorder (D'Amato & Hicks, 1965) that is accompanied by reduced muscle development (P. C. Chen et al., 2009), reduced synaptic transmission at the neuromuscular junction (NMJ; Wilson et al., 2002), and altered NMJ structure (P. C. Chen et al., 2011; P. C. Chen et al., 2009). Transgenic restoration of USP14 in the ax^J nervous system dramatically improves lifespan, mobility, and NMJ structure and function (Crimmins et al., 2006), indicating that the neuromuscular phenotype of the ax^J mice results exclusively from neuronal dysfunction. This study, and the lack of pathology in non-neuronal tissues taken from ax^J mice (Crimmins et al., 2009), demonstrates that USP14 is critical in the nervous system but dispensable in other tissues.

While studies of the ax^J mice have established a need for USP14 in the nervous system, the types of processes that USP14 regulates in the brain and spinal cord remain unclear. Although only 50% of neuronal USP14 is associated with the proteasome (Crimmins et al., 2006), USP14's ubiquitin hydrolase activity towards model substrates

has only been observed when it is proteasome-bound (B. H. Lee et al., 2010; Leggett et al., 2002). Therefore, one way for USP14 to support nervous system function is by modulating protein turnover at the proteasome, and there is a wealth of evidence from yeast and immortalized cell lines that loss or inhibition of USP14 alters proteasome function (Hanna et al., 2006; B. H. Lee et al., 2010; Leggett et al., 2002; Liu et al., 2014; Peth, Besche, & Goldberg, 2009; Tian et al., 2014). A second, related, avenue is the maintenance of ubiquitin homeostasis. As previously mentioned, the proteasome-associated DUBs help maintain the free ubiquitin pool by preventing the degradation of ubiquitin and, indeed, loss of USP14 in both yeast (Chernova et al., 2003; Hanna, Meides, Zhang, & Finley, 2007) and the *ax^J* mice (P. C. Chen et al., 2011; P. C. Chen et al., 2009) leads to ubiquitin reduction. These two suggestions assume that, in keeping with its association with the proteasome, USP14 primarily acts on proteasome-targeting K48-linked ubiquitin chains. However, there is evidence that USP14 disassembles K63-linked ubiquitin chains in some circumstances (Jung et al., 2013), raising the possibility that USP14 is required for proteasome-independent ubiquitin signaling in the nervous system.

Regulation of Protein Turnover by USP14

USP14 is a structural and functional homologue of the yeast DUB ubiquitin-specific protease 6 (Ubp6; Chernova et al., 2003), and much of the initial characterization of the protein was carried out in yeast. Ubp6/USP14 associates with the proteasome by binding to regulatory particle non-ATPase 1 (RPN1), a component of the RP's base, via its ubiquitin-like (UBL) domain (Leggett et al., 2002). This binding event causes a

conformational change in USP14 in which the two regulatory loops that normally obscure the active site, which is composed of the catalytic triad of cysteine, histidine, and aspartic acid, are translocated, allowing ubiquitin to enter the catalytic cleft (Hu et al., 2005) and immensely increasing Ubp6/Uspl4's DUB activity towards model deubiquitinase substrates (B. H. Lee et al., 2010; Leggett et al., 2002). It is likely that there is a reciprocal conformational change in either the RP's base or lid upon Ubp6/USP14 docking, because the binding of ubiquitinated proteins with Ubp6/USP14's active site stimulates the opening of the gate to the CP to accelerate the degradation of small peptides by proteasomes isolated from rabbit myocytes (Peth et al., 2009) and stimulates the activity of the RP's ATPases, which unfold proteasomal substrates, in proteasomes isolated from yeast (Peth, Kukushkin, Bosse, & Goldberg, 2013). Intriguingly, even Ubp6 that has been rendered catalytically inactive by mutation of its active site cysteine residue (Ubp6-C118A) is capable of stimulating gate opening (Peth et al., 2009) and ATPase activity (Peth et al., 2013).

Further support for a non-catalytic role for USP14 in the modulation of protein turnover comes from a study done in isolated yeast proteasomes, which showed that both Ubp6 and Ubp6-C118A are capable of delaying the degradation of the model proteasomal substrate cyclin-B when it is ubiquitinated *in vitro* (Hanna et al., 2006). Addition of catalytically active Ubp6 to proteasomes purified from Ubp6 null yeast causes a gradual reduction in the molecular weight of polyubiquitinated cyclin-B, consistent with the idea that USP14/Ubp6 trims ubiquitin chains to weaken the interaction between the proteasome and the ubiquitinated substrate. In contrast, Ubp6-C118A is unable to trim ubiquitin chains, but stabilizes cyclin-B through some other

mechanism. Notably, although these studies provide clear evidence that USP14/Ubp6 can non-catalytically modulate protein turnover, there is no consensus on whether USP14 accelerates (as in Peth et al., 2009; Peth et al., 2013) or delays (as in Hanna et al., 2006) protein degradation. Thus, the impact of USP14 binding to the proteasome may be cell type or substrate specific.

There are also conflicting findings on the impact of USP14's catalytic activity on the turnover of ubiquitinated proteins by the proteasome. While catalytically competent Ubp6 and USP14 delay the degradation of cyclin B by proteasomes purified from Ubp6 null yeast (Hanna et al., 2006), the same research group reported that inhibition of USP14's DUB activity can accelerate the proteasome-mediated degradation of some aggregate-prone proteins in murine embryonic fibroblasts (MEFs; B. H. Lee et al., 2010). To add another layer of complexity, the compound b-AP15, a potent USP14/UCH37 inhibitor, appears to provide the same level of proteasome inhibition as bortezomib, a proteasome inhibitor used clinically to treat multiple myeloma, resulting in cessation of the cell cycle and apoptosis (D'Arcy et al., 2011). The tumor-reducing effects of the antirheumatic drug Auranofin (Fiskus et al., 2014; Mirabelli et al., 1986; Mirabelli et al., 1985) have also been attributed to inhibition of USP14 and UCHL37, which, in turn, inhibits the proteasome (Liu et al., 2014).

Overall, these reports suggest that, similar to the non-catalytic effects of USP14 on proteasome function, regulation of protein turnover by USP14's catalytic activity depends on the cell type in question. The same is true of regulatory particle non-ATPase 13 (RPN13), the proteasomal subunit that enables UCH37 to dock on the RP (Hamazaki et al., 2006). Whereas knockdown of RPN13 in HeLa cells does not have a discernable

effect on proteasome function (Jorgensen et al., 2006), RPN13 knockout mice have accelerated protein degradation in the adrenal gland and lymph organs and reduced proteasome activity in the brain and reproductive system (Al-Shami et al., 2010). Therefore, while the studies described above certainly demonstrate that USP14 can alter protein turnover, the disparity in the effects of loss or inhibition of USP14 on proteasome-mediated protein degradation make it difficult to predict the role of USP14 in the intact nervous system.

Maintenance of Ubiquitin Homeostasis by USP14

In contrast, the maintenance of ubiquitin homeostasis by USP14/Ubp6 is relatively consistent across model systems. Ubiquitin is degraded by the proteasome in Ubp6 null yeast (Leggett et al., 2002), resulting in a significant depletion of both free ubiquitin and ubiquitin conjugates (Hanna, Leggett, & Finley, 2003; Hanna et al., 2007; Leggett et al., 2002). Moreover, Ubp6 null yeast are more sensitive to a variety of cellular stressors, including the protein synthesis inhibitors anisomycin and cycloheximide, than wild type yeast (Amerik, Li, & Hochstrasser, 2000; Chernova et al., 2003). Exogenous expression of the yeast polyubiquitin gene *UBI4* suppresses this increased stress sensitivity, demonstrating a central role for ubiquitin depletion in these phenotypes (Chernova et al., 2003). Ubiquitin depletion is also present in both neuronal and non-neuronal tissues from the *ax^J* mice (Anderson et al., 2005; P. C. Chen et al., 2009) and, similar to what is observed in yeast, nervous system-specific expression of a single open reading frame of the mammalian polyubiquitin gene *Ubb* increases the lifespan and dramatically improves the NMJ structure of the *ax^J* mice (P. C. Chen et al., 2011).

While the ability of neuronal ubiquitin complementation to improve the viability of the ax^J mice suggests that maintenance of ubiquitin pools is the predominant role of USP14 in the nervous system, ubiquitin does not fully rescue the ax^J phenotype (P. C. Chen et al., 2011). For example, while the body mass and the mass of the gastrocnemius muscles in the ax^J , *TgUb* mice are significantly improved over the ax^J mice, both measures fall below wild type levels as the ax^J , *TgUb* mice transition from early to mature adulthood between 8 and 12 weeks of age. In assays of motor behavior, done at 4 weeks of age, ax^J , *TgUb* mice also show considerable improvement over ax^J mice, but they have significantly less muscle strength and require significantly longer to traverse an elevated beam than wild type mice. The incomplete rescue of motor function, body mass, and muscle mass cannot be attributed to incomplete restoration of ubiquitin levels, as more ubiquitin conjugates and free ubiquitin are observed in the brains of the ax^J , *TgUb* mice than wild type mice. Therefore, maintenance of ubiquitin homeostasis is unlikely to be the only function of USP14 in the nervous system. Moreover, expression of *TgUb* in the ax^J mice causes the frequency of miniature endplate currents (MEPCs) recorded at the NMJs of the ax^J , *TgUb* mice to be greater than what is observed in wild type mice (P. C. Chen et al., 2011), and overexpression of ubiquitin in wild type mice also causes altered NMJ structure late in life (Hallengren, Chen, & Wilson, 2013). Together, these findings raise the possibility that ubiquitin has independent effects on the structure and function of the NMJ, and that these effects that mask the deficits observed in the ax^J mice during early postnatal development without correcting the underlying mechanism through which the deficits occur.

Regulation of Non-Proteolytic Ubiquitin Signaling by USP14

In addition to modulating protein turnover and maintaining ubiquitin homeostasis, USP14 has also been reported to modulate the activity or localization of a small group of proteins. The ataxia observed in the *ax^J* mice was initially ascribed to cerebellar dysfunction due to the prominent axonal swellings observed in cerebellar Purkinje cells (PCs; D'Amato & Hicks, 1965). Because transgenic expression of USP14 under the *Thy1.2* promoter, which is not expressed in PCs, rescues the majority of the motor deficits observed in the *ax^J* mice (Crimmins et al., 2006), it is more likely that the ataxic phenotype results directly from NMJ dysfunction (P. C. Chen et al., 2009). However, both spontaneous and evoked inhibitory post synaptic currents (IPSCs) in the PCs of the *ax^J* mice are larger than what is observed in their wild type counterparts, and cell surface expression of the GABA_A receptor (GABA_AR), which mediates fast inhibitory transmission, is also increased (Lappe-Siefke et al., 2009). The increased presence of the GABA_AR on the cell surface is not due to greater GABA_AR abundance, as both mRNA and protein levels are unchanged. Furthermore, USP14 directly interacts with the $\alpha 1$ subunit of the GABA_AR, making it unlikely that USP14 regulates GABA_AR localization by controlling the abundance of another protein.

USP14 also directly interacts with another plasma membrane protein, chemokine (C-X-C motif) receptor 4 (CXCR4), to regulate both its localization and activity (Cane, Ponnappan, & Ponnappan, 2012; Mines, Goodwin, Limbird, Cui, & Fan, 2009).

Treatment of human embryonic kidney (HEK) cells with the CXCR4 ligand (C-X-C motif) chemokine 12 (CXCL12; also known as stromal-derived factor-1, SDF-1) induces the ubiquitination and endocytosis of CXCR4, as well as the association of CXCR4 with

USP14 (Mines et al., 2009). Pharmacological inhibition of USP14 reduces ligand-driven endocytosis of CXCR4 in CD4⁺ T-cells and, similar to what is observed with the GABA_AR (Lappe-Siefke et al., 2009), increases the basal cell surface expression of CXCR4 (Cane et al., 2012). RNAi-mediated knockdown of USP14 increases the levels of ubiquitinated CXCR4 and decreases CXCR4-mediated chemotactic cell migration (Mines et al., 2009). Intriguingly, overexpression of USP14, which reduces CXCR4 ubiquitination, also reduces chemotactic cell migration, suggesting that USP14 is required for a temporally regulated cycle of CXCR4 ubiquitination that promotes its activity.

Although the linkage of the ubiquitin chains that USP14 removes from CXCR4 has not been determined, CXCR4 is a known substrate of the E3 ubiquitin ligase atrophin interacting protein 4 (AIP4), which builds K63-linked ubiquitin chains (Bhandari, Robia, & Marchese, 2009; Marchese et al., 2003). As K63-linked chains are more commonly associated with regulation of protein location and activity than K48-linked chains, USP14's effects on both the GABA_AR and CXCR4 suggest that it can disassemble K63-linked chains. More recently, it has been directly demonstrated that inhibition of USP14's ubiquitin hydrolase activity leads to enhanced K63-linked ubiquitination of Disheveled 2 (Dvl2), a component of the Wnt signaling cascade (Jung et al., 2013). USP14-mediated deubiquitination of Dvl2 promotes its phosphorylation and the activation of both canonical and non-canonical Wnt signaling. Combined, these findings suggest that USP14 may regulate proteasome-independent ubiquitin signaling mediated by K63-linked chains in the nervous system.

As previously mentioned, K63-linked chains have a well-characterized impact on the activation of kinases (Z. J. Chen et al., 1996; Deng et al., 2000; Humphrey et al., 2013; W. L. Yang et al., 2009; W. L. Yang et al., 2010; A. Y. Zhou et al., 2013), so a role for USP14 in the disassembly of K63-linked chains is consistent with the widespread kinase activation observed in the hippocampus of the *ax^J* mice (Y. N. Jin et al., 2012). In fact, the phosphorylation of both AKT, which requires K63-linked ubiquitination to become activated (W. L. Yang et al., 2009), and c-Jun N-terminal kinase (JNK), which is downstream of the ubiquitin-activated kinase MLK3 (Humphrey et al., 2013), are increased in the *ax^J* mice. Given the prominent structural pathology at the NMJs of the *ax^J* mice (P. C. Chen et al., 2011; P. C. Chen et al., 2009), the increase in pJNK is especially suggestive, as JNK is an important determinant of axon structure.

During development, pJNK contributes to axon path finding (Qu et al., 2013; Shafer, Onishi, Lo, Colakoglu, & Zou, 2011), elongation (Tararuk et al., 2006), and branching (G. Yang et al., 2012), largely through phosphorylation of cytoskeletal proteins in developing axons (Chang, Jones, Ellisman, Goldstein, & Karin, 2003; Feltrin et al., 2012). Axonal JNK is also activated in response to nerve damage and contributes to the injury response through retrograde transport to the nucleus, where it activates transcription factors to alter gene expression (Lindwall & Kanje, 2005; Shin et al., 2012). Furthermore, aberrant JNK activation has detrimental effects on both NMJ structure (Collins et al., 2006; Drerup & Nechiporuk, 2013; Etter et al., 2005) and function (Etter et al., 2005). Over active JNK contributes to the synaptic overgrowth in the *Drosophila highwire (hiw)* mutants (Collins et al., 2006), and expression of constitutively active JNK causes similar structural abnormalities in both *Drosophila* (Etter et al., 2005) and zebra

fish (Drerup & Nechiporuk, 2013) NMJs. Moreover, temporally controlled induction of constitutively active JNK in *Drosophila* causes a reduction in neurotransmitter release from the NMJ (Etter et al., 2005).

USP14 as a Regulator of Protein Kinase Activation

The primary goal of the research described in this dissertation was to determine what type of ubiquitin signaling USP14 regulates in the nervous system. At the outset of this work, there was a great deal of interest in using USP14 inhibitors to treat neurological diseases (Dantuma & Bott, 2014; Edelmann, Nicholson, & Kessler, 2011; B. H. Lee, Finley, & King, 2012; Ristic, Tsou, & Todi, 2014; Schmidt & Finley, 2014; Todi & Paulson, 2011; Ying, Wang, & Wang, 2013), following the demonstration that inhibition of USP14 accelerates the degradation of aggregate-prone proteins in MEFs (B. H. Lee et al., 2010). Given the devastating, nervous-system-specific, effects of loss of USP14 in the *ax^J* mice (Crimmins et al., 2006; Wilson et al., 2002), it was important to establish whether USP14's essential role in the nervous system relied on its non-catalytic modulation of the proteasome rather than its ubiquitin hydrolase activity.

To this end, we generated a transgenic mouse expressing a ubiquitin-hydrolase-inactive, dominant-negative USP14 species in the nervous system. The USP14 catalytic mutant mice, referred to as *TgUsp14CA* mice, had a normal life span, but replicated all other aspects of the neuromuscular disease observed in the *ax^J* mice. Expression of USP14CA caused increased K63-linked ubiquitination of MLK3 and over-activation of JNK in the spinal cords of *TgUsp14CA* mice. Notably, there was no change in the overall abundance of MLK3 or JNK, nor was there evidence of global alterations in protein

turnover. The NMJ pathology, muscle development, and motor deficits of the *TgUsp14CA* mice were significantly improved by treatment with a JNK inhibitor, demonstrating a central role of aberrant JNK activation in the phenotype of the *TgUsp14CA* mice and suggesting that regulation of non-proteolytic ubiquitin signaling is a critical aspect of USP14 function in the nervous system. These studies are presented in Chapter 2.

In Chapter 3, we investigated the interplay between ubiquitin homeostasis and the neuromuscular deficits observed in the *ax^J* and *TgUsp14CA* mice. Similar to what is observed in the *ax^J* mice (P. C. Chen et al., 2011), ubiquitin complementation reduced the presynaptic swelling and ultra-terminal sprouting at the NMJs of the *TgUsp14CA* mice. Consistent with the JNK inhibitor studies reported in Chapter 2, the improved NMJ structure in *TgUsp14CA* mice expressing the ubiquitin transgene was accompanied by reduced pJNK immunoreactivity at the NMJ. However, whereas overexpression of ubiquitin partially rescued the deficits in motor function and muscle development in the *ax^J* mice (P. C. Chen et al., 2011), *TgUsp14CA* mice expressing the ubiquitin transgene had smaller muscles and displayed less voluntary ambulation than *TgUsp14CA* mice without ubiquitin complementation. We ascribed this discrepancy to the differential effects of loss of USP14 and expression of USP14CA on ubiquitin pools: whereas there was a 50% decrease in the total ubiquitin pool in the spinal cords of the *ax^J* mice, expression of USP14CA shifted the balance between free ubiquitin and ubiquitin conjugates without altering the overall abundance of ubiquitin. This conclusion was supported by the finding that, when USP14's catalytic activity was intact, moderate ubiquitin overexpression improved muscle development and motor function, while more

robust ubiquitin overexpression was detrimental. For reference, the mouse lines discussed in Chapters 2 and 3 are summarized in Table 1.

Table 1. Descriptions of mutant and transgenic mice.

Mouse	Notes
<i>ax^J</i>	Spontaneous recessive mutation in <i>Usp14</i> that reduces USP14 levels to 5% of wild type.
Tg <i>Usp14</i>	Transgenic mouse expressing wild type <i>Usp14</i> under the neuronal <i>Thy1.2</i> promoter. USP14 expression in nervous system is 5X higher than in wild type mice.
Tg <i>Usp14CA</i> (Chapter 2)	Transgenic mouse expressing <i>Usp14C118A</i> , in which the active site cysteine is mutated to an alanine, under the neuronal <i>Thy1.2</i> promoter. Expression level matches Tg <i>Usp14</i> .
TgCA (Chapter 3)	Transgenic mouse expressing <i>Usp14C118A</i> , in which the active site cysteine is mutated to an alanine, under the neuronal <i>Thy1.2</i> promoter. Expression level matches Tg <i>Usp14</i> .
Tg <i>Ub</i>	Transgenic mouse expressing a single open reading frame of the ubiquitin gene <i>Ubb</i> under the neuronal <i>Thy1.2</i> promoter. Abundance of free ubiquitin and ubiquitin conjugates in the nervous system is 2X and 1.5X higher than in wild type mice, respectively.
Tg <i>Ub</i> -High	Another founder line created during the generation of the Tg <i>Ub</i> mice. The <i>Ubb</i> gene is expressed under the <i>Thy1.2</i> promoter, resulting in levels of free ubiquitin that are 3X what is observed in wild type mice and levels of ubiquitin conjugates that are 2X what is observed in wild type mice.
<i>ax^J</i> , Tg <i>Ub</i>	<i>ax^J</i> mice expressing Tg <i>Ub</i> in the nervous system.
TgCA, Tg <i>Ub</i>	Transgenic mouse expressing both TgCA and Tg <i>Ub</i> in the nervous system.

UBIQUITIN-SPECIFIC PROTEASE 14 REGULATES C-JUN N-TERMINAL KINASE
SIGNALING AT THE NEUROMUSCULAR JUNCTION

by

JADA H. VADEN, BULA J. BHATTACHARYYA, PING-CHUNG CHEN,
JENNIFER A. WATSON, ANDREA G. MARSHALL, SCOTT E. PHILLIPS, JULIE A.
WILSON, GWENDALYN D. KING, RICHARD J. MILLER,
AND SCOTT M. WILSON

Molecular Neurodegeneration 2015, **10**:3

Copyright
2015
by
BioMed Central

Used under the Creative Commons Attribution (CC-BY) license

Format adapted and errata corrected for dissertation

Abstract

Background: Ubiquitin-specific protease 14 (USP14) is one of three proteasome-associated deubiquitinating enzymes that remove ubiquitin from proteasomal substrates prior to their degradation. *In vitro* evidence suggests that inhibiting USP14's catalytic activity alters the turnover of ubiquitinated proteins by the proteasome, although whether protein degradation is accelerated or delayed seems to be cell-type and substrate specific. For example, combined inhibition of USP14 and the proteasomal deubiquitinating enzyme UCH37 halts protein degradation and promotes apoptosis in multiple myeloma cells, whereas USP14 inhibition alone accelerates the degradation of aggregate-prone proteins in immortalized cell lines. These findings have prompted interest in USP14 as a therapeutic target both inside and outside of the nervous system. However, loss of USP14 in the spontaneously occurring *ataxia* mouse mutant leads to a dramatic neuromuscular phenotype and early perinatal lethality, suggesting that USP14 inhibition may have adverse consequences in the nervous system. We therefore expressed a catalytically inactive USP14 mutant in the mouse nervous system to determine whether USP14's catalytic activity is required for neuromuscular junction (NMJ) structure and function.

Results: Mice expressing catalytically inactive USP14 in the nervous system exhibited motor deficits, altered NMJ structure, and synaptic transmission deficits that were similar to what is observed in the USP14-deficient *ataxia* mice. Acute pharmacological inhibition of USP14 in wild type mice also reduced NMJ synaptic transmission. However, there was no evidence of altered proteasome activity when USP14 was inhibited either genetically or pharmacologically. Instead, these manipulations increased the levels of non-proteasome targeting ubiquitin conjugates. Specifically, we observed

enhanced proteasome-independent ubiquitination of mixed lineage kinase 3 (MLK3). Consistent with the direct activation of MLK3 by ubiquitination, we also observed increased activation of its downstream targets MAP kinase kinase 4 (MKK4) and c-Jun N-terminal kinase (JNK). *In vivo* inhibition of JNK improved motor function and synapse structure in the USP14 catalytic mutant mice.

Conclusions: USP14's catalytic activity is required for nervous system structure and function and has an ongoing role in NMJ synaptic transmission. By regulating the ubiquitination status of protein kinases, USP14 can coordinate the activity of intracellular signaling pathways that control the development and activity of the NMJ.

Introduction

Protein ubiquitination is an exceptionally flexible post-translational modification because ubiquitin can be conjugated onto substrates in different lengths and linkages, enabling it to regulate a wide variety of signaling pathways (Kravtsova-Ivantsiv, Sommer, & Ciechanover, 2012; Welchman, Gordon, & Mayer, 2005). For example, lysine 63 (K63)-linked chains regulate the endocytosis and sorting of plasma membrane receptors (Lauwers, Jacob, & Andre, 2009). There is also an emerging link between K63-linked ubiquitination and kinase activation (Schmukle & Walczak, 2012; Zhou et al., 2013), with K63-linked chains serving as a scaffold for the recruitment of signaling components or, in the case of MLK3, directly inducing dimerization and kinase activation (Humphrey et al., 2013). In contrast, K48-linked ubiquitin chains target proteins for proteasomal degradation.

USP14 is one of three proteasome-associated deubiquitinating enzymes (DUBs) that remove ubiquitin from proteasomal substrates prior to their degradation, thus terminating the ubiquitin signal and maintaining a stable pool of free ubiquitin (Anderson et al., 2005; Kraut, Prakash, & Matouschek, 2007; M. J. Lee, Lee, Hanna, King, & Finley, 2010). In addition, USP14's catalytic activity may alter the turnover of ubiquitinated proteins by the proteasome in a cell-type and substrate specific manner (Hanna et al., 2006; B. H. Lee et al., 2010; Peth, Besche, & Goldberg, 2009; Tian et al., 2014). Combined inhibition of USP14 and the proteasomal DUB ubiquitin C-terminal hydrolase 37 (UCH37) in multiple myeloma cells delays proteasome-mediated protein degradation, halts the cell cycle, and leads to tumor cell apoptosis (D'Arcy et al., 2011). In contrast, in immortalized cell lines, inhibition of USP14 appears to accelerate the

degradation of proteins known to aggregate in neurological diseases (B. H. Lee et al., 2010). Additional proteolysis-independent functions for USP14 have also been described, including deconjugating K63-linked ubiquitin chains on Disheveled 2 (Jung et al., 2013) and controlling the cell-surface expression of GABA receptors (Lappe-Siefke et al., 2009).

Despite the growing interest in USP14 inhibition as a treatment for neurological diseases ((B. H. Lee, Finley, & King, 2012; B. H. Lee et al., 2010) but see (Hyrskyluoto et al., 2014)) and cancers (D'Arcy et al., 2011; Liu et al., 2014; Tian et al., 2014; Wu, Zhang, Bai, Han, & Li, 2014), loss of USP14 in the spontaneously occurring *ataxia* (ax^J) mouse mutant causes a severe loss of mobility and early postnatal lethality (Wilson et al., 2002). The neuromuscular phenotype of the ax^J mice is rescued by neuronal-specific expression of USP14 (Crimmins et al., 2006), demonstrating a critical need for USP14 in the nervous system. In this study, we used genetic and pharmacological inhibition of USP14 to investigate the contributions of USP14's catalytic activity to NMJ structure and function. Expression of a catalytically inactive form of USP14 in the nervous system caused developmental deficits in NMJ structure and synaptic transmission. However, acute pharmacological inhibition of USP14 at adult NMJs also significantly reduced synaptic transmission, indicating that USP14 participates in dynamic ubiquitin signaling events that support neurotransmitter release. This ubiquitin signaling appears to be independent of proteasomal-mediated protein degradation. Instead, our data suggest that USP14 disassembles non-proteasomal-targeting ubiquitin chains and indicate that loss of USP14's DUB activity leads to enhanced K63-linked ubiquitination of MLK3 and hyperactivation of its signaling cascade. Inhibition of pJNK, which is downstream of

MLK3, significantly improved the motor deficits and NMJ pathology caused by loss of USP14's DUB activity. These findings demonstrate that USP14 is involved in regulating multiple ubiquitin signals in the nervous system, ranging from acute ubiquitination for the maintenance of synaptic activity to long-term control of ubiquitin pools.

Results

TgUsp14CA Displaces Endogenous USP14 from the Proteasome without Altering Proteasome Activity

To investigate the contributions of USP14's DUB activity to nervous system structure and function, we generated transgenic mice expressing a catalytically inactive form of USP14 in the nervous system. The coding sequence for USP14's active site cysteine was changed to an alanine residue using PCR-site-directed mutagenesis, and the resulting *Usp14C114A* cDNA was cloned behind the neuronal *Thy1.2* promoter (Fig. 1A). Expression of this transgene, referred to as *TgUsp14CA*, caused a robust increase in USP14 expression in the spinal cords of both wild type and USP14-deficient *ax^J* mice (Fig. 1B) that was easily detectible by postnatal day (P) 8 (Supplemental Figure 1). Because reduced ubiquitin levels (Chen et al., 2009) and altered NMJ structure (Chen et al., 2011) are observed in *ax^J* mice prior to P8, we chose to study the effects of *TgUsp14CA* in wild type mice. Importantly, using RNA transcriptome analysis, we determined that *TgUsp14CA* did not alter the expression of endogenous *Usp14* mRNA in the brains of wild type mice, and that transgenic *Usp14CA* mRNA accounted for 90% of total *Usp14* transcripts (Fig. 1C). We therefore interpreted the robust increase in USP14 abundance observed in the brains and spinal cords of wild type mice expressing

TgUsp14CA (henceforth *TgUsp14CA* mice) as evidence of USP14CA expression (Supplemental Figure 1). In contrast, USP14 abundance was not increased in non-neuronal tissues of *TgUsp14CA* mice, indicating that USP14CA was expressed exclusively in the nervous system (Supplemental Figure 1). Overall, the localization and abundance of USP14CA were consistent with that we have previously observed when wild type USP14 is expressed under the *Thy1.2* promoter (Crimmins et al., 2006).

While USP14 can be found both free and bound to the proteasome, its catalytic activity has only been observed when associated with the proteasome (Crimmins et al., 2006). We found that expression of *TgUsp14CA* caused increased USP14 abundance in proteasome fractions isolated from the brains of 4- to 6-week old mice that was similar to what was observed when wild type USP14 was overexpressed in the *TgUsp14* mice (Fig. 1D). To determine whether USP14CA was the predominant USP14 species on *TgUsp14CA* proteasomes, we used a ubiquitin vinyl-methyl-ester (Ub-VME) assay (Borodovsky et al., 2001). Ub-VME labels catalytically active USP14 by forming a covalent bond with its active site cysteine residue, creating a shift in molecular weight that can be detected by immunoblotting. Because the active site cysteine is mutated to alanine in USP14CA, it cannot be labeled by Ub-VME. As expected, when proteasome fractions isolated from the brains of wild type and *TgUsp14* mice were incubated with Ub-VME, all USP14 was labeled within 1 hr (Fig. 1E). In contrast, only minimal USP14 labeling was observed in proteasomes isolated from *TgUsp14CA* mice, demonstrating that USP14CA displaces endogenous USP14 from the proteasome.

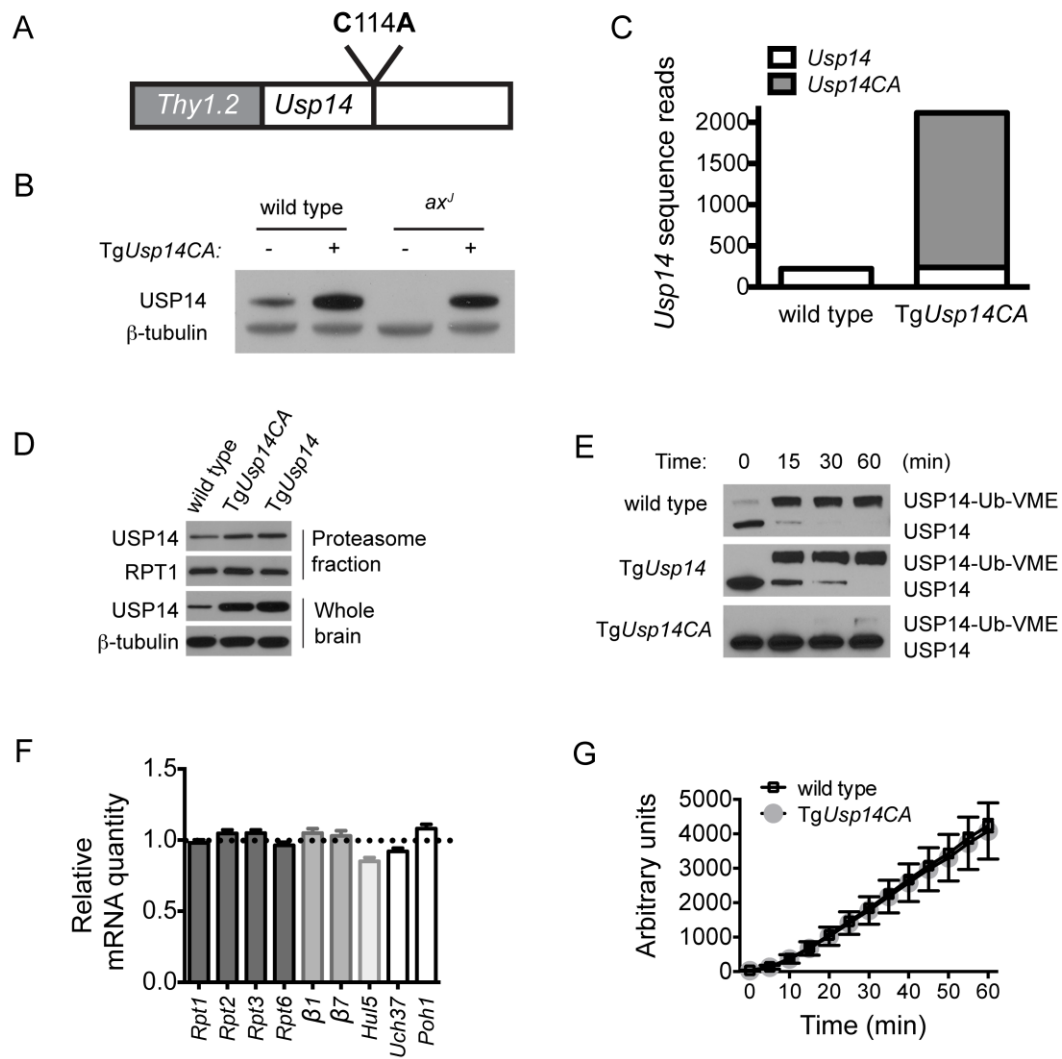
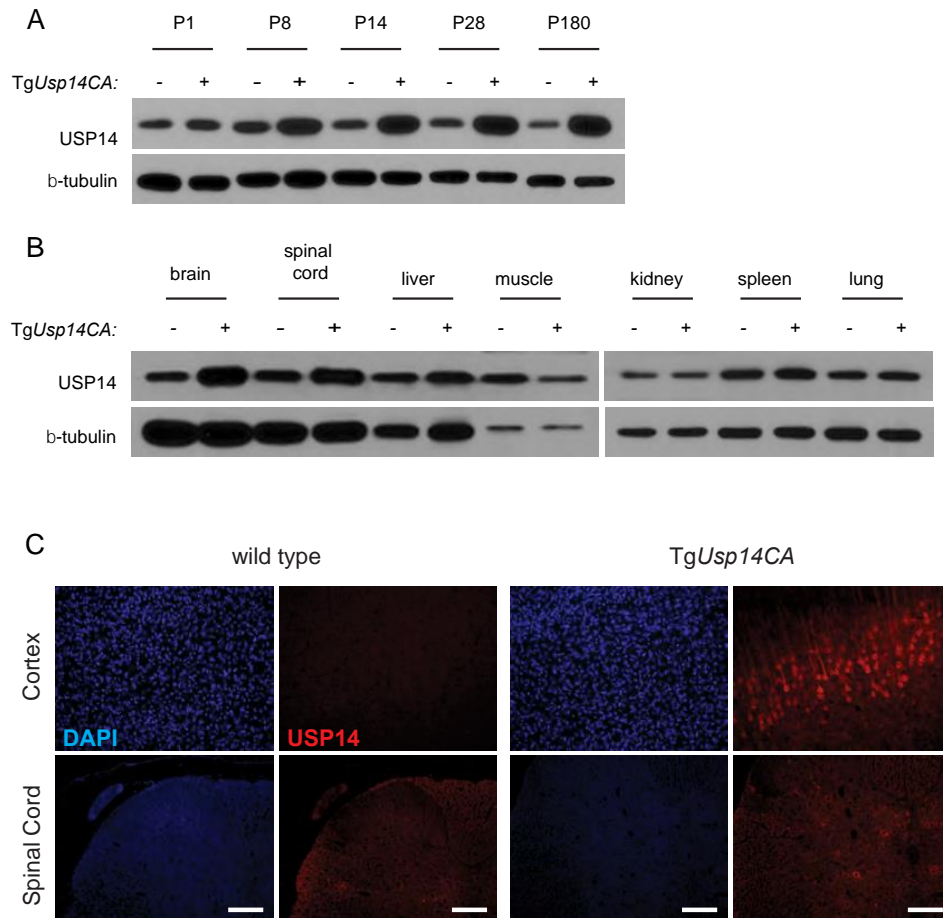


Figure 1. See legend on next page.

See figure on previous page.

Figure 1. Transgenic expression of USP14CA in the nervous system (A) Full length *Usp14* cDNA containing a mutation of the active site cysteine to alanine (C114A) was cloned behind the *Thy1.2* promoter. (B) Representative immunoblot of spinal cord extracts taken from 4- to 6-week-old wild type and *ax^J* mice (\pm Tg*Usp14CA*) using USP14-specific antisera. β -tubulin was included as a loading control. (C) Abundance of wild type *Usp14* and transgenic *Usp14CA* transcripts obtained by RNA transcriptome analysis of brain tissue taken from 4- to 6-week-old wild type and Tg*Usp14CA* mice. (D) Representative Immunoblots of USP14 in whole brain lysates and brain proteasome fractions from 4- to 6-week-old wild type, Tg*Usp14CA*, and Tg*Usp14* mice. β -tubulin was included as a loading control for whole brain and RPT1 was a loading control for the proteasome fraction. Tg*Usp14* mice express wild type USP14 behind the *Thy1.2* promoter. (E) Ubiquitin vinyl methyl ester (Ub-VME) assay for DUB activity in proteasome fractions from the brains of 4- to 6-week-old wild type, Tg*Usp14*, and Tg*Usp14CA* mice. Ubiquitin is covalently attached to the active site cysteine of USP14, resulting in a slower migrating USP14 species denoted as USP14-Ub-VME. The mutant USP14CA cannot be labeled by Ub-VME. (F) Relative mRNA quantity of proteasome subunits and associated factors determined by qPCR, normalized to wild type (represented by dotted line on graph), from spinal cords of 6-week-old wild type and Tg*Usp14CA* mice. $n = 3$ mice per genotype, run in triplicate. Data are shown as mean \pm SEM (G) Assay of trypsin-like activity of proteasomes isolated from 4- to 6-week-old wild type and Tg*Usp14CA* mice using the fluorogenic Boc-LRR-AMC substrate. $n = 3$ mice per genotype, and data are shown as mean \pm SEM. See also Supplemental Figure 1.



Supplemental Figure 1, related to Figure 1. USP14CA is expressed specifically in the nervous system. (A) Developmental time course of USP14 expression in spinal cords of wild type (-) and TgUsp14CA (+) mice on postnatal days (P) 1-180 showing robust expression of the transgene by P8. β -tubulin was included as a loading control. (B) Representative immunoblots of USP14 from 4- to 6-week old wild type (-) and TgUsp14CA (+) mice demonstrating neuronal expression of the transgene. USP14 overexpression is assumed to reflect transgene expression. β -tubulin was included as a loading control (C) Representative immunostaining for USP14 (red) and DAPI (blue) in cerebral cortices and spinal cords of 8-week-old wild type and TgUsp14CA mice. Scale bar = 100 μ m.

Because inhibition of Upb6, the yeast ortholog of USP14, delays the degradation of ubiquitinated proteins by the proteasome and induces increased transcription of proteasomal subunits (Hanna et al., 2006), we looked for signs of proteasome dysfunction in the nervous systems of *TgUsp14CA* mice. In contrast to what is observed in yeast, we did not observe transcriptional upregulation of components of the proteasome's catalytic core or regulatory particle in the brains of *TgUsp14CA* mice (Fig. 1F). Similarly, when the trypsin-like activity of proteasomes isolated from *TgUsp14CA* mice was compared to that of wild type proteasomes, the activity profile was identical (Fig. 1G). Therefore, expression of *TgUsp14CA* almost completely eliminated the DUB activity of USP14 on the proteasome, but did not cause proteasome stress.

TgUsp14CA Reduces Muscle Mass, Strength, and Coordination, But Does Not Cause Early Postnatal Lethality

Unlike loss of neuronal USP14 in the *ax^J* mice (Crimmins et al., 2006; Wilson et al., 2002), inhibition of USP14's DUB activity in the nervous system did not alter the lifespan of the *TgUsp14CA* mice (Fig. 2A). However, *TgUsp14CA* did have deficits in muscle development, muscle strength, and motor coordination similar to what is observed in *ax^J* mice, and could be easily distinguished from wild type littermates by 3 weeks of age due to a resting tremor and hind limb clasp upon tail suspension (Fig. 2B). The *TgUsp14CA* mice were significantly smaller than wild type mice by 12 weeks of age (Fig. 2C), and had reduced muscle mass (Fig. 2D) and fore limb grip strength (Fig. 2E) by 4 weeks of age. Similarly, 4-week-old *TgUsp14CA* mice required more time than wild type controls to cross an elevated beam, and 24-week-old *TgUsp14CA* mice were

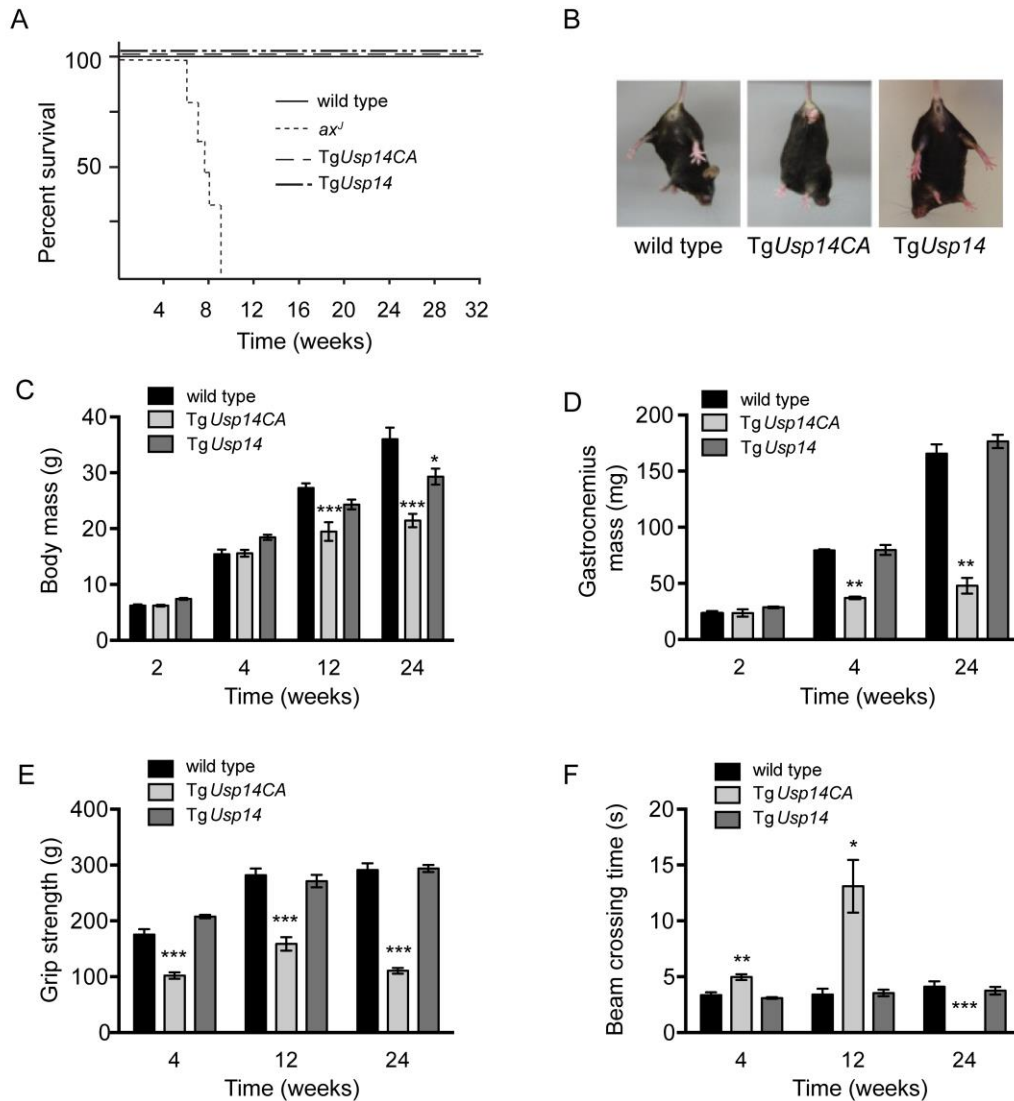


Figure 2. Neuronal expression of USP14CA leads to decreased body weight, muscle weight, and motor performance. (A) Survival curves for wild type, *TgUsp14CA*, *TgUsp14*, and *ax^J* mice. *TgUsp14* mice express wild type USP14 under the *Thy1.2* promoter and serve as a control for neuronal USP14 overexpression in *TgUsp14CA* mice. *ax^J* mice have a 95% reduction of USP14 in all tissues. (B) Tail suspension assays show hind limb clasp in *TgUsp14CA* mice versus the typical splaying observed in 6-week-old wild type and *TgUsp14* mice. Assays of (C) body mass, (D) muscle mass, (E) muscle strength and (F) motor performance of 2- to 24-week-old wild type, *TgUsp14CA*, and *TgUsp14* mice. Muscle strength was assessed by a forelimb grip-force assay and motor performance was assessed by time required to traverse an elevated beam. 24-week-old *TgUsp14CA* mice were unable to traverse beam. All data are shown as mean \pm SEM. Symbols represent Mann-Whitney tests compared against wild type and corrected for multiple comparisons with a Bonferroni adjustment where appropriate; * $p < 0.05$, ** $p < 0.01$, *** $p < 0.001$; $n =$ at least 4 animals per genotype per time point.

completely unable to traverse the beam (Fig. 2F). Because the deficits in body mass, muscle development, and motor performance observed in the *TgUsp14CA* mice were not replicated by overexpression of wild type USP14 in the *TgUsp14* mice, they were attributed to loss of USP14's catalytic activity and not to USP14 overexpression.

USP14's Ubiquitin Hydrolase Activity Supports NMJ Structure and Function

The reduced muscle mass and motor coordination observed in *TgUsp14CA* mice suggested that neuronal expression of catalytically-inactive USP14 caused deficits in synaptic transmissions similar to what we have previously observed in the USP14-deficient *ax^J* mice (Chen et al., 2011; Wilson et al., 2002). To test this, we used two-electrode voltage clamp to record miniature endplate currents (MEPCs) in diaphragm muscles from 4- to 6-week-old wild type, *ax^J*, and *TgUsp14CA* mice (Fig. 3A). Like the *ax^J* mice, *TgUsp14CA* mice had a marked reduction in frequency MEPCs, and the amplitude and decay constant of MEPCs were increased compared to controls (Fig. 3B-D).

A change in MEPC kinetics, such as the increased decay constant observed in *TgUsp14CA* mice (Fig. 3D), often reflects a change in the properties of the postsynaptic receptor. When we examined expression of muscle acetylcholine receptor (AChR) subunits in 4-week-old mice, we found a greater than 100-fold increase in transcripts of the fetal AChR- γ subunit in *TgUsp14CA* gastrocnemius muscles compared to wild type muscles (Fig. 3G). Consistent with the increased decay constant observed at the *TgUsp14CA* NMJ, AChRs containing the γ -subunit have a longer channel open time than

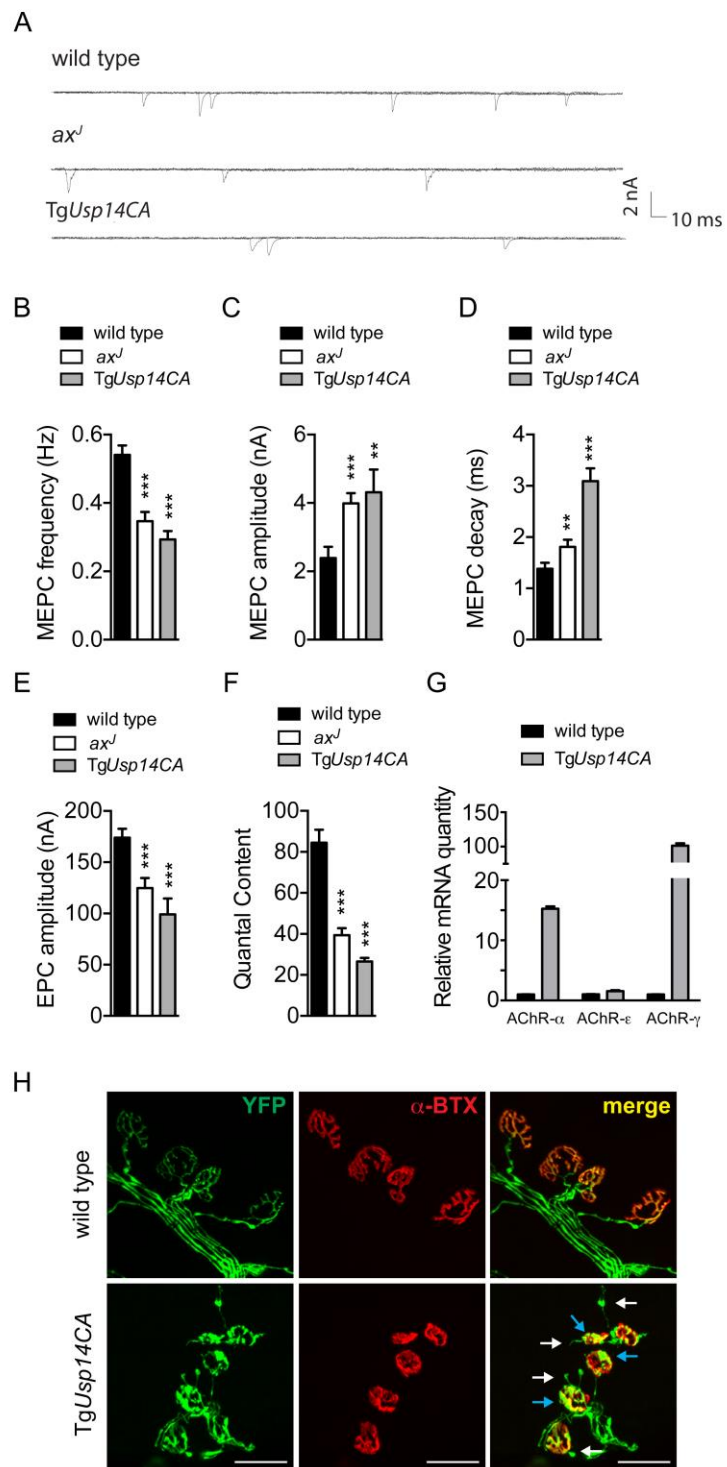
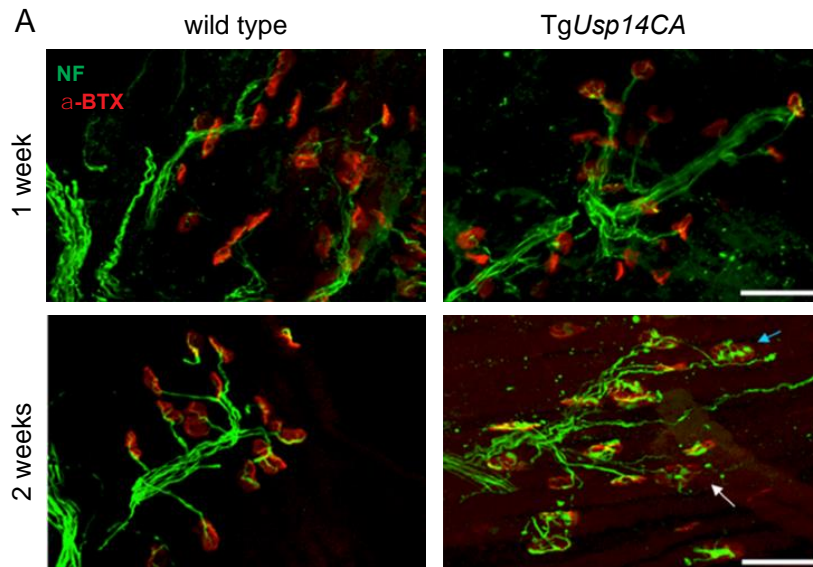


Figure 3. See legend on next page.

See figure on previous page.

Figure 3 Expression of *TgUsp14CA* causes functional and structural deficits at the NMJ. (A) Example traces of MEPCs recorded from diaphragms of 4- to 6-week-old wild type, *ax^J*, and *TgUsp14CA* mice. (B) MEPC frequency in wild type (n = 56 endplates, 10 mice), *TgUsp14CA* (n = 23 endplates, 4 mice), and *ax^J* (n = 75 endplates, 10 mice) muscles. (C) MEPC amplitude in wild type (n = 45 endplates, 10 mice), *TgUsp14CA* (n = 21 endplates, 4 mice) and *ax^J* (n = 75 endplates, 10 mice). (D) MEPC decay constant in wild type (n = 42 endplates, 10 mice), *TgUsp14CA* (n = 17 endplates, 4 mice) and *ax^J* (n = 23 endplates, 10 mice) muscles. (E) Evoked EPC amplitudes in wild type (n = 55 endplates, 10 mice), *TgUsp14CA* (n = 15 endplates, 4 mice) and *ax^J* (n = 75 endplates, 10 mice) muscles. (F) Quantal content in wild type (n = 40 endplates, 10 mice), *TgUsp14CA* (n = 15 endplates, 4 mice) and *ax^J* (n = 59 endplates, 10 mice) muscles. (G) qPCR of AChR subunits in the gastrocnemius muscles of 4-week-old wild type and *TgUsp14CA* mice. Data were normalized to wild type and n = at least 3 mice per genotype. All data in (B)-(G) are shown as mean \pm SEM. Symbols represent Mann-Whitney tests compared against wild type and corrected for multiple comparisons with a Bonferonni adjustment. * p < 0.05, ** p < 0.01, and ***p < 0.001. (H) Immunostaining of TA muscles from 4-week-old wild type and *TgUsp14CA* mice. Axons were visualized via expression of YFP (green) under the neuronal *Thy1.2* promoter and AChRs were labeled with rhodamine-conjugated α -bungarotoxin (α -BTX, red). White arrows indicate ultra-terminal sprouting and blue arrows indicate axonal and terminal swellings, scale bars = 50 μ m. See also Supplemental Figure 2.



Supplemental Figure 2, related to Figure 3. *TgUsp14CA* mice have abnormal NMJ structure starting at 2 weeks of age.(A) Whole-mount immunostaining of TA muscles from wild type and *TgUsp14CA* mice in 1- and 2-week-old. Motor neuron axons were stained with antibodies against neurofilament (green), and AChRs were labeled with rhodamine-conjugated α -bungarotoxin (α -BTX, red). White arrows indicate ultra-terminal sprouting and blue arrows indicate axonal swellings, scale bars = 50 μ m.

receptors containing the adult ϵ -subunit (Michler & Sakmann, 1980). The γ -containing receptors and upregulation of the α - and ϵ - AChR subunits observed in the *TgUsp14CA* mice are also observed following denervation and nerve block (Kues, Brenner, Sakmann, & Witzemann, 1995), and may represent postsynaptic compensation for reduced neurotransmission. However, despite these postsynaptic compensations, the *TgUsp14CA* endplates displayed reduced synaptic responses upon nerve stimulation (Fig. 3E) and decreased quantal content (Fig. 3F). We also observed significant pathology when we examined NMJ structure using whole mount immunostaining of the tibialis anterior (TA) muscle. Presynaptic swelling and ultra-terminal sprouting were detectable by 2 weeks of age (Supplemental Figure 2), and by 4 weeks of age, 57% of the *TgUsp14CA* terminals displayed focal swellings and 56% had ultra-terminal sprouting (Fig. 3H).

Acute Inhibition of USP14 Leads to Reduced Neurotransmitter Release at the NMJ

To differentiate between abnormal development and an ongoing need for USP14's DUB activity in synaptic transmission at the adult NMJ, we measured spontaneous and evoked transmission following acute treatment with the USP14 inhibitor IU1 in phrenic nerve/diaphragm preparations from adult wild type and *TgUsp14CA* mice. Example traces for each condition are shown in Fig. 4A. IU1 treatment of wild type NMJs replicated the decrease in MEPC frequency (Fig. 4B) and the increase in the MEPC decay constant (Fig. 4D) observed in the *ax^J* and *TgUsp14CA* mice (Fig. 3B and D). In contrast, we did not observe any effect of IU1 treatment on *TgUsp14CA* NMJs, indicating that the IU1-mediated alterations in synaptic transmission were due to inhibition of USP14's DUB activity. Acute inhibition of USP14 in wild type mice also

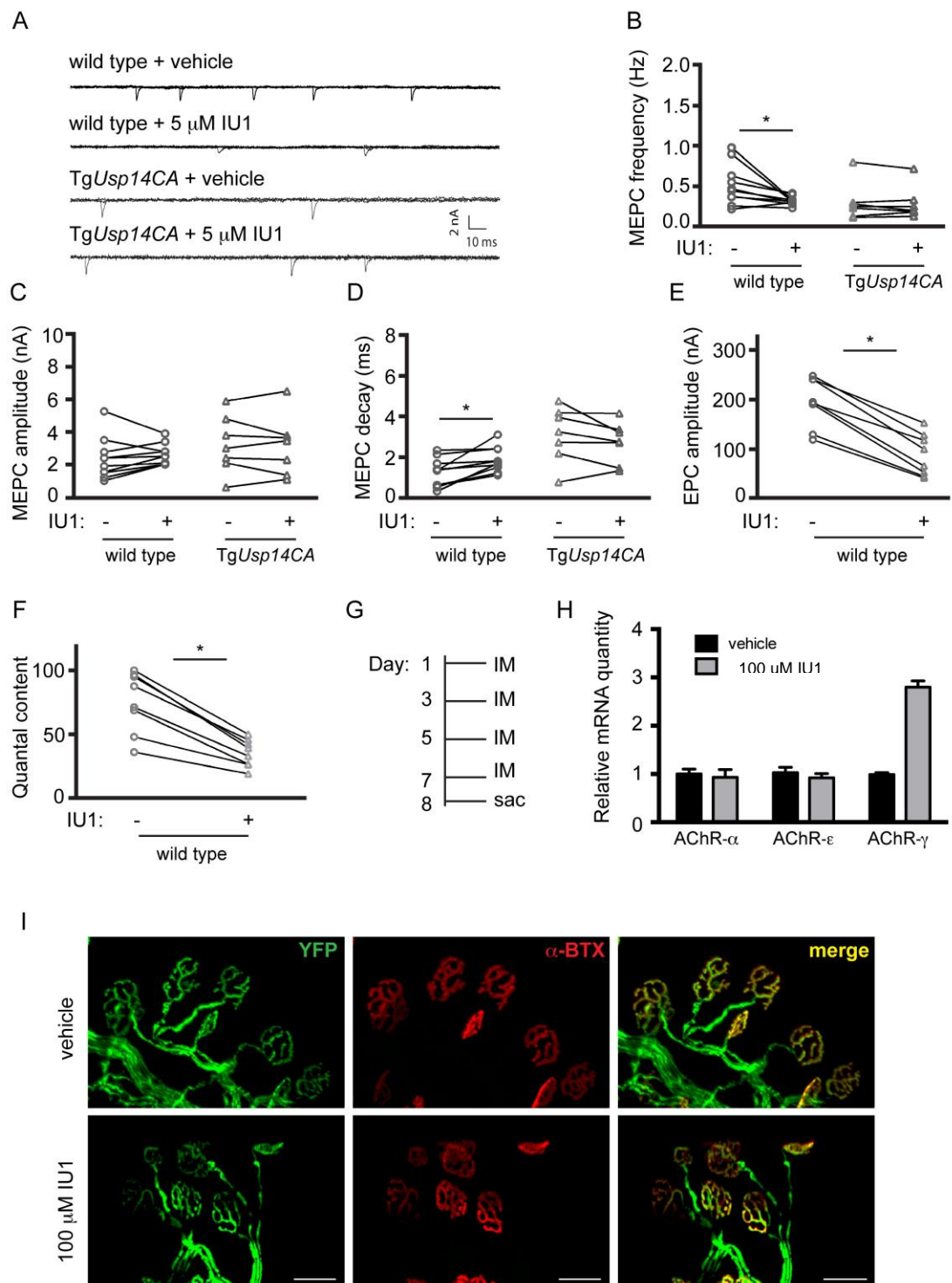


Figure 4. See legend on next page.

See figure on previous page.

Figure 4. Acute inhibition of USP14 causes synaptic transmission deficits at the adult NMJ. (A) Example traces of MEPCs recorded from diaphragm muscle fibers isolated from 4- to 6-week-old wild type (n = 10 endplates, 4 mice) and *TgUspl4CA* (n = 7 endplates, 3 mice) muscles in the presence of vehicle or the USP14 inhibitor IU1. Quantitation of (B) MEPC frequency, (C) amplitude, and (D) decay constants in muscles from wild type and *TgUspl4CA* muscles before (-) and after (+) 5 μ M IU1 application. Quantitation of (E) EPC amplitude and (F) quantal content in wild type muscles (n = 10 endplates, 4 mice) before (-) and after (+) addition of 5 μ M IU1. In (B)-(F), symbols represent Wilcoxon matched-pairs signed rank tests, where *p<0.05 (G) Schematic of experimental design, where adult wild type mice (12- to 14-weeks-old) were given intramuscular injections of 100 μ L of 100 μ M IU1 or vehicle every other day for 1 week, and (H) the abundance of AChR subunit mRNA in gastrocnemius muscles was compared using qPCR. Data are shown as mean \pm SEM and were normalized to vehicle treatment. n = 3 muscles per condition, run in triplicate. (I) Whole mount immunostaining of gastrocnemius muscles from wild type mice given intramuscular injections of IU1 or vehicle as described above. Endplates were labeled with rhodamine-conjugated α -BTX, and motor neurons were visualized via expression of YFP under the *Thy1.2* promoter. Scale bars = 50 μ m.

recapitulated the deficits in EPC amplitude and quantal content (Fig. 4E and F) observed in *TgUsp14CA* mice (Fig. 3E and F). Only the increase in MEPC amplitude observed in *ax^J* and *TgUsp14CA* mice was not mimicked by IU1 treatment (Fig. 4C). These data indicate that the synaptic deficits observed in *TgUsp14CA* mice are not due to aberrant development, but rather reflect an ongoing need for USP14's DUB activity at the adult NMJ.

The increase in the MEPC decay constant in *TgUsp14CA* mice was associated with increased expression of the fetal AChR- γ subunit in gastrocnemius muscles (Fig. 3G). Similarly, 1 week of IU1 injections into the gastrocnemius muscles of adult, wild type mice (Fig. 4G) caused an increase in AChR- γ abundance compared to what was observed in vehicle-injected control muscles (Fig. 4H), indicating that USP14-inhibition at the adult NMJ is sufficient to cause induction of the embryonic AChR- γ subunit. We also examined NMJ structure following IU1 treatment. Unlike in *TgUsp14CA* mice (Fig. 3H), no swollen terminals or ultra-terminal sprouts were observed in IU1-treated wild type mice, and the endplates retained their mature, arborized appearance (Fig. 4I). These experiments demonstrate that abnormal terminal structure is not a prerequisite for deficient synaptic transmission, and suggests that these deficits may have distinct underlying mechanisms.

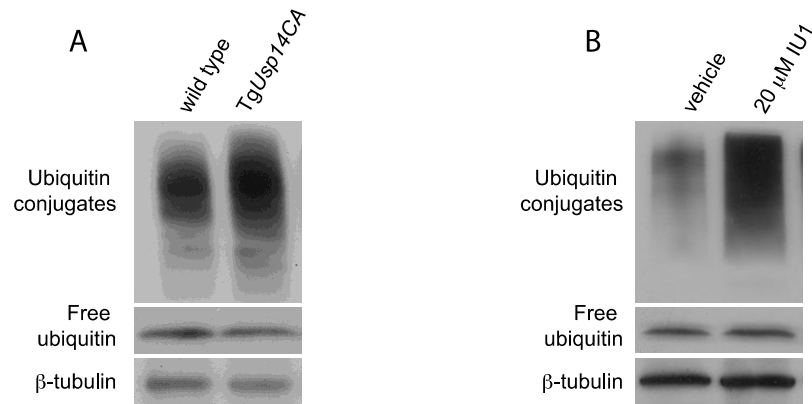
Inhibition of USP14's DUB Activity Causes Accumulation of K63-linked Ubiquitin

Chains

The role of USP14 in the maintenance of ubiquitin homeostasis is well established, so we reasoned that aberrant ubiquitin signaling might underlie the

neuromuscular phenotype of the *TgUsp14CA* mice and the synaptic deficits caused by acute inhibition of USP14. Consistent with USP14's ubiquitin hydrolase activity, we found an increase in ubiquitinated proteins in the spinal cords of *TgUsp14CA* mice compared to controls and in cortical neurons treated with IU1 (Supplemental Figure 3).

Although we found no difference in the catalytic capacity of *TgUsp14CA* and wild type proteasomes towards the fluorogenic Boc-LRR-AMC substrate (Fig. 1G), this increase in ubiquitin conjugates was consistent with decreased turnover of ubiquitinated proteins by the proteasome. Because the Boc-LRR-AMC substrate is not ubiquitinated and can bypass the proteasome's regulatory particle and enter the catalytic core directly, the turnover of this substrate may not accurately reflect the turnover of ubiquitinated proteins *in vivo*. However, when we measured the abundance of proteasomal-targeting K48-linked ubiquitin conjugates, which serve as a robust and sensitive marker of ubiquitin proteasome system function (E. J. Bennett et al., 2007), we found no difference between wild type and *TgUsp14CA* spinal cords or between IU1- and vehicle-treated neurons (Fig. 5A and B). Instead, we observed increased K63-linked ubiquitin conjugates in both *TgUsp14CA* spinal cords and IU1-treated neurons (Fig. 5C and D). K63-linked ubiquitin chains do not appear to target proteins for proteasomal degradation (Ikeda & Dikic, 2008; Jacobson et al., 2009; Xu et al., 2009), but, instead, regulate receptor internalization, endosomal sorting, and intracellular signaling (Ikeda & Dikic, 2008).



Supplemental Figure 3, related to Figure 5. Genetic inactivation and pharmacological inhibition of USP14's ubiquitin hydrolase activity lead to increased ubiquitin conjugates. (A) Representative immunoblot from spinal cords of wild type and *TgUsp14CA* mice probed for ubiquitin. β -tubulin was used as a loading control. (B) Representative immunoblot of cortical neurons from wild type mice treated with vehicle (DMSO) or 20 μ M IU1 for 24 h.

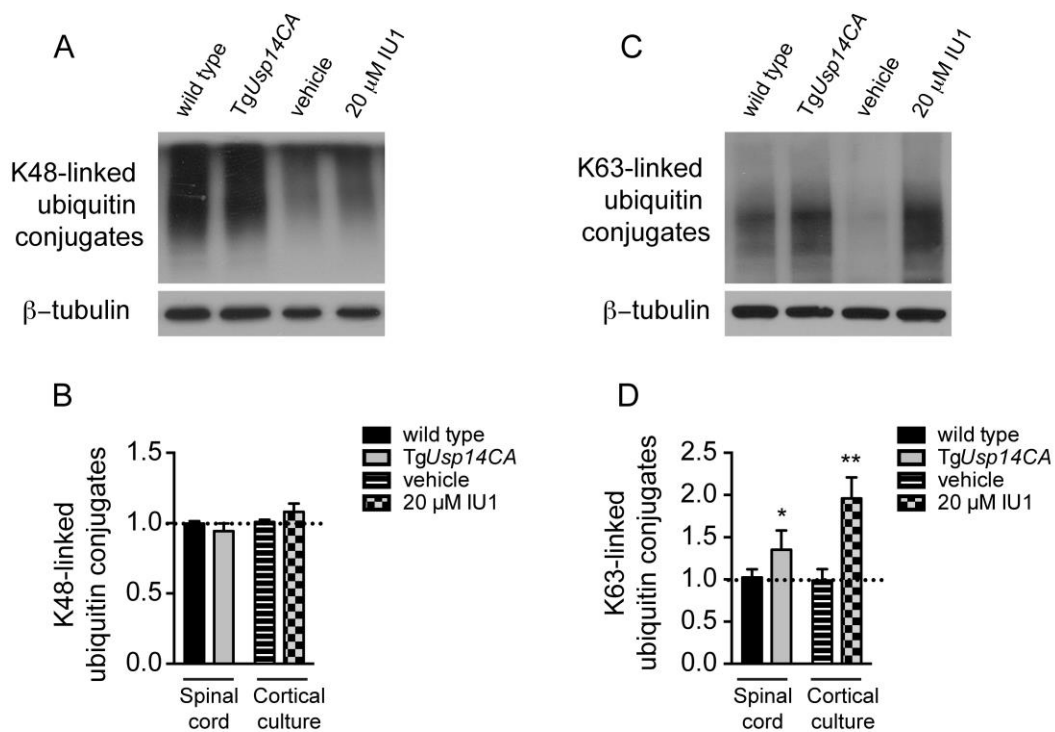


Figure 5. Loss of USP14's ubiquitin hydrolase activity results in accumulation of non-proteasomal associated ubiquitin conjugates. (A) Representative immunoblot of spinal cord extracts from 4- to 6-week-old wild type and *TgUsp14CA* mice and cortical neurons treated with vehicle or 20 μM IU1 for 24 h and probed with an antibody specific for K48-linked ubiquitin chains. (B) Quantitation of (A). (C) As in (A) except with anti-K63-linked ubiquitin chain antibody. β-tubulin was used as a loading control in all experiments. (D) Quantitation of (C). Data are shown as mean ± SEM, and n = at least 3 animals per genotype or condition run in duplicate. Symbols represent Mann-Whitney tests, where *p<0.05 and **p<0.01. See also Supplemental Figure 3.

USP14's DUB Activity Regulates the MLK3 Signaling Cascade

K63-linked ubiquitination of MLK3 leads to dimerization and auto-phosphorylation on threonine 277/ serine 281 (Humphrey et al., 2013). This auto-phosphorylation enables MLK3 to phosphorylate mitogen-activated protein kinase kinase 4 (MKK4), which, in turn, phosphorylates JNK. Because MLK3 is activated by K63-linked ubiquitination and elevated pJNK has been demonstrated to cause terminal swelling (Drerup & Nechiporuk, 2013) and sprouting (Collins, Wairkar, Johnson, & DiAntonio, 2006) at the NMJ that is similar to what we observed in the *TgUsp14CA* mice (Fig. 3H), we investigated whether this pathway was hyperactivated in the *TgUsp14CA* mice. When we immunoprecipitated MLK3 from spinal cord extracts, we observed increased K63-linked ubiquitination and enhanced serine/threonine phosphorylation of high molecular weight MLK3 species in *TgUsp14CA* lysates compared to wild type lysates (Fig. 6A and B). We also observed increased phosphorylation of MLK3's target MKK4, even though total MKK4 abundance was decreased in *TgUsp14CA* mice relative to controls (Fig. 6C and D). Although we observed a significant decrease in *Mkk4* mRNA in *TgUsp14CA* spinal cords compared to wild type spinal cords (Supplemental Figure 4), the magnitude of the effect may not explain the 39% reduction in MKK4 protein.

When compared to wild type mice, we observed increased pJNK1/2 in spinal cord extracts of *TgUsp14CA* and *ax^J* mice and decreased pJNK1/2 in spinal cord extracts of *TgUsp14* mice, (Fig. 6E and F) indicating that USP14's DUB activity can bidirectionally modulate JNK activation, likely by controlling MLK3 ubiquitination. Notably, there was no change in the activation of the MAP kinases p38 and ERK in the spinal cords of *TgUsp14CA* mice compared to wild type mice, and, although pJNK can induce cell

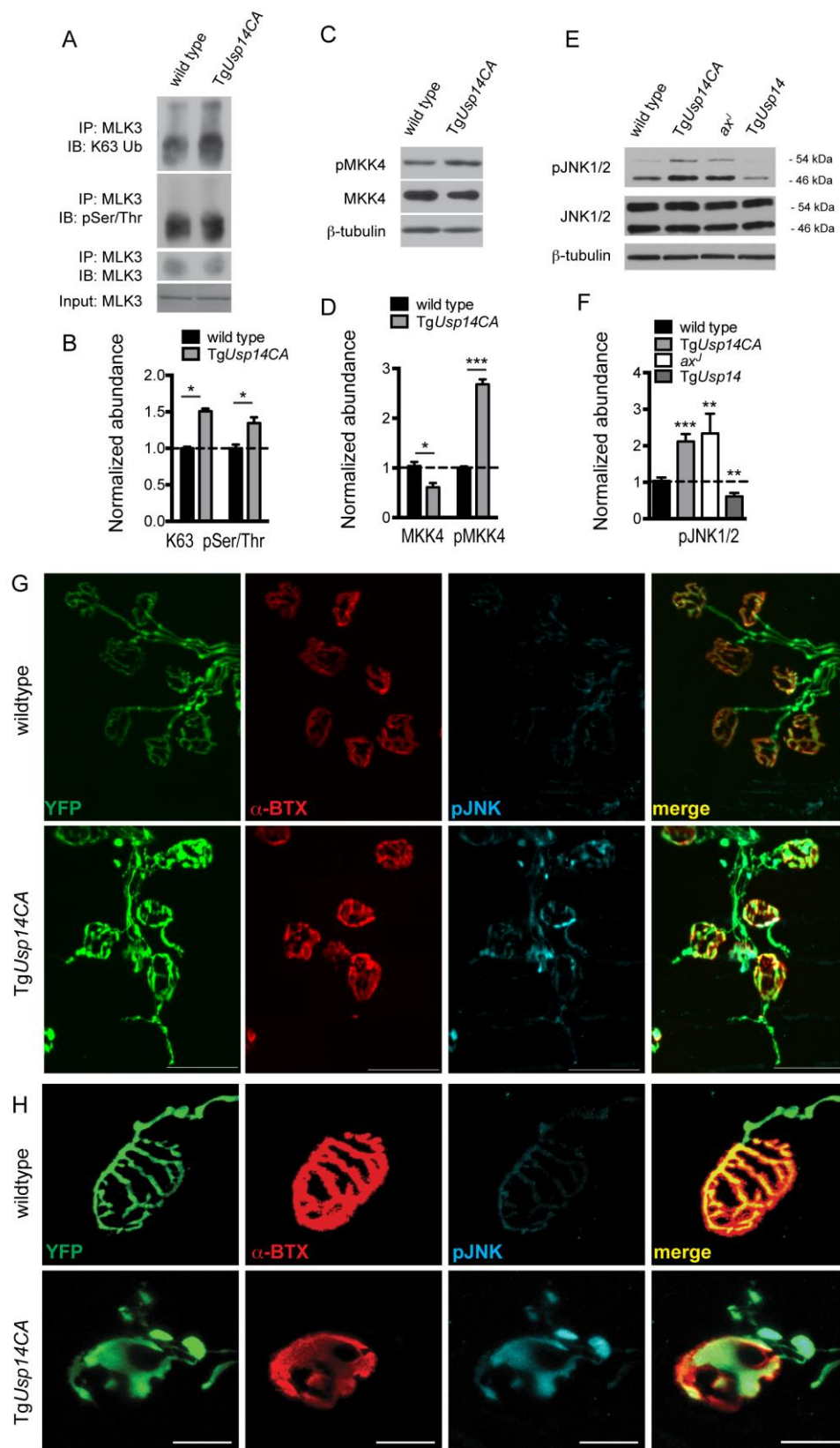
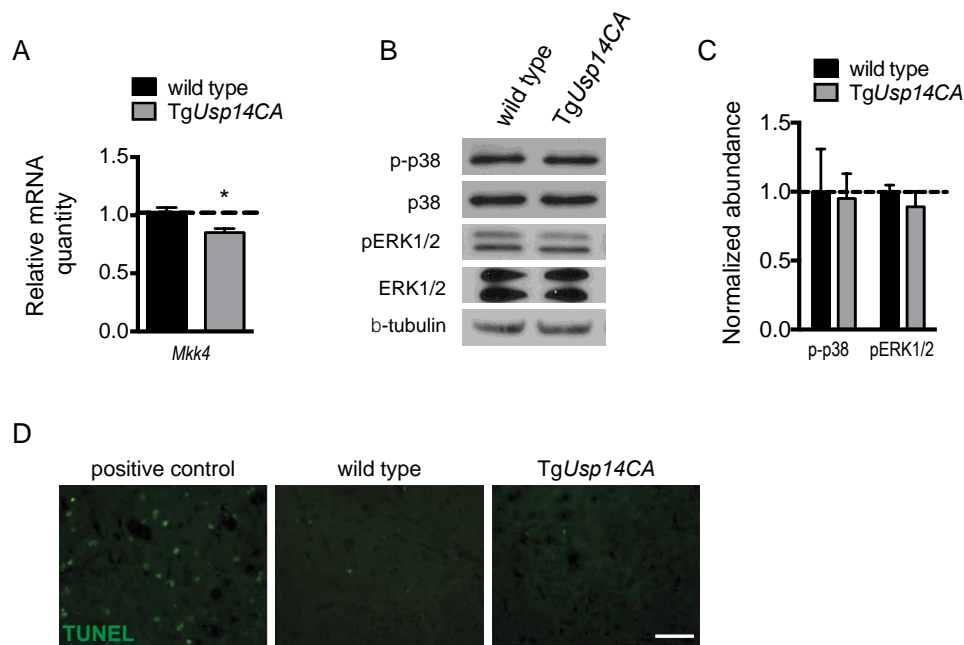


Figure 6. See legend on next page.

See figure on previous page.

Figure 6. Inhibition of USP14's DUB activity leads to enhanced activation of the MLK3 signaling cascade. (A) Representative immunoprecipitates (IP) of MLK3 from spinal cord lysates from 4- to 6-week-old wild type and *TgUsp14CA* mice, immunoblotted (IB) for K63-linked ubiquitin, phospho-serine/threonine, and MLK3. (B) Quantitation of (A), K63- and pSer/Thr- modified MLK3 were normalized to total immunoprecipitated MLK3. (C) Representative immunoblots of wild type and *TgUsp14CA* spinal cord extracts probed for pMKK4 and total MKK4. β -tubulin was used as a loading control. (D) Quantitation of (C), pMKK4 was normalized to MKK4. (E) Representative immunoblots from spinal cords from 4- to 6-week-old wild type, *TgUsp14CA*, *ax^J*, and *TgUsp14* mice, probed for pJNK1/2 and total JNK1/2. JNK 1 and 2 migrate to 46 and 54 kDa, respectively. β -tubulin was used as a loading control. (F) Quantitation of (E), pJNK was normalized to JNK and quantitation includes both the 46 and 54 kDa bands. Data in (B), (D), and (F) are shown as mean \pm SEM, and n = 3 animals per genotype. Symbols represent Mann-Whitney tests compared against wild type mice and corrected for multiple comparisons with a Bonferonni adjustment where appropriate; *p<0.05, **p<0.01, ***p<0.001. (G) Representative images of whole-mount immunostaining of TA muscles from 4-week-old wild type and *TgUsp14CA* mice using a pJNK antibody (blue). AChRs were labeled with rhodamine-conjugated α -BTX (red), and motor neuron axons were visualized via expression of YFP under the *Thy1.2* promoter (green). Scale bars = 50 μ m. (H) As in (G), except that scale bars = 20 μ m. See also Supplemental Figure 4.



Supplemental Figure 4, related to Figure 6. No evidence of cell death in *TgUsp14CA* spinal cord. (A) Relative abundance of *Mkk4* mRNA in spinal cords from 4- to 6- week-old wild type and *TgUsp14CA* mice. n = 3 animals per genotype, run in triplicate. (B) Representative immunoblots of p-p38 MAP kinase, p38 MAP kinase, pERK1/2, and ERK1/2 in spinal cords from 4- to 6 week-old wild type and *TgUsp14CA* mice. β-tubulin was used as a loading control. (C) Quantitation of (B), pERK quantitation includes both the 42 and 44 kDa bands. (D) TUNEL staining in spinal cord sections taken from 8-week-old wild type and *TgUsp14CA* mice. Brain slices from wild type mice were treated with DNase 1 to generate the positive control. Scale bar = 50 μm.

death, there was no evidence of apoptosis in spinal cords of TgUsp14CA mice (Supplemental Figure 4). We next performed whole mount immunostaining of TA muscles of wild type and TgUsp14CA mice using an antibody against pJNK (Fig. 6G and H) and found a significant correlation between pJNK staining and TgUsp14CA terminal pathology. In the TgUsp14CA mice, 94% of the terminal swellings and 90% of the ultra-terminal sprouts were pJNK positive.

Elevated pJNK Contributes to the Structural and Functional Deficits Caused by Loss of USP14's DUB Activity

Because excess pJNK at the NMJ has previously been shown to cause motor endplate disease (Collins et al., 2006) and JNK inhibition causes increased neurotransmitter release in the central nervous system (Costello & Herron, 2004), we hypothesized that the elevated pJNK observed in the TgUsp14CA spinal cords and motor neuron terminals may cause deficits in NMJ structure and function. To test this, we administered the JNK inhibitor SP600125 (SP) to 3-week-old wild type and TgUsp14CA mice via intraperitoneal (IP) injections. Daily IP injections were given at a dose of 16 mg/kg for 2 weeks, and control mice received an equivalent volume of DMSO vehicle alone. SP inhibits JNK by reversibly occupying its ATP binding pocket to prevent kinase activity towards its substrates. Because JNK is autophosphorylated, SP causes a reduction of pJNK (Fig. 7A) that is equivalent to the reduction of activated JNK substrates (B. L. Bennett et al., 2001). On average, we observed an approximately 30% reduction of pJNK in the spinal cords of SP-treated mice compared to their vehicle-treated counterparts

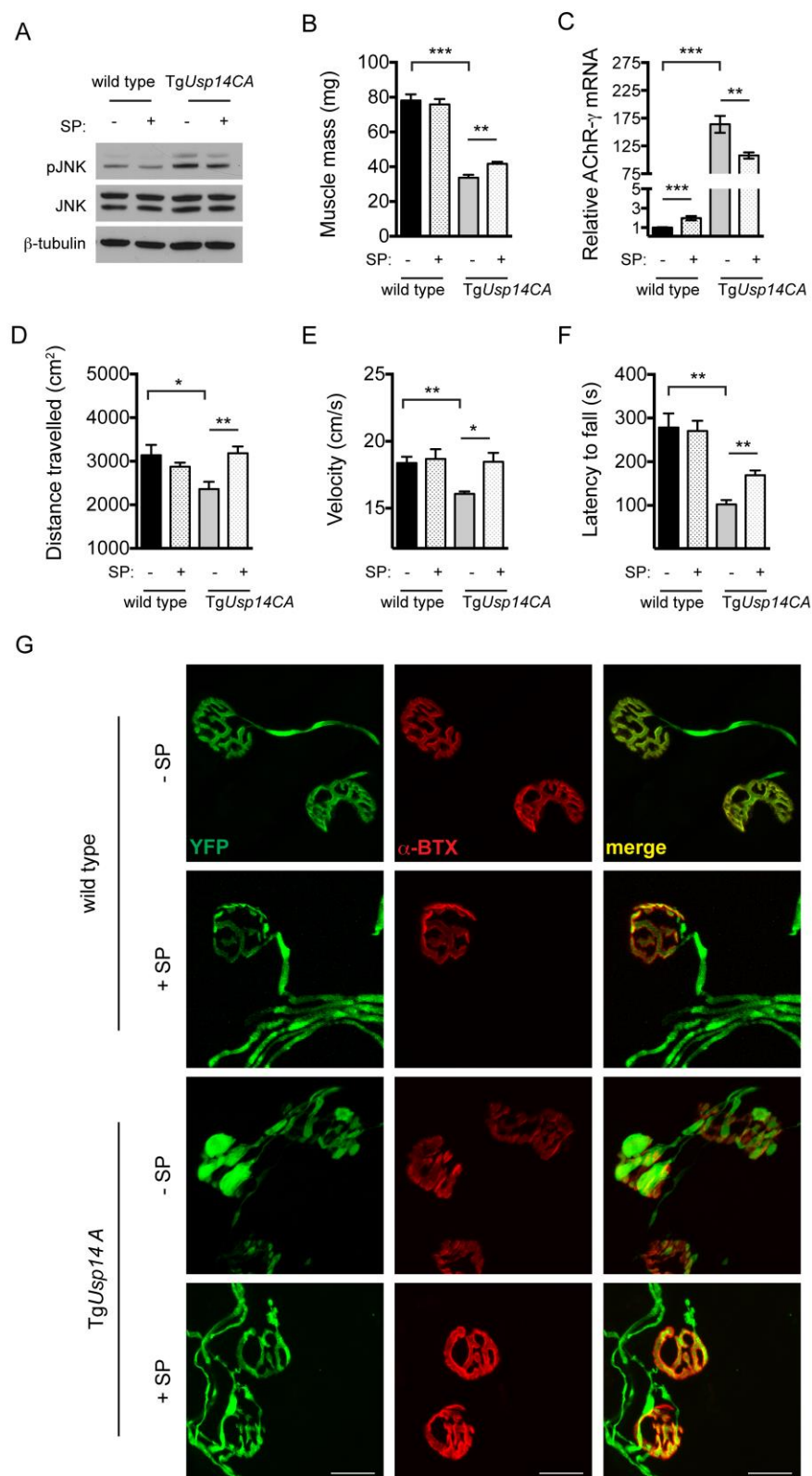


Figure 7. See legend on next page.

See figure on previous page.

Figure 7. Inhibition of pJNK improves the structural and functional deficits caused by inhibition of USP14's DUB activity. (A) Representative immunoblots of pJNK1/2 and JNK1/2 in spinal cords from 5-week-old wild type or *TgUspl4CA* mice following 2 weeks of IP injections of the JNK inhibitor SP600125 (SP, +) or vehicle control (DMSO, -). β -tubulin was used as a loading control. Wild type mice given SP had pJNK levels that were $71.2 \pm 10.3\%$ ($p < 0.01$, Mann-Whitney test) of what was observed in vehicle-treated wild type controls and SP-treated *TgUspl4CA* mice had pJNK levels that were $66.6 \pm 19.4\%$ ($p < 0.01$, Mann-Whitney test) of vehicle-treated *TgUspl4CA* mice. (B) Gastrocnemius muscle masses from male wild type or *TgUspl4CA* mice treated with vehicle alone (-) or SP (+) as described above. The same effect was observed in female mice. (C) Relative *AChR- γ* mRNA abundance in gastrocnemius muscles. (D) Total distance travelled and (E) ambulatory velocity during 10 min in an open field. (F) Latency to fall from beam in the rotarod assay. For (B) – (F), all data are shown as mean \pm SEM and $n = 5$ to 7 animals per condition. Symbols represent Mann-Whitney tests corrected for multiple comparisons with a Bonferonni adjustment, where * $p < 0.05$, ** $p < 0.01$, and *** $p < 0.001$. (G) High magnification images of whole-mount immunostaining of TA muscles from mice described above. AChRs were labeled with rhodamine-conjugated α -BTX (red), and motor neuron axons were visualized via expression of YFP under the *Thy1.2* promoter (green). Scale bars = $20 \mu\text{m}$.

(wild type: normalized pJNK abundance 1.01 ± 0.07 for vehicle-treated mice versus 0.71 ± 0.10 for SP-treated mice, $p < 0.01$, Mann-Whitney test; *TgUsp14CA*: 1.03 ± 0.08 for vehicle-treated mice versus 0.67 ± 0.19 for SP-treated mice, $p < 0.01$, Mann-Whitney test).

Although we found no difference between the gastrocnemius muscle masses of wild type mice treated with SP or vehicle alone, SP injections resulted in a significant increase in the gastrocnemius mass of *TgUsp14CA* mice (Fig. 7B). This effect was observed in both male and female *TgUsp14CA* mice but was not significant when male and female data were pooled because of the disparity in muscle hypertrophy between genders. We also observed a significant decrease in the abundance of *AChR- γ* mRNA in SP-treated *TgUsp14CA* mice compared to vehicle-treated *TgUsp14CA* mice (Fig. 7C). Although there was a significant upregulation of *AChR- γ* mRNA in SP-treated wild type mice compared to vehicle-treated controls, this effect cannot explain the decrease in *AChR- γ* transcript abundance observed in the *TgUsp14CA* mice. Because neuronal activity can promote muscle hypertrophy and *AChR* transcript abundance is inversely proportional to synaptic transmission, both the increase in muscle mass and the decrease in *AChR* transcript abundance observed in *TgUsp14CA* mice following JNK inhibition are consistent with improved presynaptic NMJ function.

When we compared locomotion while exploring a novel, open field, we found a significant decrease in distance traveled (Fig. 7D) and ambulatory velocity (Fig. 7E) in *TgUsp14CA* mice compared to wild type mice. However, SP-treated *TgUsp14CA* mice traveled as far and as fast as wild type mice in the open field (Fig. 7D and E). In the more demanding rotarod assay, the performance of the SP-treated *TgUsp14CA* mice was improved over vehicle-treated *TgUsp14CA* mice, but was still significantly worse than

wild type mice (Fig. 7F). We next used whole mount immunostaining to determine if the improvements in NMJ function observed in the *TgUsp14CA* mice following SP treatment were accompanied by improved NMJ structure. We found that, while the NMJs of SP-treated *TgUsp14CA* mice were still abnormal compared to wild type mice, there was an appreciable decrease in presynaptic swelling and an increase in endplate arborization compared to vehicle-treated *TgUsp14CA* mice (Fig. 7G).

Discussion

The purpose of this study was to determine whether USP14's catalytic activity is required for NMJ function and to investigate the effects of USP14 inhibition on proteasomal-dependent and -independent ubiquitin signaling in the nervous system. Indeed, our results demonstrate that USP14's ubiquitin hydrolase activity modulates NMJ development and synaptic transmission (Fig. 3 and 4) and regulates proteasomal-independent ubiquitin signaling (Fig. 5 and 6). We observed enhanced K63-linked ubiquitination of MLK3 and hyperactivation of its downstream kinase JNK in the spinal cords of mice expressing catalytically-inactive USP14 (Fig. 6), and JNK inhibition significantly improved both NMJ structure and motor function in these mice (Fig. 7), demonstrating that the regulation of pJNK by USP14 is critical to nervous system structure and function. In addition, we uncovered an ongoing need for USP14's DUB activity at adult NMJs by demonstrating that the synaptic transmission deficits in mice expressing USP14CA (Fig. 5) were replicated by acute inhibition of USP14 (Fig. 4).

USP14 Regulates Proteasome-Independent Ubiquitin Signaling

The increases in ubiquitin conjugates observed in the spinal cords of *TgUsp14CA* mice and in neuronal cultures when USP14 is pharmacologically inhibited (Supplemental Figure 3) mimic the effects on ubiquitin conjugates when the proteasome is inhibited (Ikeda & Dikic, 2008; Jacobson et al., 2009). However, the level of K48-linked ubiquitin conjugates was unchanged in spinal cords from *TgUsp14CA* mice compared to wild type mice and in cortical neurons with and without IU1 (Fig. 5A and B). Because K48-linked ubiquitin chains are a robust biomarker of ubiquitin proteasome system function (E. J. Bennett et al., 2007), and we found no difference in the catalytic capacity of *TgUsp14CA* and wild type proteasomes *in vitro* (Fig. 1G), it is unlikely that USP14 inhibition in the nervous system causes global alterations in proteasome activity. Instead, we observed an increase in K63-linked ubiquitin conjugates, which do not accumulate following proteasome inhibition (Ikeda & Dikic, 2008; Jacobson et al., 2009), in both *TgUsp14CA* spinal cords and IU1-treated cortical neurons (Fig. 5C and D), suggesting that USP14 disassembles non-proteasomal-targeting ubiquitin chains.

Expression of catalytically inactive USP14 in the nervous systems of *TgUsp14CA* mice led to enhanced K63-linked ubiquitination of MLK3 (Fig. 6A and B), which has previously been demonstrated to induce its dimerization, auto-phosphorylation, and ability to phosphorylate MKK4 (Humphrey et al., 2013). Consistent with this finding, we observed enhanced phosphorylation of MLK3 (Fig. 6A and B) and MKK4 (Fig. 6C and D), as well as MKK4's target JNK (Fig. 6E and F), in *TgUsp14CA* spinal cords. We also observed prominent pJNK immunoreactivity in the swollen terminals and within the ultra-terminal sprouts of *TgUsp14CA* motor neurons (Fig. 6G). In fact, treatment with the

JNK inhibitor SP600125 improved the muscle development (Fig. 7B), motor function (Fig. 7D-F), and NMJ structure (Fig. 7G) of the *TgUsp14CA* mice, even though we began administration of the drug after the neuromuscular phenotype was established (Fig. S2). More robust JNK inhibition or beginning JNK inhibitor treatment at an earlier age may have led to a more complete rescue of the *TgUsp14CA* phenotype. Alternatively, the JNK pathway may be one of multiple pathways that are regulated by USP14's catalytic activity. Support for the later explanation comes from studies of the *Drosophila highwire* (*hiw*) mutant, which has NMJ pathology and synaptic transmission deficits that are similar to what we observed in *TgUsp14CA* mice (Collins et al., 2006). Genetic inactivation of the JNK signaling cascade in the *hiw* mutants corrects their NMJ pathology, but their deficits in synaptic transmission persist.

USP14 Has an Ongoing Role in Synaptic Transmission

We observed decreased MEPC frequency, EPC amplitude, and quantal content at the NMJs of *TgUsp14CA* and *ax^J* mice (Fig. 3A-F). Surprisingly, these deficits were mimicked by acute inhibition of USP14 at the NMJs of adult, wild type mice (Fig. 4A-F), likely indicating that USP14 has an ongoing role in synaptic transmission and that the synaptic deficits in *TgUsp14CA* and *ax^J* mice do not arise from aberrant development. This conclusion is supported by the finding that intramuscular injections of IU1 were sufficient to cause alterations in AChR mRNA expression but did not alter NMJ structure (Fig. 4G-I), suggesting that the structural and functional deficits at the *TgUsp14CA* NMJs arise through different mechanisms. Because synaptic proteins are turned over very slowly *in vivo*, with an average turnover rate of 9 days (Zhang et al., 2011), and we found

no evidence of proteasome dysfunction in the Tg*Usp14CA* mice or in IU1-treated neurons, the rapid effects of IU1 on synaptic transmission are unlikely to result from altered protein turnover. Instead, the rapid effect of USP14 inhibition on MEPC frequency, the accumulation of K63-linked chains upon USP14 inhibition (Fig. 6), and the regulation of JNK phosphorylation by USP14 activity (Fig. 7E and F) all support a model in which USP14 dynamically deubiquitinates proteins to affect their activity and not their abundance.

Conclusion

In this study, we demonstrated that USP14's catalytic activity is required for NMJ structure and function, and provided evidence that USP14 regulates non-proteasomal ubiquitin signaling in the nervous system. Although our results are consistent with a recently published report demonstrating that USP14 removes K63-linked ubiquitin chains from Dvl2 (Jung et al., 2013), both studies raise the question of how a proteasome-associated DUB could disassemble proteasome-independent ubiquitin chains. Further study will be required to determine if proteasome-bound USP14 can interact with K63-linked ubiquitin chains or, alternatively, whether USP14's DUB activity can be stimulated by a novel binding partner, allowing it to be active when not bound to the proteasome. In either case, our findings demonstrate a novel role for USP14 and establish non-canonical ubiquitin signaling as an important contributor to both the long-term health of the nervous system and synaptic transmission.

Methods

Animals

C57BL/6J mice (wild type), *Usp14^{axJ}* mice (Jackson Laboratories, Bar Harbor, MA) Thy1-*YFP* mice (16JRS, Jackson Laboratories), transgenic mice expressing wild type USP14 (Tg*Usp14*) (Crimmins et al., 2006), and transgenic mice expressing catalytically inactive USP14 (Tg*Usp14CA*) have been maintained in our breeding colony at the University of Alabama at Birmingham, which is fully accredited by the Association for Assessment and Accreditation of Laboratory Animal Care International. All mouse lines were maintained on a C57BL/6J background. Homozygous *Usp14^{axJ}* mice (which we refer to as *ax^J* mice) were generated by intercrossing heterozygous *ax^J* siblings. Research was conducted without bias toward the sex of animals used for each study, and male and female mice were used equally. All research complied with the United States Animal Welfare Act and other federal statutes and regulations relating to animals and experiments involving animals and adhered to principles stated in the Guide for the Care and Use of Laboratory Animals, United States National Research Council.

Construction of TgUsp14CA Transgene

The full-length *Usp14* cDNA, including the *Usp14* Kozak consensus sequence, was generated by using reverse transcription-PCR (RT-PCR). USP14's active site cysteine (C114) was replaced with an alanine residue via PCR site-directed mutagenesis. The cDNA was cloned into the *XhoI* site of the *pThy1.2* expression cassette (gift from Dr. Pico Caroni at the Friedrich Institute, Basel, Switzerland). The transgene was excised from the vector by using *EcoRI* and *NdeI* and prepared for microinjection via standard

procedures.

RNA Transcriptome Analysis

Total RNA was isolated from hippocampal lysates of 4-week-old wild type and TgUSP14CA mice using RNA-STAT60 (Tel-Test, Friendswood, TX). Poly(A) RNAs were subsequently purified using an RNeasy Mini Kit (Qiagen, Valencia, CA). cDNAs were generated and paired-end sequencing was performed at Hudson Alpha (Huntsville, AL).

Neuronal Culture

Dissociated cortical cultures were prepared as described (Moore et al., 2007). Cultured neurons were treated with the USP14 inhibitor IU1 (20 μ M) or an equivalent volume of vehicle (DMSO) at 10 to 11 days *in vitro*, and protein or mRNA was harvested 24 h later as described below.

Isolation of Proteins

Mice 4- to 6- weeks of age were deeply anesthetized via isoflurane prior to rapid decapitation. Tissues were removed and homogenized in 1 to 3 mL of buffer containing 50 mM Tris, 150 mM NaCl, 5 mM MgCl₂, 2mM N-ethylmaleimide, 0.5% SDS, Complete protease inhibitors (Roche, Indianapolis, IN) and phosphatase inhibitor cocktail I (Sigma Aldrich, St. Louis, MO), pH 7.5. PR-619 (Life Sensors, Malvern, PA) was added to a final concentration of 50 μ M to inhibit a wide range of DUBs. After homogenization, tissues were centrifuged at 17,000 x g for 10 min at 4°C, and

supernatants were removed and immediately frozen at -80°C . Protein concentrations were determined by using the bicinchoninic acid (BCA) protein assay kit from Pierce (Rockford, IL).

Isolation of Proteasomes and Assays of Proteasome Activity

Proteasomes were isolated and assayed as described (Anderson et al., 2005).

Immunoblotting

Protein electrophoresis and blotting was performed as described (Chen et al., 2011). Immunoblots probed for ubiquitin were pretreated with 0.1% glutaraldehyde for 20 min prior to blocking.

Immunoprecipitation

Proteins were isolated as described above in a modified RIPA buffer containing 0.5% SDS and heated to 95°C for 5 min. Protein lysates were diluted 1:10 in a buffer containing 25 mM Tris and 150 mM NaCl with a pH of 7.2 and incubated with 10 μg of MLK3 antibody overnight at 4°C with constant agitation. The antibody/antigen complex was added to 100 μL of Immobilized Protein A/G resin slurry (Thermo Scientific, Waltham, MA) and incubated with constant agitation at 4°C for 6 hours. Immunoprecipitates were collected by centrifugation according to manufacturer instructions.

Antibodies

The following antibodies were used: USP14 (Anderson et al., 2005); β -tubulin (Developmental Studies Hybridoma Bank, Iowa City, IA); Rpt1 and MLK3 (Santa Cruz Biotechnologies, Dallas, TX); Ubiquitin (UAB Hybridoma Facility, Birmingham, AL), K48 Ubiquitin and K63 Ubiquitin (Millipore, Billerica, MA); pMKK4, MKK4, pJNK, and JNK (Cell Signaling Technology, Danvers, Massachusetts).

Quantitation of Immunoblots.

Blots were quantitated using ImageJ software (NIH, Bethesda, MD). Each value represents the average and standard error from at least two blots using at least three different animals of each genotype.

Labeling of Proteasome-Associated DUBs

Activity of proteasomal DUBs was assayed as previously described (Crimmins et al., 2006).

Immunocytochemistry (ICC)

ICC of PFA-fixed brain sections was performed as described previously (King et al., 2011). Briefly, following perfusion with Tyrode's solution and 4% PFA, serial coronal sections of brain (50 μ m) were prepared, and free-floating immunohistochemistry was performed. Spinal cords were paraffin embedded. USP14 was detected using Alexa Fluor anti-rabbit 594 antibody (Invitrogen, Carlsbad, CA). Sections were washed in PBST containing DAPI (Invitrogen) to detect nuclei. Free-floating sections were

mounted on gelatinized slides and dehydrated in graded ethanol and xylenes. Coverslips for all sections were secured in Prolong-gold anti-fade mounting media (Invitrogen). TUNEL staining was performed using the Roche TUNEL labeling kit per manufacturer instructions (Roche Diagnostics Corporation, Indianapolis, IN).

Grip Strength Test

Forelimb grip strength was determined using an animal grip strength system (SDI, San Diego, CA). Each trial consisted of five repetitions of this assay ($n > 5$ mice per genotype per time point).

Elevated Beam Assay

Ability to traverse an elevated beam 2 cm in diameter was assessed as previously described (Crimmins et al., 2006), $n > 5$ mice per genotype per time point.

Rotarod Assay

Motor coordination was tested by placing mice on a rotating rod (ENV-575, Med Associates, St. Albans, VT), which accelerated from 3.5 rpm to 35 rpm over a 5-min period. Latency to fall was recorded over 3 trials, each separated by 1 h, and the individual trials for each animal were averaged.

Open Field Assay.

Animals were handled 1 day prior to open field testing. Locomotor activity was measured in an open field chamber (43.2 cm x 43.2 cm x 30.5 cm) for 15 min by an

automated video tracking system. The first 5 min were not analyzed to account for habituation to the chamber.

NMJ Immunostaining and Confocal Imaging

Whole mount immunostaining of the tibialis anterior (TA) muscle was performed as described (Chen et al., 2009), with minor modifications. The TA muscle was immersed in ice-cold PBS containing 2% PFA for 1 h following dissection and immediately teased into thin bundles. Muscle bundles were then transferred to PBS containing 1% PFA and 1% Triton and permeabilized overnight at 4°C with constant rocking. To improve visualization of axons and ultra-terminal sprouting, all mice used for NMJ immunostaining carried the *Thy1-YFP* transgene in addition to the transgene(s) of interest. For pJNK immunostaining, muscle bundles were incubated with primary antibody (pJNK, #81E11, Cell Signaling Technology, Danvers, MA) for 5 days at 4°C with constant rocking. Images were captured using a Zeiss LSM 510 Meta confocal microscope (Carl Zeiss, Oberkochen, Germany).

Quantitative PCR

RNA isolation and quantitative PCR (qPCR) were performed as described (Chen et al., 2009). Individual gene assay kits were purchased from Applied Biosystems for each of the RNAs analyzed. n = at least 3 animals per genotype per time point run in triplicate.

Electrophysiology

Two-electrode voltage clamp was performed as described (Chen et al., 2011). Diaphragms, with ribs and intact phrenic nerves, were dissected from 5- to 6-week-old mice. All experiments were performed at room temperature. For experiments using IU1, measurements were taken in the presence of vehicle alone prior to the introduction of 20 μ M IU1 into the perfusing solution.

Intramuscular Injections of IU1

Adult mice (12- to 14-weeks old) were lightly anesthetized with isoflurane for injections into the gastrocnemius muscle. Injections (100 μ L) contained IU1 (100 μ M) or vehicle with 0.1% India blue ink, to ensure correct injection location, and 0.05 mg/kg RIMADYL (Pfizer, New York City, NY), to reduce discomfort, in sterile PBS. Each animal ($n = 3$) received vehicle injection and IU1 injection into the left and right gastrocnemius muscles, respectively.

Intraperitoneal Injections of SP600125

3-week-old wild type and TgUsp14CA mice were given daily intraperitoneal injections of the JNK inhibitor SP600125 (Fisher Scientific, Rockford, IL) for two weeks. SP600125 was dissolved in DMSO at a concentration of 91 mM and this solution was directly administered at a dose of 16 mg/kg using a 25 μ L Hamilton syringe (Hamilton Company, Reno, NV). This procedure was used to minimize the injection volume, as SP600125 is not soluble in aqueous solutions and DMSO was not tolerated at higher doses. Animals were weighed every other day to adjust doses and to monitor potential

adverse effects of the injections. At the doses given, both DMSO and SP600125 were well tolerated.

References

- Anderson, C., Crimmins, S., Wilson, J. A., Korbel, G. A., Ploegh, H. L., & Wilson, S. M. (2005). Loss of Usp14 results in reduced levels of ubiquitin in ataxia mice. *J Neurochem*, 95(3), 724-731. doi: 10.1111/j.1471-4159.2005.03409.x
- Bennett, B. L., Sasaki, D. T., Murray, B. W., O'Leary, E. C., Sakata, S. T., Xu, W., . . . Anderson, D. W. (2001). SP600125, an anthrapyrazolone inhibitor of Jun N-terminal kinase. *Proc Natl Acad Sci U S A*, 98(24), 13681-13686. doi: 10.1073/pnas.251194298
- Bennett, E. J., Shaler, T. A., Woodman, B., Ryu, K. Y., Zaitseva, T. S., Becker, C. H., . . . Kopito, R. R. (2007). Global changes to the ubiquitin system in Huntington's disease. *Nature*, 448(7154), 704-708. doi: 10.1038/nature06022
- Borodovsky, A., Kessler, B. M., Casagrande, R., Overkleeft, H. S., Wilkinson, K. D., & Ploegh, H. L. (2001). A novel active site-directed probe specific for deubiquitylating enzymes reveals proteasome association of USP14. *Embo J*, 20(18), 5187-5196. doi: 10.1093/emboj/20.18.5187
- Chen, P. C., Bhattacharyya, B. J., Hanna, J., Minkel, H., Wilson, J. A., Finley, D., . . . Wilson, S. M. (2011). Ubiquitin homeostasis is critical for synaptic development and function. *J Neurosci*, 31(48), 17505-17513.
- Chen, P. C., Qin, L. N., Li, X. M., Walters, B. J., Wilson, J. A., Mei, L., & Wilson, S. M. (2009). The proteasome-associated deubiquitinating enzyme Usp14 is essential for the maintenance of synaptic ubiquitin levels and the development of neuromuscular junctions. *J Neurosci*, 29(35), 10909-10919.
- Collins, C. A., Wairkar, Y. P., Johnson, S. L., & DiAntonio, A. (2006). Highwire restrains synaptic growth by attenuating a MAP kinase signal. *Neuron*, 51(1), 57-69. doi: 10.1016/j.neuron.2006.05.026
- Costello, D. A., & Herron, C. E. (2004). The role of c-Jun N-terminal kinase in the A beta-mediated impairment of LTP and regulation of synaptic transmission in the hippocampus. *Neuropharmacology*, 46(5), 655-662. doi: 10.1016/j.neuropharm.2003.11.016
- Crimmins, S., Jin, Y., Wheeler, C., Huffman, A. K., Chapman, C., Dobrunz, L. E., . . . Wilson, S. M. (2006). Transgenic rescue of ataxia mice with neuronal-specific expression of ubiquitin-specific protease 14. *J Neurosci*, 26(44), 11423-11431.
- D'Arcy, P., Brnjic, S., Olofsson, M. H., Fryknas, M., Lindsten, K., De Cesare, M., . . . Linder, S. (2011). Inhibition of proteasome deubiquitinating activity as a new cancer therapy. *Nat Med*, 17(12), 1636-1640. doi: 10.1038/nm.2536

- Drerup, C. M., & Nechiporuk, A. V. (2013). JNK-interacting protein 3 mediates the retrograde transport of activated c-Jun N-terminal kinase and lysosomes. *PLoS Genet*, 9(2), e1003303. doi: 10.1371/journal.pgen.1003303
- Hanna, J., Hathaway, N. A., Tone, Y., Crosas, B., Elsassner, S., Kirkpatrick, D. S., . . . Finley, D. (2006). Deubiquitinating enzyme Ubp6 functions noncatalytically to delay proteasomal degradation. *Cell*, 127(1), 99-111. doi: 10.1016/j.cell.2006.07.038
- Humphrey, R. K., Yu, S. M., Bellary, A., Gonuguntla, S., Yebra, M., & Jhala, U. S. (2013). Lysine 63-linked ubiquitination modulates mixed lineage kinase-3 interaction with JIP1 scaffold protein in cytokine-induced pancreatic beta cell death. *J Biol Chem*, 288(4), 2428-2440. doi: 10.1074/jbc.M112.425884
- Hyrskyluoto, A., Bruelle, C., Lundh, S. H., Do, H. T., Kivinen, J., Rappou, E., . . . Korhonen, L. (2014). Ubiquitin-specific protease-14 reduces cellular aggregates and protects against mutant huntingtin-induced cell degeneration: involvement of the proteasome and ER stress-activated kinase IRE1alpha. *Hum Mol Genet*. doi: 10.1093/hmg/ddu317
- Ikeda, F., & Dikic, I. (2008). Atypical ubiquitin chains: new molecular signals. 'Protein Modifications: Beyond the Usual Suspects' review series. *EMBO Rep*, 9(6), 536-542. doi: 10.1038/embor.2008.93
- Jacobson, A. D., Zhang, N. Y., Xu, P., Han, K. J., Noone, S., Peng, J., & Liu, C. W. (2009). The lysine 48 and lysine 63 ubiquitin conjugates are processed differently by the 26 s proteasome. *J Biol Chem*, 284(51), 35485-35494. doi: 10.1074/jbc.M109.052928
- Jung, H., Kim, B. G., Han, W. H., Lee, J. H., Cho, J. Y., Park, W. S., . . . Jho, E. H. (2013). Deubiquitination of Dishevelled by Usp14 is required for Wnt signaling. *Oncogenesis*, 2, e64. doi: 10.1038/oncsis.2013.28
- King, G. D., Muhammad, A. K., Larocque, D., Kelson, K. R., Xiong, W., Liu, C., . . . Lowenstein, P. R. (2011). Combined Flt3L/TK gene therapy induces immunological surveillance which mediates an immune response against a surrogate brain tumor neoantigen. *Mol Ther*, 19(10), 1793-1801. doi: 10.1038/mt.2011.77
- Kraut, D. A., Prakash, S., & Matouschek, A. (2007). To degrade or release: ubiquitin-chain remodeling. *Trends Cell Biol*, 17(9), 419-421. doi: 10.1016/j.tcb.2007.06.008
- Kravtsova-Ivantsiv, Y., Sommer, T., & Ciechanover, A. (2012). The Lysine48-Based Polyubiquitin Chain Proteasomal Signal: Not a Single Child Anymore. *Angew*

- Kues, W. A., Brenner, H. R., Sakmann, B., & Witzemann, V. (1995). Local neurotrophic repression of gene transcripts encoding fetal AChRs at rat neuromuscular synapses. *J Cell Biol*, 130(4), 949-957.
- Lappe-Siefke, C., Loebrich, S., Hevers, W., Waidmann, O. B., Schweizer, M., Fehr, S., . . . Kneussel, M. (2009). The ataxia (axJ) mutation causes abnormal GABAA receptor turnover in mice. *PLoS Genet*, 5(9), e1000631.
- Lauwers, E., Jacob, C., & Andre, B. (2009). K63-linked ubiquitin chains as a specific signal for protein sorting into the multivesicular body pathway. *J Cell Biol*, 185(3), 493-502. doi: 10.1083/jcb.200810114
- Lee, B. H., Finley, D., & King, R. W. (2012). A High-Throughput Screening Method for Identification of Inhibitors of the Deubiquitinating Enzyme USP14. *Curr Protoc Chem Biol*, 4(4), 311-330. doi: 10.1002/9780470559277.ch120078
- Lee, B. H., Lee, M. J., Park, S., Oh, D. C., Elsasser, S., Chen, P. C., . . . Finley, D. (2010). Enhancement of proteasome activity by a small-molecule inhibitor of USP14. *Nature*, 467(7312), 179-184.
- Lee, M. J., Lee, B. H., Hanna, J., King, R. W., & Finley, D. (2010). Trimming of ubiquitin chains by proteasome-associated deubiquitinating enzymes. *Mol Cell Proteomics*, 10(5), R110 003871.
- Liu, N., Li, X., Huang, H., Zhao, C., Liao, S., Yang, C., . . . Liu, J. (2014). Clinically used antirheumatic agent auranofin is a proteasomal deubiquitinase inhibitor and inhibits tumor growth. *Oncotarget*, 5(14), 5453-5471.
- Michler, A., & Sakmann, B. (1980). Receptor stability and channel conversion in the subsynaptic membrane of the developing mammalian neuromuscular junction. *Dev Biol*, 80(1), 1-17.
- Moore, C. D., Thacker, E. E., Larimore, J., Gaston, D., Underwood, A., Kearns, B., . . . Theibert, A. (2007). The neuronal Arf GAP centaurin alpha1 modulates dendritic differentiation. *J Cell Sci*, 120(Pt 15), 2683-2693. doi: 10.1242/jcs.006346
- Peth, A., Besche, H. C., & Goldberg, A. L. (2009). Ubiquitinated proteins activate the proteasome by binding to Usp14/Ubp6, which causes 20S gate opening. *Mol Cell*, 36(5), 794-804.
- Schmukle, A. C., & Walczak, H. (2012). No one can whistle a symphony alone - how different ubiquitin linkages cooperate to orchestrate NF-kappaB activity. *J Cell Sci*, 125(Pt 3), 549-559. doi: 10.1242/jcs.091793

- Tian, Z., D'Arcy, P., Wang, X., Ray, A., Tai, Y. T., Hu, Y., . . . Anderson, K. C. (2014). A novel small molecule inhibitor of deubiquitylating enzyme USP14 and UCHL5 induces apoptosis in multiple myeloma and overcomes bortezomib resistance. *Blood*, 123(5), 706-716. doi: 10.1182/blood-2013-05-500033
- Welchman, R. L., Gordon, C., & Mayer, R. J. (2005). Ubiquitin and ubiquitin-like proteins as multifunctional signals. *Nat Rev Mol Cell Biol*, 6(8), 599-609. doi: 10.1038/nrm1700
- Wilson, S. M., Bhattacharyya, B., Rachel, R. A., Coppola, V., Tessarollo, L., Householder, D. B., . . . Jenkins, N. A. (2002). Synaptic defects in ataxia mice result from a mutation in Usp14, encoding a ubiquitin-specific protease. *Nat Genet*, 32(3), 420-425.
- Wu, N., Zhang, C., Bai, C., Han, Y. P., & Li, Q. (2014). MiR-4782-3p inhibited non-small cell lung cancer growth via USP14. *Cell Physiol Biochem*, 33(2), 457-467. doi: 10.1159/000358626
- Xu, P., Duong, D. M., Seyfried, N. T., Cheng, D., Xie, Y., Robert, J., . . . Peng, J. (2009). Quantitative proteomics reveals the function of unconventional ubiquitin chains in proteasomal degradation. *Cell*, 137(1), 133-145. doi: 10.1016/j.cell.2009.01.041
- Zhang, Y., Reckow, S., Webhofer, C., Boehme, M., Gormanns, P., Egge-Jacobsen, W. M., & Turck, C. W. (2011). Proteome scale turnover analysis in live animals using stable isotope metabolic labeling. *Anal Chem*, 83(5), 1665-1672. doi: 10.1021/ac102755n
- Zhou, A. Y., Shen, R. R., Kim, E., Lock, Y. J., Xu, M., Chen, Z. J., & Hahn, W. C. (2013). IKKepsilon-Mediated Tumorigenesis Requires K63-Linked Polyubiquitination by a cIAP1/cIAP2/TRAF2 E3 Ubiquitin Ligase Complex. *Cell Rep*. doi: 10.1016/j.celrep.2013.01.031

DISTINCT EFFECTS OF UBIQUITIN OVEREXPRESSION ON NMJ STRUCTURE
AND MOTOR PERFORMANCE IN MICE EXPRESSING CATALYTICALLY
INACTIVE USP14

by

JADA H. VADEN, JENNIFER A. WATSON, ALAN D. HOWARD,
PING-CHUNG-CHEN, JULIE A. WILSON, AND SCOTT M. WILSON

Submitted to *Frontiers in Molecular Neuroscience*

Format adapted for dissertation

Abstract

Ubiquitin-specific protease 14 (USP14) is a major deubiquitinating enzyme and a key determinant of neuromuscular junction (NMJ) structure and function. We have previously reported dramatic ubiquitin depletion in the nervous systems of the USP14-deficient *ataxia* (ax^J) mice and demonstrated that transgenic ubiquitin overexpression partially rescues the ax^J neuromuscular phenotype. However, ubiquitin overexpression does not correct the ax^J deficits in hippocampal short term plasticity, and transgenic expression of a catalytically-inactive form of USP14 in the nervous system mimics the neuromuscular phenotype observed in the ax^J mice, but causes only a modest reduction of free ubiquitin. In this report, we demonstrate that restoring free ubiquitin levels in the USP14 catalytic mutant mice improved NMJ structure and reduced pJNK immunofluorescence at the NMJ, but had a negative impact on measures of NMJ function, such as motor performance and muscle development. Transgenic expression of ubiquitin had a dose-dependent effect on NMJ function in wild type mice: moderate levels of overexpression improved NMJ function while more robust ubiquitin overexpression reduced muscle development and motor coordination. Combined, these results suggest that maintenance of free ubiquitin levels by USP14 contributes to NMJ structure, but that USP14 also regulates NMJ function through a separate pathway.

Key words: neuromuscular junction, ubiquitin, USP14, pJNK, proteasomes, motor neuron and deubiquitinating enzyme

Non-standard abbreviations: TgCA (transgene expressing catalytically inactive USP14, generated by mutating the active site cysteine to an alanine residue, expressed under the neuronal *Thy1.2* promoter; also refers to mice expressing this transgene), TgUb

(transgene expressing ubiquitin under the *Thy1.2* promoter; also refers to mice expressing this transgene), *TgUb-H* (a transgenic line with more robust ubiquitin overexpression than *TgUb*), *TgCA,TgUb* (mice expressing both *TgCA* and *TgUb*).

Introduction

Ubiquitination can regulate a diverse array of cellular pathways depending on the number of ubiquitin monomers conjugated onto a protein and the way those monomers are linked. These pathways regulate protein stability (Hershko & Ciechanover, 1998), activity (Humphrey et al., 2013; Schmukle & Walczak, 2012; Zhou et al., 2013), and localization (Tanno & Komada, 2013). The accumulation of ubiquitin-positive aggregates is a hallmark of neurodegenerative diseases (Jara, Frank, & Ozdinler, 2013; Lowe et al., 1988; Perry, Friedman, Shaw, & Chau, 1987), suggesting that sequestration of ubiquitin, and the consequent reduction of ubiquitin availability, causes neuronal dysfunction. This suggestion is supported by the hypothalamic dysfunction and neurodegeneration observed in mice lacking the ubiquitin gene *Ubb* (Ryu, Garza, Lu, Barsh, & Kopito, 2008).

Although ubiquitin is encoded by four genes in the mammalian genome (Baker & Board, 1987, 1991; Finley, Bartel, & Varshavsky, 1989; Lund et al., 1985; Redman & Rechsteiner, 1989; Wiborg et al., 1985), the equilibrium between ubiquitin conjugated onto proteins and free ubiquitin is largely controlled by the opposing actions of ubiquitin ligases and deubiquitinating enzymes (DUBs) (Hallengren, Chen, & Wilson, 2013). We have previously shown that loss of the proteasome-associated DUB USP14 in the *ataxia*

(ax^J) mice severely hampers ubiquitin homeostasis by causing a dramatic depletion of free ubiquitin in the brain and spinal cord (Anderson et al., 2005; Chen et al., 2009). In fact, neuronal-specific transgenic expression of ubiquitin corrects the reduced muscle development, altered NMJ structure, reduced synaptic transmission, and perinatal lethality observed in the ax^J mice (Chen et al., 2011). Although these findings suggest a role for USP14 in the maintenance of free ubiquitin pools in the nervous system, later work showed ubiquitin complementation does not rescue the deficits in hippocampal short-term plasticity observed in the ax^J mice (Walters et al., 2014).

Furthermore, we recently reported that transgenic expression of a dominant-negative, catalytically-inactive USP14 species in the murine nervous system recreates many of the phenotypes observed when USP14 is lost in the ax^J mice, including altered NMJ structure and reduced muscle development (Vaden et al., 2015). In contrast to the ax^J mice, however, the USP14 catalytic mutant mice have a normal lifespan and only a modest decrease in free ubiquitin. Instead, the spinal cords of the USP14 catalytic mutant mice show an increase in levels of ubiquitin conjugates linked through lysine 63 (K63), which are known to promote kinase activation (Humphrey et al., 2013; Yang, Wu, Wu, & Lin, 2010). Consistent with this finding, the USP14 catalytic mutant mice have increased activation of the ubiquitin-dependent mixed lineage kinase 3 (MLK3) pathway, which signals through c-Jun N-terminal kinase (JNK) (Vaden et al., 2015). As expected from the well-documented role of pJNK in rearranging synaptic architecture in invertebrates (Collins, Wairkar, Johnson, & DiAntonio, 2006; Drerup & Nechiporuk, 2013; Etter et al., 2005), *in vivo* inhibition of JNK significantly improved NMJ structure and muscle development in the USP14 catalytic mutant mice (Vaden et al., 2015).

These findings led us to hypothesize that, in addition to maintaining ubiquitin homeostasis, USP14's catalytic activity is required for the termination of ubiquitin signaling cascades and, consequently, that the increase in ubiquitin conjugates observed in the spinal cords of the USP14 catalytic mutant mice can alter neuronal function independent of the reduction of free ubiquitin. To directly test this hypothesis, we generated mice expressing both catalytically inactive USP14 (TgCA) and ubiquitin (TgUb) under the neuronal *Thy1.2* promoter. The spinal cords of the resulting TgCA, TgUb mice had control levels of free ubiquitin and a nearly 2-fold increase in ubiquitin conjugates. The motor performance and muscle development of the double transgenic TgCA,TgUb mice were reduced compared to both TgCA mice and controls, underlining the need for USP14-dependent deubiquitination events in the nervous system. However, despite the detrimental effects of ubiquitin complementation on the overall phenotype of the TgCA mice, the structure of the NMJ was improved, and the amount of pJNK-positive pathology was decreased, in the TgCA,TgUb mice compared to TgCA mice,. Additionally, we found that overexpression of ubiquitin had a bidirectional, dose-dependent effect on muscle mass, motor function, and measures of synaptic transmission even in wild type mice where USP14's activity was intact. These data suggest that ubiquitin complementation in *ax^J* mice indirectly corrects the functional deficits caused by loss of USP14 and demonstrate that increased protein ubiquitination alters motor function.

Results

Loss of USP14's DUB Activity Increases Ubiquitin Conjugates

To assess the impact of USP14 on cellular ubiquitin pools, we performed immunoblot analysis on spinal cord extracts from wild type, TgCA, and *ax^J* mice (Fig. 1A). Tg*Usp14* mice, which overexpress wild type USP14 in the nervous system (Crimmins et al., 2006), were included as a control. As previously reported (Anderson et al., 2005; Chen et al., 2009), loss of USP14 in the *ax^J* mice resulted in significant decreases in free ubiquitin levels, whereas neuronal expression of catalytically inactive USP14 in the TgCA mice led to only a modest reduction in free ubiquitin levels (Fig. 1A, C). Instead, loss of USP14's catalytic activity led to the retention of more proteins in a ubiquitinated state, as indicated by the increase in ubiquitin conjugates observed in the spinal cords of TgCA mice compared to controls (Fig. 1A, B). We also observed both an increase in free ubiquitin and a reduction in ubiquitin conjugates in the spinal cords of the mice overexpressing wild type USP14 (Tg*Usp14*), suggesting that USP14's DUB activity makes a significant contribution to protein deubiquitination.

Proteomic screening indicates that, within the cellular ubiquitin pool, 40% of ubiquitin is conjugated and 60% is in a free, monomeric form (Kaiser et al., 2011). Therefore, an estimate of cellular ubiquitin levels can be obtained by multiplying the relative levels of conjugated and monomeric ubiquitin by 0.4 and 0.6, respectively. The overall ubiquitin level remains similar to wild type levels when USP14 is overexpressed or when its ubiquitin hydrolase activity is lost (Fig. 1D); however, these manipulations

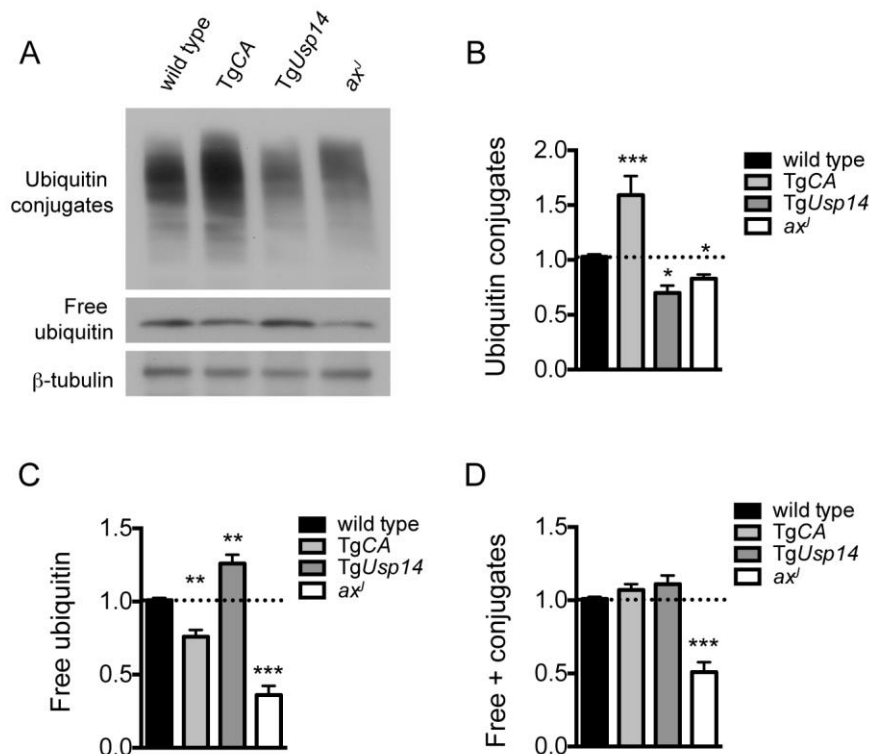


Figure 1. Analysis of USP14 mutations on neuronal ubiquitin pools. (A) Representative immunoblot of spinal cord lysates taken from 4-week-old wild type, TgCA, TgUsp14, and ax^J mice, probed for ubiquitin. β-tubulin was used as a loading control. (B-D) Quantitation of ubiquitin conjugates, free ubiquitin, and total ubiquitin pool in spinal cord lysates. Data were normalized to wild type levels and are shown as mean ± SEM. Free + conjugates is the sum of the relative levels of free ubiquitin x 0.6 and ubiquitin conjugates x 0.4 from reports that free ubiquitin and ubiquitin conjugates represent 40% and 60% of the total ubiquitin pool, respectively (Kaiser et al., 2011). In all cases, a one-way ANOVA revealed a significant effect of genotype (p<0.0001). Symbols represent unpaired t-tests compared against wild type and corrected for multiple comparisons with a Bonferonni adjustment, where *p<0.05, **p<0.01, ***p<0.001. n = at least 3 animals per genotype, run in duplicate.

shift the monomeric ubiquitin/conjugated ubiquitin balance in opposite directions (Fig. 1B, C). The increase in ubiquitin conjugates in TgCA mice corresponds to a decrease in monomeric ubiquitin, and the reciprocal is true in TgUsp14 mice. In contrast, the overall level of cellular ubiquitin is drastically decreased in *ax^J* mice compared to wild type mice (Fig. 1D).

Neuronal-Specific Overexpression of Ubiquitin is Detrimental to TgCA Mice

To test the hypothesis that increased ubiquitin conjugates, and not depletion of free ubiquitin, cause the motor neuron dysfunction in TgCA mice, we restored free ubiquitin levels in the TgCA mice by generating double transgenic mice expressing both TgUb and TgCA under the neuronal *Thy1.2* promoter. The resulting TgCA,TgUb mice expressed wild type levels of free ubiquitin as well as the increased ubiquitin conjugates that were observed in the TgCA mice (Fig. 2A, B, C). Consistent with our previous report (Vaden et al., 2015), there was no difference in body mass between 4-week-old TgCA mice and controls (Fig. 2D), but there was a significant reduction in the mass of the gastrocnemius muscles in the TgCA mice compared to controls (Fig. 2E). While transgenic expression of ubiquitin increased body and muscle mass in the *ax^J* mice (Chen et al., 2011), both parameters were significantly reduced in the TgCA,TgUb mice compared to both control and TgCA mice (Figs. 2D and E). Furthermore, whereas rotarod performance in *ax^J*TgUb mice is improved over *ax^J* mice (Chen et al., 2011), the TgCA,TgUb mice did not perform better than TgCA mice in this assay (Fig. 2F). In fact, when we measured motor function in the less demanding open field assay, the TgCA,TgUb mice showed reduced ambulatory distance (Fig. 2G) and velocity (Fig. 2H)

See figure on previous page.

Figure 2. Ubiquitin complementation does not rescue muscle mass or motor deficits in TgCA mice. (A) Representative immunoblots of ubiquitin and USP14 from spinal cords of 4-week-old wild type; *TgCA*; *TgCA,TgUb*; and *TgUb* mice. β -tubulin was used as a loading control. Relative levels of ubiquitin conjugates and free ubiquitin, normalized to wild type levels, are quantitated in (B) and (C), respectively. (D) Body mass and (E) gastrocnemius muscle mass of 4-week-old mice. $n =$ at least 12 animals per genotype. (F) Latency to fall from beam during a rotarod assay. (G) Total ambulatory distance and (H) velocity during 10 min open field assay. For (F)- (H), $n =$ at least 5 animals per genotype. All data are shown as mean \pm SEM. In all cases, a one-way ANOVA revealed a significant effect of genotype. Symbols represent unpaired T-tests compared against wild type and corrected for multiple comparisons with a Bonferonni adjustment, where * $p < 0.05$, ** $p < 0.01$, *** $p < 0.001$. In (B) and (C), an additional unpaired T-test with Bonferonni adjustment was used to compare *TgCA* and *TgCA,TgUb* mice.

compared to both wild type and TgCA mice. In contrast, ubiquitin overexpression alone, in TgUb mice, caused increased body and gastrocnemius mass (Figs. 2D and E) and ambulatory distance in the open field assay (Fig. 2G) compared to controls.

The transcription of muscle AChR transcripts is dramatically increased by manipulations, such as denervation and nerve block, that decrease synaptic transmission (Kues, Brenner, Sakmann, & Witzemann, 1995). We have previously shown that deficits in motor function and NMJ synaptic transmission are inversely related to muscle *AChR* transcript levels, and, in particular, that expression of the fetal *AChR*- γ subunit is dramatically increased in adult animals with motor and synaptic deficits (Chen et al., 2011; Chen et al., 2009; Vaden et al., 2015). In 4-week-old USP14-deficient *ax^J* mice, transgenic ubiquitin overexpression corrects deficits in mEPC frequency at the NMJ and also normalizes muscle *AChR* transcript levels (Chen et al., 2011), suggesting that *AChR* transcript abundance can act as a surrogate measure of synaptic transmission. We therefore compared *AChR* transcript levels in gastrocnemius muscles taken from wild type; TgCA; TgCA,TgUb; and TgUb mice at 4 to 6 weeks of age, the same time period over which the rotarod and open field assays were conducted, and found a significant effect of genotype on *AChR*- α , - ϵ , and - γ transcript expression.

As predicted by their poor open field performance, *AChR*- α , - ϵ , and - γ transcripts were significantly increased in TgCA,TgUb mice over all other genotypes, including TgCA (Fig. 3A, B, C). Finally, there was a significant decrease in *AChR*- γ transcripts in TgUb mice compared to controls (Fig. 3C), and a trend towards decreased *AChR*- α and - ϵ transcripts (Figs. 3A, B). Together with our previous report, these data demonstrate that

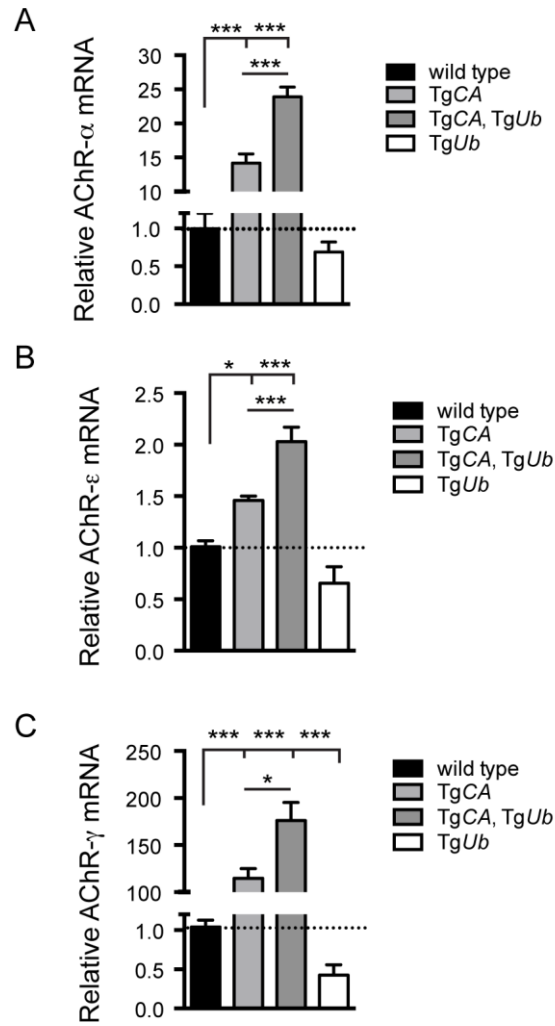


Figure 3. Effects of ubiquitin overexpression on AChR transcript levels in TgCA mice. qPCR analysis of *AChR* (A) - α , (B) - ϵ , and (C) - γ subunit mRNA abundance in 4-week-old wild type; *TgCA*; *TgCA,TgUb*;; and *TgUb* mice expressed as relative fold change from wild type. n = at least 3 animals per genotype, run in triplicate. Data are shown as mean \pm SEM. In all cases, a one-way ANOVA revealed a significant effect of genotype ($p < 0.0001$). Symbols represent unpaired T-tests corrected for multiple comparisons with a Bonferonni adjustment where * $p < 0.05$, ** $p < 0.01$, *** $p < 0.001$.

increased ubiquitin expression in the presence of catalytically inactive USP14 (in the TgCA,TgUb mice) has drastically different effects than when USP14 is reduced (ax^J TgUb mice). Because ubiquitin overexpression (TgUb mice) and genetic inactivation of USP14 (TgCA mice) had opposite effects on motor performance, gastrocnemius mass, and muscle AChR transcript levels, the deleterious effects of ubiquitin complementation in TgCA,TgUb mice cannot be ascribed to independent, additive, effects of the two transgenes. Instead, the beneficial effects of ubiquitin overexpression seem to be blocked by catalytically inactive USP14, which causes increased ubiquitin to become harmful.

Ubiquitin has a Dose-Dependent Effect on Motor Function

Loss of USP14's catalytic activity leads to a greater increase in ubiquitin conjugates in TgCA,TgUb spinal cords than ubiquitin overexpression alone causes in the spinal cords of TgUb mice. To determine whether this increase in protein ubiquitination could contribute to the severe motor phenotype observed in TgCA,TgUb mice, we compared muscle mass, AChR expression, and rotarod performance in the TgUb mice used in previous experiments with another transgenic founder line (TgUb-High) that has higher levels of ubiquitin expression (Fig. 4A, B, C). The gastrocnemius muscles of 4- to 6-week-old female TgUb mice were significantly larger than those of controls (Fig. 4D). In contrast, the increased ubiquitin expression in the TgUb-H mice resulted in significantly decreased gastrocnemius mass compared to controls (Fig. 4D). The same was true for male wild type, TgUb, and TgUb-High mice (data not shown). Further, we found that TgUb-H mice had a significant increase in the abundance of fetal AChR- γ

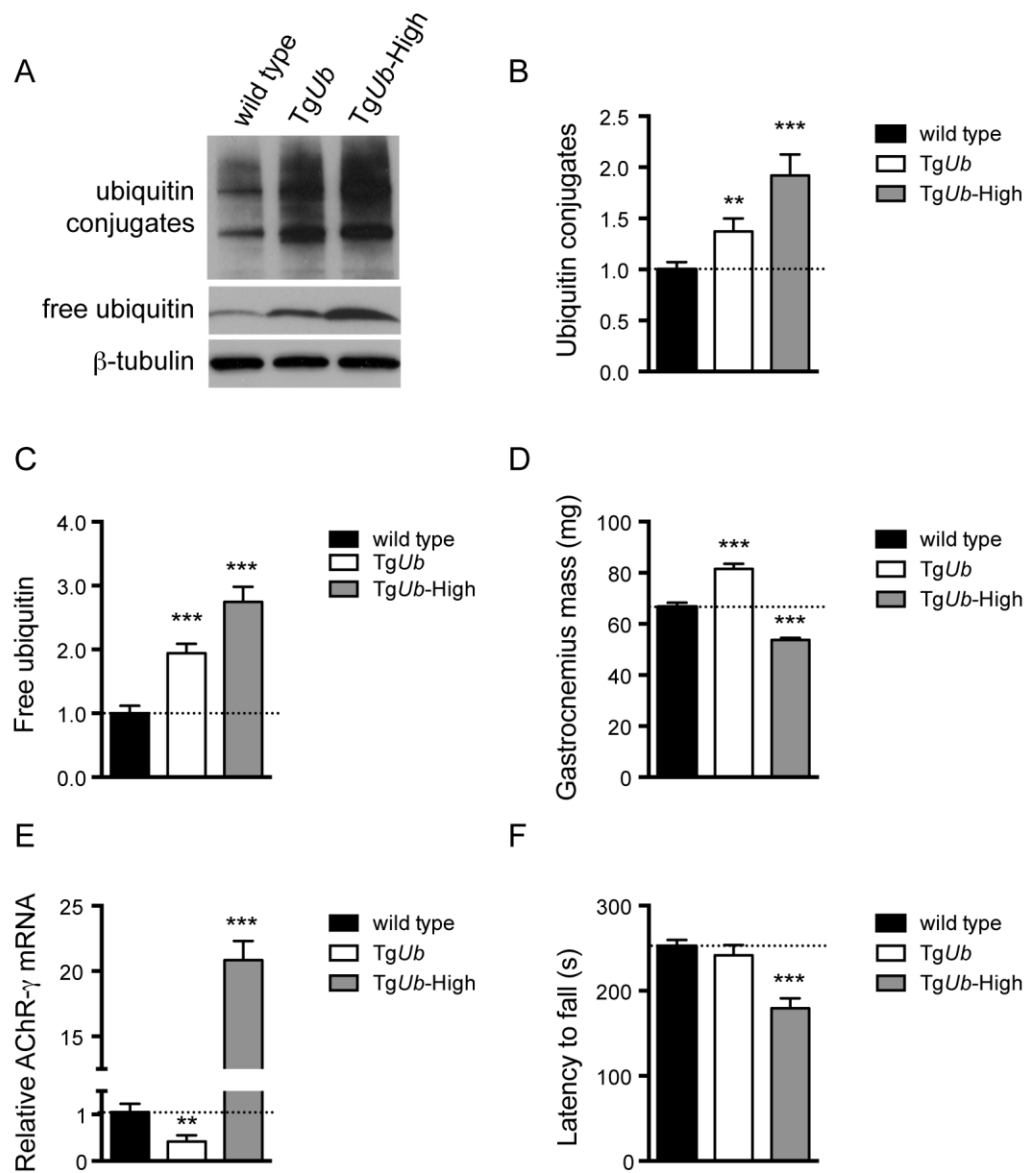


Figure 4. See legend on next page.

See figure on previous page.

Figure 4. Dose-dependent effects of ubiquitin on muscle development and motor function. (A) Representative immunoblots of free and conjugated ubiquitin in spinal cord from two lines of transgenic mice over-expressing ubiquitin under the neuronal *Thy1.2* promoter. β -tubulin was used as a loading control. Relative levels of ubiquitin conjugates and free ubiquitin, normalized to wild type levels, are quantitated in (B) and (C), respectively. (D) Comparison of gastrocnemius muscle mass from 4 to 5-week old female mice. The same effect was observed in male mice. A one-way ANOVA revealed a significant effect of genotype ($p < 0.0001$) (E) Comparison of *AChR- γ* transcript abundance, normalized to wild type. A one-way ANOVA revealed a significant effect of genotype ($p < 0.0001$) (F) Latency to fall from beam during a rotarod assay. A one-way ANOVA revealed a significant effect of genotype ($p < 0.01$). For (D)- (F), $n =$ at least 5 animals per genotype. All data are shown as mean \pm SEM. Symbols represent unpaired T-tests compared against wild type and corrected for multiple comparisons with a Bonferonni adjustment where ** $p < 0.01$, *** $p < 0.001$.

transcripts (Fig. 4E), a marker of synaptic deficits and motor dysfunction in adult animals (Chen et al., 2011; Chen et al., 2009). In fact, *TgUb*-H mice had a more than 20-fold increase in *AChR-γ* abundance compared to controls, which is similar to what is seen in the USP14-deficient *ax^J* mice (Chen et al., 2011) and contrasted with the significant decrease in *AChR-γ* transcript abundance observed in *TgUb* mice (Fig. 4E). Finally, whereas overexpression of ubiquitin in the *TgUb* mice had no effect on rotarod performance, increased levels of ubiquitin in the *TgUb*-H mice caused them to fall from the rotating beam more quickly than controls (Fig. 4F), and display an abnormal gait while performing this task (data not shown). Together, these data show that ubiquitin has dose-dependent effects on motor function and muscle development. These independent effects of ubiquitin may partially explain the improved motor function and muscle development observed in *ax^JTgUb* mice compared to *ax^J* mice (Chen et al., 2011) and the increased deficits in motor function and muscle development observed in *TgCA,TgUb* mice compared to *TgCA* mice (Fig. 2).

Ubiquitin overexpression corrects presynaptic structural deficits at the TgCA NMJ

We have previously reported that NMJs of 4 to 6-week-old USP14-deficient *ax^J* mice have poor motor endplate arborization, swollen presynaptic terminals, and ultra-terminal sprouting, and that these deficits are corrected in *ax^JTgUb* mice (Chen et al., 2011). Because *TgCA* mice recapitulate these *ax^J* NMJ deficits (Vaden et al., 2015), we investigated whether NMJ structure was improved in *TgCA,TgUb* mice (Fig. 5A).

Whereas 56% of *TgCA* NMJs had presynaptic swellings, ubiquitin overexpression

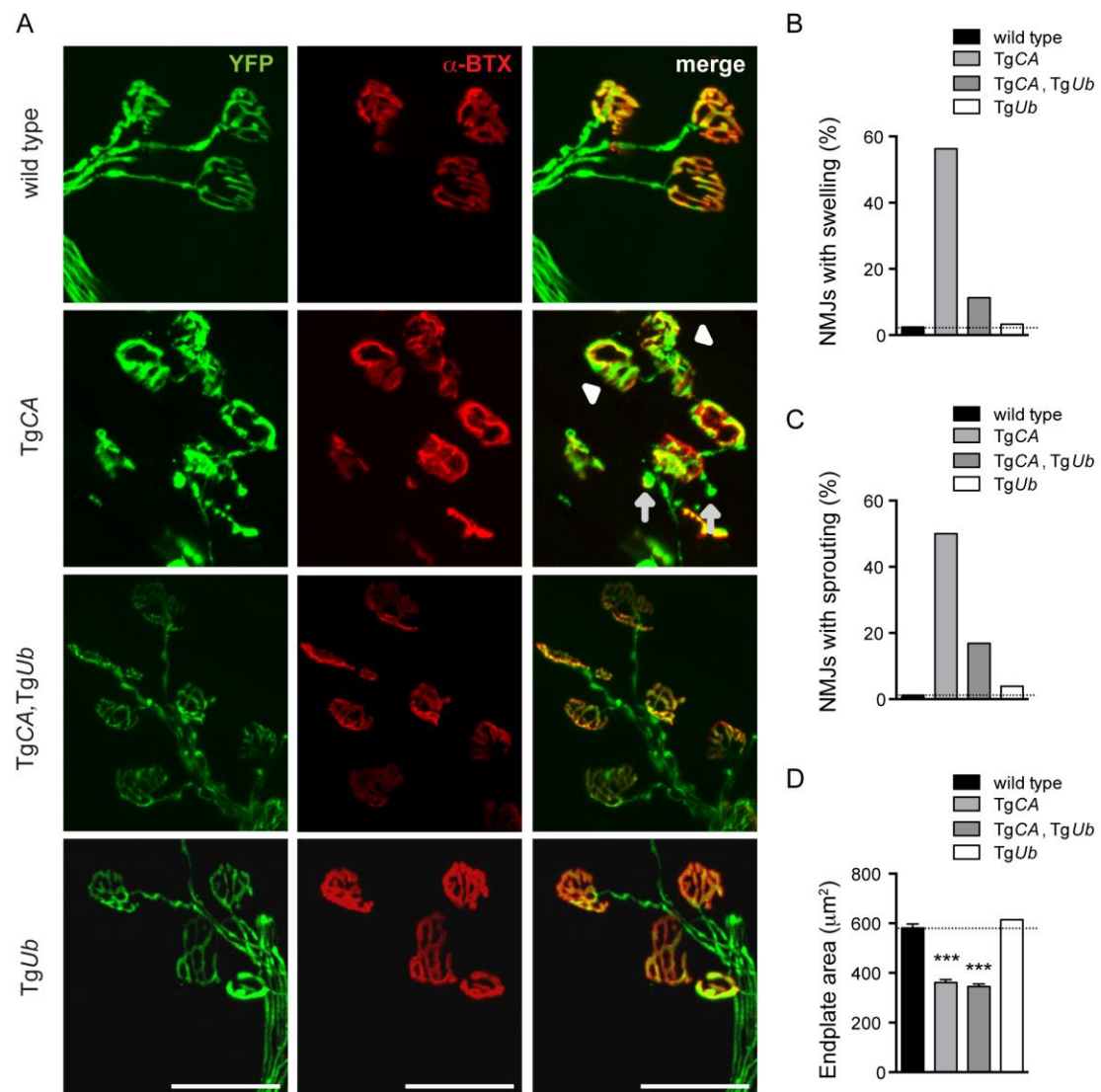


Figure 5. See legend on next page.

See figure on previous page.

Figure 5. Ubiquitin complementation improves NMJ structure in TgCA mice. (A) Whole-mount immunostaining of tibialis anterior (TA) muscles from 4 to 5-week-old wild type; *TgCA*; *TgCA,TgUb*; and *TgUb* mice expressing YFP (green) under the neuronal *Thy1.2* promoter. AChR clusters were visualized with rhodamine-conjugated α -bungarotoxin (α -BTX, red). Arrowhead indicates terminal swelling and arrows indicate ultra-terminal sprouting. Scale bar represents 50 μ M. **(B)** Percent of NMJs with presynaptic swellings or **(C)** sproutings. **(D)** Quantitation of α -BTX-positive endplate area shown as mean \pm SEM. A one-way ANOVA revealed a significant effect of genotype ($p < 0.0001$). Symbols represent unpaired T-tests compared against wild type and corrected for multiple comparisons with a Bonferonni adjustment, where *** $p < 0.001$. For (B)-(D), $n =$ at least 130 NMJs from 5 animals.

improved NMJ structure and only 11% of TgCA,TgUb terminals were swollen (Fig. 5B). Similarly, we observed ultra-terminal or ultra-axonal sprouting in 50% of the terminals of the TgCA mice compared to only 17% in the TgCA,TgUb mice (Fig. 5C). Terminal swelling and sprouting were seen only rarely in wild type and TgUb mice (Figs. 5B and C). We found a significant effect of genotype on endplate area, with smaller, more plaque-like endplates in the TgCA and TgCA,TgUb mice than wild type and TgUb mice (Figure 5D), consistent with the increase in *AChR* mRNA abundance observed in these mice (Fig. 3).

Ubiquitin Complementation Reduces pJNK at the NMJs, but not the Spinal Cords, of the TgCA Mice

We recently reported that pJNK is a prominent component of the terminal swellings and sproutings in TgCA mice, and that the extent of this pathology is reduced by treatment with the JNK inhibitor SP600125 (Vaden et al., 2015). Because ubiquitin complementation improved the structure of the TgCA endplates (Fig. 5), we investigated whether this reduction in pathology was associated with a reduction of pJNK at the NMJ. As previously reported, we observed strong pJNK immunostaining in the presynaptic terminals of TgCA mice (Fig. 6A): 55.8% of terminals contained pJNK-positive swellings (Fig. 6B) and 43.5% of terminals contained pJNK-positive ultra-terminal sprouts (Fig. 6C). In contrast, ubiquitin overexpression in the TgCA,TgUb mice reduced the pathology, and only 8.3% of terminals contained pJNK-positive swelling or sprouting (Figs. 6B and C). pJNK-positive pathology was negligible in wild type mice and absent

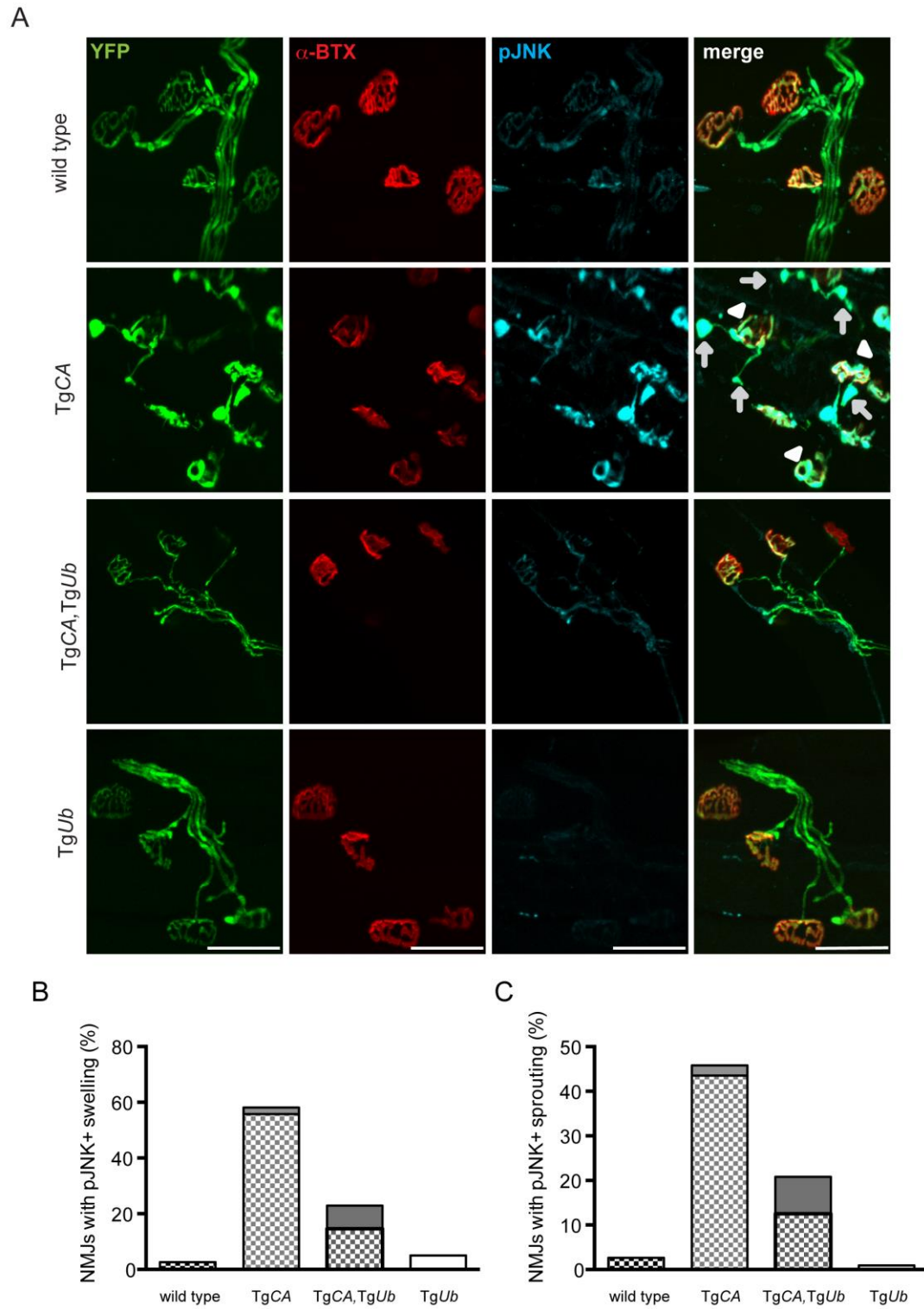


Figure 6. See legend on next page.

See figure on previous page.

Figure 6. Ubiquitin complementation reduces pJNK levels at the NMJs of TgCA mice. (A) Whole-mount immunostaining of tibialis anterior (TA) muscles from 4 to 5-week-old wild type; *TgCA*; *TgCA,TgUb*; and *TgUb* mice expressing YFP (green) under the neuronal *Thy1.2* promoter using an antibody against pJNK (light blue). Endplates were visualized with rhodamine-conjugated α -bungarotoxin (α -BTX, red). Arrowheads indicate pJNK-positive terminal swelling and arrows indicate pJNK-positive ultra-terminal sprouting. Scale bar represents 50 μ M. Quantitation of (B) presynaptic swellings or (C) ultra-terminal sproutings, where the height of each bar represents the total percent of swollen NMJs and the patterned portion of each bar represents pJNK-positive swellings. n = at least 60 NMJs from 3 animals per genotype.

in the *TgUb* mice. Together with our previous work (Vaden et al., 2015) and the work of others (Collins et al., 2006; Drerup & Nechiporuk, 2013; Etter et al., 2005) demonstrating that elevated pJNK at the NMJ can cause ultra-terminal sprouting and swelling, these data suggest that ubiquitin complementation in *TgCA* mice may directly rescue the structural deficits at the NMJ by reducing levels of pJNK in the presynaptic terminal.

In our previous report, we demonstrated elevated levels of pJNK and enhanced K63-linked ubiquitination of MLK3 in spinal cords of *TgCA* mice (Vaden et al., 2015). MLK3 ubiquitination causes dimerization, autophosphorylation, and activation of MKK4, which in turn activates JNK (Humphrey et al., 2013). Given that activation of this pathway is ubiquitin-dependent, it was surprising that pJNK-positive pathology was reduced in the NMJs of *TgCA,TgUb* mice compared to *TgCA* mice. However, when we immunoblotted spinal cord lysates from wild type, *TgCA*, *TgCA,TgUb*, and *TgUb* mice with a pJNK-specific antibody, we found that the levels of pJNK in *TgCA,TgUb* mice were elevated over the levels observed in *TgCA* mice, and that spinal cord lysates of both genotypes had significantly more pJNK than spinal cord lysates from wild type mice (Figs. 7A and B). There was no change in total JNK abundance in the *TgCA* or *TgCA,TgUb* mice compared to controls, indicating that USP14 and ubiquitin regulate JNK activation and not JNK stability.

We also observed a significant decrease in the abundance of pJNK, but not total JNK, in *TgUb* spinal cord lysates compared to controls (Figs. 7A and B). The dramatic difference in pJNK abundance between *TgCA,TgUb* and *TgUb* spinal cord lysates demonstrates that the effect of ubiquitin on JNK activation is modulated by USP14's catalytic activity. Further, when we examined the axons of motor neurons immediately

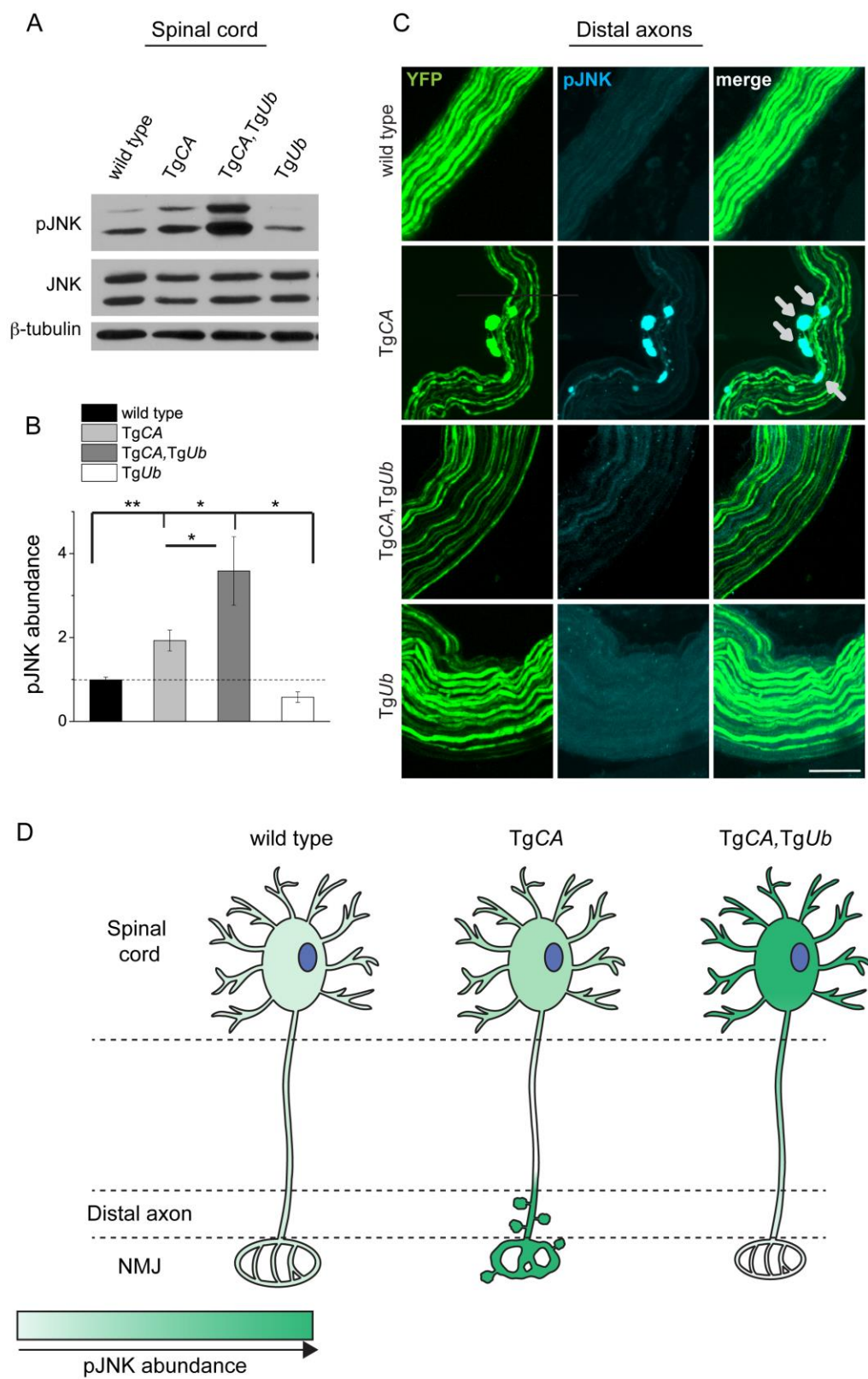


Figure 7. See legend on next page.

See figure on previous page.

Figure 7. Ubiquitin overexpression does not reduce pJNK abundance in TgCA spinal cords. (A) Representative immunoblots of pJNK and total JNK from spinal cords of 4 week-old wild type, TgCA, TgCA,TgUb, and TgUb mice. β -tubulin was used as a loading control. (B) Quantitation of pJNK levels in 4-week-old mice normalized to wild type and total JNK abundance. $n = 4$ animals per genotype. A one-way ANOVA revealed a significant effect of genotype ($p < 0.001$). Symbols represent unpaired T-tests corrected for multiple comparisons with a Bonferroni adjustment, where * $p < 0.05$, ** $p < 0.01$. (C) Images of distal axons of motor neurons, immediately adjacent to the NMJ, captured from whole-mount immunostaining of TA muscles from 4 to 5-week-old mice following incubation with a pJNK specific antibody. Arrows represent pJNK-positive axonal inclusions. (D) Schematic representation of the levels of pJNK abundance observed in the spinal cords, distal axons of motor neurons, and NMJs of 4- to 5-week-old mice of the genotypes indicated, where darker green indicates greater pJNK abundance.

proximal to the NMJ and distal to the spinal cord in the *TgCA* mice, we noticed pJNK-positive inclusions (Fig. 7C) that were similar to what is observed in the motor axons of mice with deficient retrograde axonal transport (Li et al., 2010; Shi, Strom, Gal, & Zhu, 2010). Together, these data demonstrate that both ubiquitin and USP14's catalytic activity regulate JNK activation in motor neurons, most likely in a compartment-specific manner. A schematic summarizing the levels of pJNK abundance observed in the spinal cords, distal motor neuron axons, and NMJs of wild type, *TgCA*, and *TgCA*, *TgUb* mice is shown in Fig. 7D.

Discussion

Three main conclusions can be drawn from these studies. First, overexpression of ubiquitin increased the abundance of ubiquitin conjugates in the spinal cord (Fig. 4), demonstrating that free ubiquitin is a limiting factor in some ubiquitin-dependent processes in the nervous system. Second, USP14's ubiquitin hydrolase activity plays a significant role in regulating the distribution of free and conjugated ubiquitin pools in neurons (Fig. 1). The increased abundance of ubiquitin conjugates, and not depletion of the free ubiquitin pool, directly correlated with impaired motor function when USP14's ubiquitin hydrolase activity was inhibited (Figs. 2, 3). Third, both ubiquitin levels and the catalytic activity of USP14 impact the abundance of pJNK at the NMJ and in the spinal cord (Figs. 6, 7) and, in turn, the levels of pJNK at the NMJ impact the structure of the presynaptic terminal.

Neuronal overexpression of ubiquitin led to increased ubiquitin conjugates in a dose-dependent manner in two transgenic founder lines, *TgUb* and *TgUb-H*, with low and high levels of ubiquitin overexpression, respectively (Fig. 4A). These ubiquitin conjugates had dose-dependent effects on motor function and muscle development in wild type mice (Fig. 4), which are illustrated schematically in Figure 8. Mild ubiquitin overexpression led to increased muscle development and reduced expression of the fetal γ subunit of the muscle *AChR*, which is correlated with enhanced NMJ synaptic transmission (Chen et al., 2011; Chen et al., 2009; Vaden et al., 2015), in *TgUb* mice compared to controls (Fig. 4B,C, D). In contrast, more dramatic ubiquitin overexpression reduced muscle development, increased *AChR*- γ abundance, and hindered motor performance in the *TgUb*-High mice compared to controls (Fig. 4B, C, D). Moreover, we have previously reported that the *TgUb*-H mice develop adult-onset motor endplate disease (Hallengren et al., 2013). Together, these data highlight the importance of maintaining ubiquitin levels within a relatively narrow window.

USP14 is an important regulator of ubiquitin homeostasis. We found that increasing the level of wild type USP14 in the nervous system resulted in an increase in the free ubiquitin pool and decreased levels of ubiquitin conjugates as compared to controls. Because both the *ax^J* mice and *TgCA* mice exhibit severe motor endplate disease, we were surprised to find differences in ubiquitin homeostasis in these two mouse lines. Loss of USP14 in the *ax^J* mice decreased the total ubiquitin pool by nearly 50% (Fig. 1) and significantly reduced the abundance of both free and conjugated ubiquitin. In contrast, expression of catalytically inactive USP14CA in the nervous system did not significantly impact the size of the total ubiquitin pool, but, instead, led to

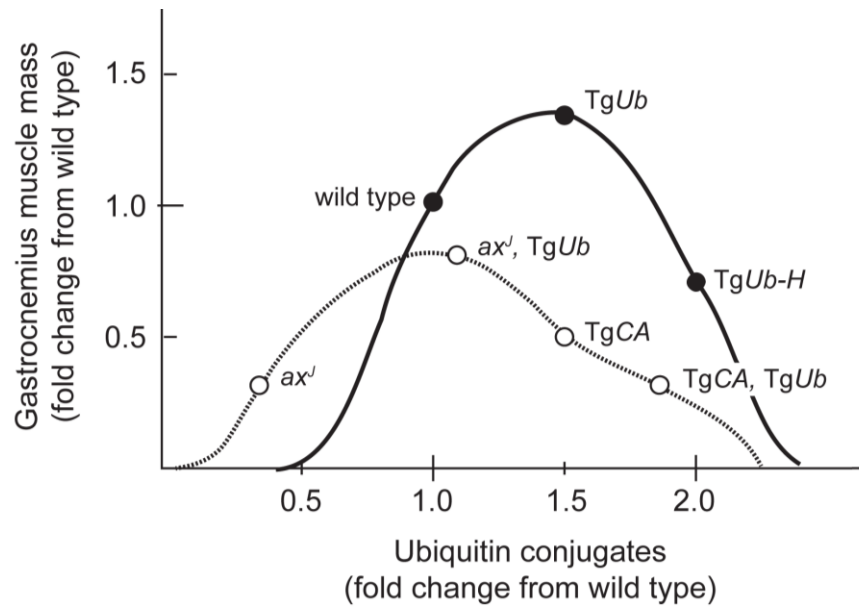


Figure 8. Relationship between the abundance of ubiquitin conjugates in the spinal cord and development of the gastrocnemius muscle. Mass of gastrocnemius muscles, expressed as fold change from wild type, plotted versus abundance of ubiquitin conjugates in the spinal cord for 4-6-week-old mice of the genotypes indicated. Mice expressing only endogenous, wild type USP14 are plotted with closed circles and mice with reduced USP14 abundance or the dominant-negative USP14CA transgene are plotted with open circles. Gastrocnemius mass and abundance of ubiquitin conjugates for the *ax^J*, *TgUb* mice are from Chen et al. (2011), as is the gastrocnemius mass of the *ax^J* mice. All other data points are from Figures 1, 2, and 4.

a 40% increase in ubiquitin conjugates and a 25% reduction of free ubiquitin. Further studies will be required to determine if these effects of USP14 on ubiquitin pools are due to changes in ubiquitin-dependent degradation by the proteasome. These differences in ubiquitin homeostasis in the spinal cords of the *ax^J* and *TgCA* mice, along with the dose-dependent impact of increased ubiquitin conjugates on motor function and muscle development, may provide a framework for understanding the opposite effects of ubiquitin overexpression in the *ax^J* and *TgCA* mice.

In the *ax^J*, *TgUb* mice, the levels of ubiquitin conjugates are slightly elevated over what is normally observed in wild type mice (Chen et al., 2011; shown schematically in Fig. 8). We have now shown that a modest increase in ubiquitin conjugates is correlated with increased muscle development and motor function, even when wild type USP14 is present (Fig. 4). In contrast, the levels of ubiquitin conjugates in the spinal cords of the *TgCA*, *TgUb* mice were nearly 2-fold what is observed in wild type mice (Fig. 2A, B), and reduced muscle development and mobility were observed in the *TgCA*, *TgUb* mice compared to both wild type and *TgCA* mice. Our studies of the *TgUb*-High mice indicated that a 2-fold increase in ubiquitin conjugates caused deficits in motor function and muscle development even when USP14's catalytic activity was intact (Fig. 4). Together, these data open the possibility that the restoration of motor neuron function in *ax^JTgUb* mice is indirect and can be attributed to increased ubiquitin conjugates, while suggesting that ubiquitin overexpression exacerbates the accumulation of ubiquitin conjugates caused by loss of USP14's DUB activity in *TgCA* mice to exaggerate the existing phenotype (Fig. 2, 3).

However, when considered together with our previous work demonstrating a role for pJNK in the NMJ pathology observed in the *TgCA* mice (Vaden et al., 2015), this study suggests that ubiquitin complementation corrects these structural deficits directly, by reducing pJNK-positive pathology (Figs. 5, 6). While we have not examined pJNK abundance at the NMJs of *ax^J* mice, the increased JNK activation in *ax^J* spinal cords suggests that the mechanism underlying NMJ pathology caused by loss of USP14 is the same as that caused by loss of USP14's DUB activity (Vaden et al., 2015). Given the reduction of pJNK at *TgCA*, *TgUb* NMJs compared to *TgCA* NMJs (Fig. 6), we were surprised by the dramatic increase in pJNK levels in the spinal cords of the *TgCA*, *TgUb* mice (Figs. 7A, B). However, we have recently reported that loss of USP14's DUB activity leads to enhanced K63-linked ubiquitination of MLK3 (Vaden et al., 2015), which drives it to dimerize, autophosphorylate, and activate its immediate downstream targets, MKK4/7, which, in turn, activate JNK (Humphrey et al., 2013). It is therefore possible that the increased JNK activation that we observed in *TgCA*, *TgUb* spinal cords compared to *TgCA* spinal cords (Figs. 7A and B) results from increased activation of MLK3.

The means by which ubiquitin complementation reduced pJNK-positive pathology at the NMJ remains unclear. One possibility is that the increased ubiquitin in *TgCA*, *TgUb* mice stimulates the degradation of pJNK or its upstream kinases at the NMJ or, alternatively, that ubiquitin contributes to the activation of phosphatases that act on pJNK. Both of these explanations are consistent with the reduction of pJNK abundance in *TgUb* spinal cords compared to wild type, but not with the increase in pJNK levels over both wild type and *TgCA* levels in the spinal cords of the *TgCA*, *TgUb* mice (Figs. 7A and

B). In contrast, the well-documented retrograde axonal transport of activated JNK (Cavalli, Kujala, Klumperman, & Goldstein, 2005; Drerup & Nechiporuk, 2013; Lindwall & Kanje, 2005; Shin et al., 2012), the pJNK-positive swellings at TgCA NMJs (Fig. 6), and the pJNK-positive inclusions in TgCA motor neuron axons (Fig. 7C) are all consistent with a deficit in the retrograde transport of pJNK out of axon terminals in the TgCA mice. The lack of pJNK-positive pathology in either the nerve terminals (Fig. 6) or distal motor neuron axons (Fig. 7C) of the TgCA,TgUb mice, combined with the robust elevation of pJNK abundance in TgCA,TgUb spinal cords (Figs. 7A and B), the site of motor neuron cell bodies, suggest that ubiquitin may stimulate the retrograde axonal transport of pJNK (Fig. 7D). Although a role for ubiquitin in retrograde axonal transport has not been demonstrated directly, it was recently reported that altered ubiquitin homeostasis contributes to the deficits in TrkB retrograde transport caused by the exposure of cultured neurons to A β oligomers (Poon et al., 2013).

Finally, our findings also suggest that the functional deficits observed in the TgCA and *ax^J* mice are not dependent on altered NMJ structure. This is consistent with our previous report that acute inhibition of USP14 at the NMJs of wild type mice causes deficits in synaptic transmission that are similar to what is observed in the TgCA and *ax^J* mice, while intramuscular injections of the same inhibitor given over the course of a week do not cause NMJ pathology (Vaden et al., 2015). Together, these findings may indicate that USP14 regulates synapse structure and function through distinct pathways. The same is true of the ubiquitin ligase highwire, which regulates the structure and function of the *Drosophila* NMJ through separate pathways (Collins et al., 2006).

Methods

Animals

Wild type C57BL/6J, *Thy1-YFP* mice (16JRS, Jackson Laboratories, Bar Harbor, ME), transgenic mice expressing catalytically inactive USP14 (TgCA; previously referred to as Tg*Usp14CA*), ubiquitin (Tg*Ub*), or both catalytically inactive USP14 and ubiquitin (TgCA,Tg*Ub*) have been maintained in our breeding colony at the University of Alabama at Birmingham, which is fully accredited by the Association for Assessment and Accreditation of Laboratory Animal Care International. We have previously described the generation of TgCA (Vaden et al., 2015) and Tg*Ub* mice (Chen et al., 2011), where both transgenes are expressed from the neuronal *Thy1.2* promoter. Generation of Tg*Ub* mice resulted in two different founder lines with differing ubiquitin expression, Tg*Ub-H* (high expresser) and Tg*Ub* (low expresser). Double transgenic (TgCA,Tg*Ub*) mice were generated by breeding male TgCA mice to female Tg*Ub* mice. All mouse lines were maintained on a C57BL/6J background and transgenic mice were heterozygous for the transgene(s) of interest. Research was conducted without bias toward the sex of animals used for each study, and equal numbers of male and female mice were used. All research complied with the United States Animal Welfare Act and other federal statutes and regulations relating to animals and experiments involving animals, and adhered to principles stated in the Guide for the Care and Use of Laboratory Animals, United States National Research Council.

Isolation of Proteins

Mice were deeply anesthetized with isoflurane prior to rapid decapitation. Spinal cords were removed and homogenized in modified RIPA buffer containing 50 mM Tris, pH 7.5, 150 mM NaCl, 5 mM MgCl₂, 0.5 mM EGTA, 1 mM EDTA, 0.5% SDS, 1% Triton X-100, and 1% sodium deoxycholate. Complete protease inhibitor (Roche, Indianapolis, IN), phosphatase inhibitor cocktail III (Sigma Aldrich, St. Louis, MO), and 50 μ M PR-619 (inhibitor of deubiquitinating enzymes, Life Sensors, Malvern, PA) were added to the homogenization buffer per manufacturer instructions. Following homogenization, samples were sonicated and centrifuged at 17,000 x g for 10 min at 4°C. The supernatants were removed and stored immediately at -80°C. Protein concentrations were determined using the bicinchoninic acid (BCA) protein assay kit from Pierce (Rockford, IL).

Immunoblotting and Quantitation

Proteins were resolved on 10% Tris-glycine gels and transferred onto nitrocellulose membranes. BSA (2%) in PBS containing 0.1% NP-40 was used to block the membranes and dilute the primary and secondary antibodies. HRP-conjugated secondary antibodies (Southern Biotechnology Associates, Birmingham, AL) and SuperSignal West Pico Chemiluminescent Substrate (Thermo Scientific, Rockford, IL) were used for detection. For detection of ubiquitin, proteins were resolved on 4-12% Nupage Tris-bis gels (Life Technologies, Grand Island, NY) and transferred onto PVDF membranes. Membranes were treated with 0.1% glutaraldehyde in PBS for 20 min prior to blocking in PBS containing 2% BSA and 0.1% NP-40. The secondary antibody was

diluted into PBS containing 1% non-fat dry milk and 0.1% NP-40. For quantitation, all blots were scanned using a Hewlett-Packard Scanjet 3970, and band density was quantified with UN-SCAN-IT gel digitizing software (Silk Scientific, Inc., Orem, Utah).

Antibodies

The following antibodies were used: USP14 (Anderson et al., 2005), β -tubulin (Developmental Studies Hybridoma Bank, Iowa City, Iowa); Ubiquitin (UAB Hybridoma Facility, Birmingham, AL); pJNK, and JNK (Cell Signaling Technology, Danvers, Massachusetts).

Open Field

Animals were handled 1 day prior to open field testing. Locomotor activity was measured in an open field chamber (43.2 cm x 43.2 cm x 30.5 cm) for 15 min by an automated video tracking system (Med Associated, St. Albans, VT). The first 5 min were not analyzed to account for habituation to the chamber.

Rotarod

Motor coordination was tested by placing mice on a rotating rod (ENV-575, Med Associates), which accelerated from 3.5 rpm to 35 rpm over a 5-min period. Latency to fall was recorded over 3 trials, each separated by 1 h, and the individual trials for each animal were averaged.

Quantitative PCR

Total RNA was isolated from gastrocnemius muscles or spinal cords using RNA-STAT60 (Tel-Test, Friendswood, TX) and reverse transcribed using the Superscript VILO cDNA synthesis kit (Life Technologies) per manufacturer instructions. Individual gene assays were purchased from Applied Biosystems for each of the RNAs analyzed: *AChR- α* (Mm00431629_m1), *AChR- ϵ* (Mm00437411_m1), and *AChR- γ* (Mm00437419_m1). $\Delta\Delta\text{Ct}$ values were generated using *Gapdh* (Mm99999915_g1) as an internal standard. All values are reported as mean \pm SEM of at least three different animals per genotype, run in triplicate.

NMJ Immunostaining and Confocal Imaging

Whole mount immunostaining of the tibialis anterior (TA) muscle was performed as described (Vaden et al., 2015), and images were captured using a Ziess LSM 510 Meta confocal microscope (Carl Ziess, Oberkochen, Germany). Endplate size was determined by tracing the circumference of the α -BTX-positive post-synaptic AChR cluster and computing area using ImageJ software (NIH, Bethesda, MD).

References

- Anderson, C., Crimmins, S., Wilson, J. A., Korbel, G. A., Ploegh, H. L., & Wilson, S. M. (2005). Loss of Usp14 results in reduced levels of ubiquitin in ataxia mice. *J Neurochem*, 95(3), 724-731. doi: 10.1111/j.1471-4159.2005.03409.x
- Baker, R. T., & Board, P. G. (1987). The human ubiquitin gene family: structure of a gene and pseudogenes from the Ub B subfamily. *Nucleic Acids Res*, 15(2), 443-463.
- Baker, R. T., & Board, P. G. (1991). The human ubiquitin-52 amino acid fusion protein gene shares several structural features with mammalian ribosomal protein genes. *Nucleic Acids Res*, 19(5), 1035-1040.
- Cavalli, V., Kujala, P., Klumperman, J., & Goldstein, L. S. (2005). Sunday Driver links axonal transport to damage signaling. *J Cell Biol*, 168(5), 775-787. doi: 10.1083/jcb.200410136
- Chen, P. C., Bhattacharyya, B. J., Hanna, J., Minkel, H., Wilson, J. A., Finley, D., . . . Wilson, S. M. (2011). Ubiquitin homeostasis is critical for synaptic development and function. *J Neurosci*, 31(48), 17505-17513.
- Chen, P. C., Qin, L. N., Li, X. M., Walters, B. J., Wilson, J. A., Mei, L., & Wilson, S. M. (2009). The proteasome-associated deubiquitinating enzyme Usp14 is essential for the maintenance of synaptic ubiquitin levels and the development of neuromuscular junctions. *J Neurosci*, 29(35), 10909-10919. doi: 10.1523/jneurosci.2635-09.2009
- Collins, C. A., Wairkar, Y. P., Johnson, S. L., & DiAntonio, A. (2006). Highwire restrains synaptic growth by attenuating a MAP kinase signal. *Neuron*, 51(1), 57-69. doi: 10.1016/j.neuron.2006.05.026
- Crimmins, S., Jin, Y., Wheeler, C., Huffman, A. K., Chapman, C., Dobrunz, L. E., . . . Wilson, S. M. (2006). Transgenic rescue of ataxia mice with neuronal-specific expression of ubiquitin-specific protease 14. *J Neurosci*, 26(44), 11423-11431.
- Drerup, C. M., & Nechiporuk, A. V. (2013). JNK-interacting protein 3 mediates the retrograde transport of activated c-Jun N-terminal kinase and lysosomes. *PLoS Genet*, 9(2), e1003303. doi: 10.1371/journal.pgen.1003303

- Etter, P. D., Narayanan, R., Navratilova, Z., Patel, C., Bohmann, D., Jasper, H., & Ramaswami, M. (2005). Synaptic and genomic responses to JNK and AP-1 signaling in *Drosophila* neurons. *BMC Neurosci*, 6, 39. doi: 10.1186/1471-2202-6-39
- Finley, D., Bartel, B., & Varshavsky, A. (1989). The tails of ubiquitin precursors are ribosomal proteins whose fusion to ubiquitin facilitates ribosome biogenesis. *Nature*, 338(6214), 394-401. doi: 10.1038/338394a0
- Hallengren, J., Chen, P. C., & Wilson, S. M. (2013). Neuronal ubiquitin homeostasis. *Cell Biochem Biophys*, 67(1), 67-73. doi: 10.1007/s12013-013-9634-4
- Hershko, A., & Ciechanover, A. (1998). The ubiquitin system. *Annu Rev Biochem*, 67, 425-479. doi: 10.1146/annurev.biochem.67.1.425
- Humphrey, R. K., Yu, S. M., Bellary, A., Gonuguntla, S., Yebra, M., & Jhala, U. S. (2013). Lysine 63-linked ubiquitination modulates mixed lineage kinase-3 interaction with JIP1 scaffold protein in cytokine-induced pancreatic beta cell death. *J Biol Chem*, 288(4), 2428-2440. doi: 10.1074/jbc.M112.425884
- Jara, J. H., Frank, D. D., & Ozdinler, P. H. (2013). Could dysregulation of UPS be a common underlying mechanism for cancer and neurodegeneration? Lessons from UCHL1. *Cell Biochem Biophys*, 67(1), 45-53. doi: 10.1007/s12013-013-9631-7
- Kaiser, S. E., Riley, B. E., Shaler, T. A., Trevino, R. S., Becker, C. H., Schulman, H., & Kopito, R. R. (2011). Protein standard absolute quantification (PSAQ) method for the measurement of cellular ubiquitin pools. *Nat Methods*, 8(8), 691-696. doi: 10.1038/nmeth.1649
- Kues, W. A., Brenner, H. R., Sakmann, B., & Witzemann, V. (1995). Local neurotrophic repression of gene transcripts encoding fetal AChRs at rat neuromuscular synapses. *J Cell Biol*, 130(4), 949-957.
- Li, Y., Ray, P., Rao, E. J., Shi, C., Guo, W., Chen, X., . . . Wu, J. Y. (2010). A *Drosophila* model for TDP-43 proteinopathy. *Proc Natl Acad Sci U S A*, 107(7), 3169-3174. doi: 10.1073/pnas.0913602107
- Lindwall, C., & Kanje, M. (2005). Retrograde axonal transport of JNK signaling molecules influence injury induced nuclear changes in p-c-Jun and ATF3 in adult

rat sensory neurons. *Mol Cell Neurosci*, 29(2), 269-282. doi: 10.1016/j.mcn.2005.03.002

Lowe, J., Blanchard, A., Morrell, K., Lennox, G., Reynolds, L., Billett, M., . . . Mayer, R. J. (1988). Ubiquitin is a common factor in intermediate filament inclusion bodies of diverse type in man, including those of Parkinson's disease, Pick's disease, and Alzheimer's disease, as well as Rosenthal fibres in cerebellar astrocytomas, cytoplasmic bodies in muscle, and mallory bodies in alcoholic liver disease. *J Pathol*, 155(1), 9-15. doi: 10.1002/path.1711550105

Lund, P. K., Moats-Staats, B. M., Simmons, J. G., Hoyt, E., D'Ercole, A. J., Martin, F., & Van Wyk, J. J. (1985). Nucleotide sequence analysis of a cDNA encoding human ubiquitin reveals that ubiquitin is synthesized as a precursor. *J Biol Chem*, 260(12), 7609-7613.

Mayer, R. J., Lowe, J., Lennox, G., Doherty, F., & Landon, M. (1989). Intermediate filaments and ubiquitin: a new thread in the understanding of chronic neurodegenerative diseases. *Prog Clin Biol Res*, 317, 809-818.

Osaka, H., Wang, Y. L., Takada, K., Takizawa, S., Setsuie, R., Li, H., . . . Wada, K. (2003). Ubiquitin carboxy-terminal hydrolase L1 binds to and stabilizes monoubiquitin in neuron. *Hum Mol Genet*, 12(16), 1945-1958.

Perry, G., Friedman, R., Shaw, G., & Chau, V. (1987). Ubiquitin is detected in neurofibrillary tangles and senile plaque neurites of Alzheimer disease brains. *Proc Natl Acad Sci U S A*, 84(9), 3033-3036.

Poon, W. W., Carlos, A. J., Aguilar, B. L., Berchtold, N. C., Kawano, C. K., Zograbyan, V., . . . Cotman, C. W. (2013). beta-Amyloid (A β) oligomers impair brain-derived neurotrophic factor retrograde trafficking by down-regulating ubiquitin C-terminal hydrolase, UCH-L1. *J Biol Chem*, 288(23), 16937-16948. doi: 10.1074/jbc.M113.463711

Redman, K. L., & Rechsteiner, M. (1989). Identification of the long ubiquitin extension as ribosomal protein S27a. *Nature*, 338(6214), 438-440. doi: 10.1038/338438a0

Ryu, K. Y., Garza, J. C., Lu, X. Y., Barsh, G. S., & Kopito, R. R. (2008). Hypothalamic neurodegeneration and adult-onset obesity in mice lacking the Ubb polyubiquitin gene. *Proc Natl Acad Sci U S A*, 105(10), 4016-4021. doi: 10.1073/pnas.0800096105

- Schmukle, A. C., & Walczak, H. (2012). No one can whistle a symphony alone - how different ubiquitin linkages cooperate to orchestrate NF-kappaB activity. *J Cell Sci*, 125(Pt 3), 549-559. doi: 10.1242/jcs.091793
- Shi, P., Strom, A. L., Gal, J., & Zhu, H. (2010). Effects of ALS-related SOD1 mutants on dynein- and KIF5-mediated retrograde and anterograde axonal transport. *Biochim Biophys Acta*, 1802(9), 707-716. doi: 10.1016/j.bbadis.2010.05.008
- Shin, J. E., Cho, Y., Beirowski, B., Milbrandt, J., Cavalli, V., & DiAntonio, A. (2012). Dual leucine zipper kinase is required for retrograde injury signaling and axonal regeneration. *Neuron*, 74(6), 1015-1022. doi: 10.1016/j.neuron.2012.04.028
- Tanno, H., & Komada, M. (2013). The ubiquitin code and its decoding machinery in the endocytic pathway. *J Biochem*, 153(6), 497-504. doi: 10.1093/jb/mvt028
- Vaden, J. H., Bhattacharyya, B. J., Chen, P. C., Watson, J. A., Marshall, A. G., Phillips, S. E., . . . Wilson, S. M. (2015). Ubiquitin-specific protease 14 regulates c-Jun N-terminal kinase signaling at the neuromuscular junction. *Mol Neurodegener*, 10(1), 3. doi: 10.1186/1750-1326-10-3
- Walters, B. J., Hallengren, J. J., Theile, C. S., Ploegh, H. L., Wilson, S. M., & Dobrunz, L. E. (2014). A catalytic independent function of the deubiquitinating enzyme USP14 regulates hippocampal synaptic short-term plasticity and vesicle number. *J Physiol*, 592(Pt 4), 571-586. doi: 10.1113/jphysiol.2013.266015
- Wiborg, O., Pedersen, M. S., Wind, A., Berglund, L. E., Marcker, K. A., & Vuust, J. (1985). The human ubiquitin multigene family: some genes contain multiple directly repeated ubiquitin coding sequences. *Embo J*, 4(3), 755-759.
- Yang, W. L., Wu, C. Y., Wu, J., & Lin, H. K. (2010). Regulation of Akt signaling activation by ubiquitination. *Cell Cycle*, 9(3), 487-497.
- Zhou, A. Y., Shen, R. R., Kim, E., Lock, Y. J., Xu, M., Chen, Z. J., & Hahn, W. C. (2013). IKKepsilon-Mediated Tumorigenesis Requires K63-Linked Polyubiquitination by a cIAP1/cIAP2/TRAF2 E3 Ubiquitin Ligase Complex. *Cell Rep*. doi: 10.1016/j.celrep.2013.01.031

DISCUSSION

The work presented in the two previous chapters has deepened our understanding of the way USP14 supports the structure and function of the NMJ. While studies of the *ax^J* mice firmly established a need for USP14 in the nervous system (Crimmins et al., 2006; D'Amato & Hicks, 1965; Wilson et al., 2002), and, in particular, at the NMJ (P. C. Chen et al., 2011; P. C. Chen et al., 2009), the capacity in which USP14 was required was not well understood. Because of its association with the proteasome, I began this work with the expectation that loss of USP14 caused nervous system dysfunction by altering proteasome-mediated protein degradation. This was a safe assumption, supported by a wealth of *in vitro* studies demonstrating modulation of the proteasome by USP14 (D'Arcy et al., 2011; Hanna et al., 2006; Hanna et al., 2007; B. H. Lee et al., 2010; Leggett et al., 2002; Peth et al., 2009; Peth et al., 2013), although the conflicting findings of previous studies, which are discussed in greater detail in the introduction, made it difficult to predict whether loss of USP14 accelerated or delayed protein turnover and whether it exerted its effects through non-catalytic modulation of the proteasome or through its ubiquitin hydrolase activity. Unexpectedly, my results suggest that, rather than altering protein turnover, USP14's ubiquitin hydrolase activity limits proteasome-independent ubiquitin signaling.

Dissociating the Ubiquitin Hydrolase-Dependent and –Independent Functions of USP14

We used two approaches to separate USP14's catalytic activity from its non-catalytic effects. The first was the generation of a new transgenic mouse that expressed catalytically-inactive USP14CA under the *Thy1.2* promoter, leading to nervous-system-specific expression of a mutant protein that displaced endogenous USP14 from the proteasome. This mouse was referred to as Tg*Usp14CA* in Chapter 2 and TgCA in Chapter 3; for the sake of simplicity, it will be referred to as TgCA in the discussion. The second approach was the use of the USP14-specific inhibitor IU1, an active-site-directed small molecule that reduces USP14's ubiquitin hydrolase activity without affecting its ability to associate with the proteasome (B. H. Lee et al., 2010).

There are several caveats to direct comparisons between the USP14-deficient *ax^j* mice and the TgCA mice. First, because USP14CA was expressed transgenically in wild type mice, the TgCA mice retained expression of endogenous USP14 and the overall levels of USP14 in the nervous system were greatly elevated. However, we showed that proteasomes isolated from TgCA mice show only minimal USP14 activity, demonstrating that USP14CA outcompetes endogenous USP14 for proteasome binding, and establishing that TgCA mice lack USP14's catalytic activity on neuronal proteasomes. Further, elevating the levels of wild type USP14 in the nervous system to levels comparable to those observed in the TgCA mice does not result in a neuromuscular disease, demonstrating that the phenotype of the TgCA mice is due to lack of USP14's ubiquitin hydrolase activity rather than USP14 overexpression. This conclusion is supported by the finding that inhibition of USP14 with IU1 replicated key observations made in the nervous systems of the TgCA mice.

Another difference between the two models is that, whereas the *ax^J* mice lack USP14 in all tissues, USP14CA is only expressed in the nervous systems of the TgCA mice. However, the reduced lifespan, motor deficits, NMJ pathology, and NMJ synaptic transmission deficits observed in the *ax^J* mice are all rescued by expression of wild type USP14 under the *Thy1.2* promoter (Crimmins et al., 2006), indicating that the TgCA mice express USP14CA in the cell populations with a critical need for USP14. Therefore, by comparing the phenotypes of the *ax^J* and TgCA mice, it is possible to determine the catalytic and non-catalytic contributions of USP14 to the nervous system.

USP14 Non-Catalytically Promotes Viability

Overall, the neuromuscular phenotype that resulted from loss of USP14's DUB activity in the TgCA mice was milder than that caused by the reduction of USP14 in the *ax^J* mice. Unlike the *ax^J* mice, which die between 8 and 10 weeks of age, the TgCA mice had a normal lifespan and did not develop the progressive hindlimb paralysis observed in the *ax^J* mice (Vaden et al., 2015). Strikingly, expression of USP14CA in the *ax^J* mice enabled them to survive for over a year (data not shown), underscoring the importance of USP14's ubiquitin-hydrolase-independent functions in the nervous system. Furthermore, although the TgCA mice had profound deficits in motor performance when compared to wild type mice, they were more ambulatory and coordinated than the *ax^J* mice. These findings are consistent with what is observed in the central nervous system of the *ax^J* mice, where expression of USP14CA rescues deficits in hippocampal paired pulse facilitation (PPF) and synaptic vesicle pools (Walters et al., 2014).

USP14's Ubiquitin Hydrolase Activity Supports NMJ Structure and Synaptic Transmission

Although the comparison between the TgCA mice and the *ax^J* mice demonstrates that the need for USP14 in the nervous system does not depend entirely on its catalytic activity, it is clear that USP14's ubiquitin hydrolase activity does support NMJ structure and function. For example, loss of USP14 in the *ax^J* mice causes severe structural pathology at the NMJ, where we observe swollen presynaptic terminals, ultra-terminal sprouting, and poor arborization of the post-synaptic AChRs, all of which were also observed in the TgCA mice. While all of the NMJs from the TA muscles of the *ax^J* mice are structurally abnormal, only 60% of NMJs from TgCA TAs contained swelling or sprouting. This could indicate that USP14 non-catalytically contributes to the maintenance of NMJ structure, but individual TgCA terminals displaying pathology were as abnormal, or more so, than *ax^J* terminals, suggesting that the reduced frequency of pathology in the TgCA mice resulted from the mosaic expression of the *Thy1.2* promoter and that USP14's regulation of NMJ structure relies exclusively on its ubiquitin hydrolase activity.

USP14 Regulates NMJ Structure through pJNK Activation

Two lines of evidence indicate that the structural deficits caused by expression of USP14CA resulted, at least in part, from over-activation of JNK. Treatment of the TgCA mice with the JNK inhibitor SP600125 improved NMJ structure, and the reduction of terminal swelling and sprouting observed when ubiquitin was overexpressed in the nervous systems of the TgCA mice was accompanied by a reduction of pJNK

immunofluorescence at the NMJ. Although JNK was originally described as an activator of the transcription factor c-Jun, it is now known to have a large number of targets inside and outside of the nucleus (reviewed in Bogoyevitch & Kobe, 2006; Coffey, 2014)

Increased JNK activation can lead to NMJ pathology both by altering gene transcription and by phosphorylating cytosolic targets in the terminal itself. For example, in the *Drosophila hiw* mutant, loss of the ubiquitin ligase *highwire* leads to enhanced stability of the *Drosophila* homologue of dual lysine zipper-bearing kinase (DLK), which is a mitogen activated protein kinase kinase kinase (MAPKKK) that is upstream of JNK (Collins et al., 2006). Expression of a dominant-negative JNK isoform in the *hiw* mutants suppresses their synaptic overgrowth at the NMJ, as does expression of a dominant-negative isoform of the *Drosophila* homologue of the transcription factor c-Fos, demonstrating that JNK-mediated changes in gene expression can cause abnormal NMJ structure. In contrast, loss of JNK-interacting protein 3 (JIP3) in zebra fish prevents the retrograde transport of activated JNK from the NMJ and leads to pJNK-positive swellings in the presynaptic terminal that are strikingly similar to what we observed in the TgCA mice (Drerup & Nechiporuk, 2013). Over-expression of constitutively active JNK replicates the NMJ pathology seen in the JIP3 knockouts, confirming that pJNK causes the swellings. In this case, JNK's targets are necessarily located within the presynaptic terminal because the deficit in the retrograde transport of pJNK precludes access to the cell body and the nucleus.

Targets of JNK at the NMJ

Because pJNK levels were increased in both the spinal cords, where motor neuron cell bodies are located, and at the NMJs of the TgCA mice, it is possible that pJNK contributed to the altered NMJ structure through changes in gene expression and/or direct phosphorylation of cytosolic targets in the TgCA mice. However, when ubiquitin was overexpressed in the TgCA mice, we observed an improvement of NMJ structure and a reduction in pJNK immunoreactivity that was specific to the NMJ. In fact, the levels of pJNK in the spinal cords of TgCA, TgUb mice were increased over what we observed in the spinal cords of the TgCA mice. This suggests that increased phosphorylation of cytosolic targets by pJNK underlies the NMJ pathology caused by expression of USP14CA, and the neuronal cytoskeleton-associated proteins phosphorylated by pJNK are attractive possibilities.

Microtubule-associated proteins. Microtubules are non-covalently linked polymers of α - and β -tubulin that can be dynamically assembled and disassembled, allowing them to shape the elongation and maintenance of neuronal processes, including axons (reviewed in Desai & Mitchison, 1997). Synaptic morphology is determined by the organization of microtubules during development and can be altered by microtubule reorganization in response to injury (Klinedinst, Wang, Xiong, Haenfler, & Collins, 2013). Microtubule-associated proteins (MAPs), which bind to microtubules to influence their polymerization, fall into two main categories: those which enhance stability and favor elongation and those which decrease stability (Desai & Mitchison, 1997). JNK directly phosphorylates microtubule-associated proteins 1B and 2 (MAP1B and MAP2), which

enhances microtubule polymerization (Chang et al., 2003). JNK also phosphorylates the microtubule destabilizing MAP superior cervical ganglion 10 (SCG10; Neidhart et al., 2001), which inhibits association of SCG10 and microtubules to improve microtubule stability (Westerlund et al., 2011). Both of these phosphorylation events favor microtubule assembly and stability, which, unchecked, could result in the swelling and ultra-terminal sprouting observed in the ax^J and TgCA mice.

Tau is another microtubule-associated protein that can be phosphorylated by JNK (Tatebayashi et al., 2006), and hyperphosphorylated tau is observed throughout the central nervous systems of the ax^J mice (Y. N. Jin et al., 2012). However, knocking tau out in the ax^J mice does not improve their phenotype (Y. N. Jin et al., 2012), making it unlikely that JNK over-activation causes structural deficits at the NMJ through tau phosphorylation.

Neurofilaments. Neurofilaments are a type of intermediate filament thought to increase axonal diameter (reviewed in Dale & Garcia, 2012), which could translate to the axonal swellings observed at the NMJs of the ax^J and TgCA mice. And, in fact, we do find focal accumulations of neurofilaments at the NMJs of both the ax^J (P. C. Chen et al., 2009) and the TgCA mice (unpublished observation). Although we have not determined whether the neurofilaments that accumulate in the ax^J and TgCA motor axons are phosphorylated, neurofilaments are known substrates of JNK (Fernyhough et al., 1999), and there is some evidence that phosphorylation favors neurofilament aggregation (Gong, Wang, Iqbal, & Grundke-Iqbal, 2003). Interestingly, although the ultra-terminal sprouting reported in the terminals of the TgCA mice was quite prominent when motor neuron axons were

visualized by the expression of YFP under the *Thy1* promoter, it was observed only rarely in axons visualized by antibodies against the neurofilaments (unpublished observation). Therefore, while neurofilament accumulation may underlie the swollen terminals observed in the TgCA mice, it is unlikely to cause the ultra-terminal sprouting.

USP14's Ubiquitin Hydrolase Activity Dynamically Regulates Synaptic Transmission

Loss of USP14 in the *ax^J* mice causes multiple deficits in synaptic transmission at the NMJ: reduced frequency of MEPCs, increased MEPC amplitude and decay constant, reduced amplitude of evoked EPCs and reduced quantal content (Bhattacharyya, Wilson, Jung, & Miller, 2011; P. C. Chen et al., 2011; Crimmins et al., 2006; Wilson et al., 2002). All of these deficits were also observed in the TgCA mice (Vaden et al., 2015), indicating that they arise from loss of USP14's ubiquitin hydrolase activity. Furthermore, acute, pharmacological inhibition of USP14 in wild type mice also reduced MEPC frequency, increased MEPC decay time, decreased EPC amplitude, and decreased quantal content, demonstrating that USP14's ubiquitin hydrolase activity has an ongoing role in synaptic transmission.

While we did not test whether inhibition of JNK relieved the synaptic transmission deficits observed at the NMJs of the TgCA mice, we did observe modest, but significant, improvements in muscle development, motor coordination, and expression of the fetal γ -subunit of the muscle AChR in TgCA mice treated with the JNK inhibitor, all of which suggested improved NMJ function. It is possible, therefore, that the increase in pJNK abundance caused by expression of USP14CA contributes to the reduced neurotransmitter release observed at the NMJ, and there is some evidence that

JNK activity can modulate synaptic transmission. In acute hippocampal slices from mice, the same JNK inhibitor used in our studies increased field excitatory postsynaptic potentials (fEPSPs) by approximately 25% within minutes of application (Costello & Herron, 2004). This enhanced fEPSP amplitude is accompanied by a decrease in PPF, suggesting that JNK inhibition increases neurotransmitter release. Similarly, expression of constitutively active JNK in *Drosophila* motor neurons reduces excitatory junction potential (EJP) amplitudes and quantal content by more than 40% (Etter et al., 2005).

Despite convincing evidence that JNK modulates synaptic transmission, little has been done to investigate the mechanism by which this modulation occurs. While it is possible that pJNK phosphorylates synaptic proteins to alter their activity or stability, more attention has been given to the activity of other MAP kinases at the synapse (reviewed in Sweatt, 2004). The decreased EJP amplitudes observed at the NMJs of flies expressing constitutively active JNK was accompanied by decreased synaptic staining for the vesicular calcium sensor synaptotagmin as well as cysteine string protein (CSP; Etter et al., 2005). CSP is a synaptic vesicle-associated protein thought to recruit dormant voltage-gated calcium channels to increase the calcium concentration at the active zone. Thus, reduction of either of these proteins is consistent with the reduced neurotransmission observed at the NMJs of the *ax^J* and *TgCA* mice, but the means by which JNK activation decreases their presence at the synapse remains unknown. Furthermore, it is unclear if the rapid effects of IU1 on synaptic transmission could be achieved by JNK-induced changes in protein abundance.

It is also possible that the synaptic transmission deficits observed in the *ax^J* and *TgCA* mice, and in wild type mice following IU1 treatment, are independent of JNK.

Indeed, while acute inhibition of USP14 with IU1 recreated the synaptic deficits seen in the TgCA mice, animals given intramuscular injections of IU1 for one week did not develop structural pathology at the NMJ. Similarly, TgCA mice expressing TgUb showed improved NMJ structure and a reduction of pJNK at the NMJ, but muscle development, motor coordination, and AChR transcript abundance were not restored to wild type levels, which suggests that synaptic transmission at the NMJs of the TgCA, TgUb mice remained deficient. These findings indicate that the deficits in synaptic transmission and the NMJ pathology caused by expression of USP14CA are not dependent on one another and suggest that they could arise through distinct mechanisms. In support of this conclusion, although the NMJ pathology observed in the *Drosophila hiw* mutants, which is similar to that of the *ax^J* and TgCA mice, is JNK dependent, the *hiw* deficit in neurotransmitter release is independent of JNK (Collins et al., 2006).

USP14 Maintains Ubiquitin Homeostasis both Catalytically and Non-Catalytically

We found that drastically reducing USP14's DUB activity on neuronal proteasomes by expressing USP14CA impacted ubiquitin homeostasis differently than did loss of USP14. There was a 60% reduction of free ubiquitin in the spinal cords of the *ax^J* mice, compared to a 20% reduction in the TgCA mice. Moreover, whereas we observed decreased ubiquitin conjugates in the spinal cords of the *ax^J* mice compared to controls, there was a significant increase in ubiquitin conjugates in the spinal cords of TgCA mice. Pharmacological inhibition of USP14 in cultured cortical neurons also resulted in increased ubiquitin conjugates, with no appreciable decrease in free ubiquitin.

Because proteomic screens indicate that, within the mouse nervous system, 60% of total ubiquitin is free and 40% is conjugated to proteins (Kaiser et al., 2011), we were able to estimate the size of the total ubiquitin pool in the ax^J and TgCA mice compared to wild type mice. When USP14 was absent, the total ubiquitin pool was reduced by nearly 50%. In contrast, expression of USP14CA did not alter overall ubiquitin levels, but, instead, shifted the balance between free ubiquitin and ubiquitin conjugates. A caveat to these estimates is that transcription of the ubiquitin gene *Ubc* is increased 20% and 250% in the nervous systems of the TgCA (unpublished observation) and ax^J mice (P. C. Chen et al., 2011), respectively. Therefore, the effects of USP14CA expression on the size of the total ubiquitin pool may be underestimated, and the effects of loss of USP14 almost certainly are. Nonetheless, these findings suggest that USP14 non-catalytically contributes to the maintenance of cellular ubiquitin levels.

Ubiquitin is degraded by yeast proteasomes in the absence of USP14/Ubp6 (Leggett et al., 2002), suggesting that the sparing of free ubiquitin in the TgCA mice compared to the ax^J mice reflects reduced proteasomal degradation. While this could result from an overall delay in the degradation of ubiquitinated proteins by the proteasome, consistent with the accumulation of ubiquitin conjugates observed when USP14CA is expressed, the lack of increase in proteasome-targeting K48-linked ubiquitin chains in the spinal cords of the TgCA mice and in cortical neurons treated with IU1 argue against this explanation. Instead, it is more likely that expression of USP14CA stabilizes the interaction of some of USP14's substrates with the proteasome, allowing them to be deubiquitinated by the other proteasomal DUBs UCH37 and POH1. In support of this argument, the presence of Ubp6-C118A on the yeast proteasome appears to

increase POH1-mediated deubiquitination of the model proteasomal substrate cyclin-B (Hanna et al., 2006). Notably, because the ubiquitin conjugates that accumulated when USP14 was inhibited were linked through K63, it is likely that USP14 is also required to terminate proteasome-independent ubiquitin signals.

Ubiquitin Complementation in the ax^J and TgCA Mice

The differences in ubiquitin homeostasis when USP14 is absent versus catalytically inactive may contribute to the more severe phenotype of the ax^J mice compared to the TgCA mice, as ubiquitin levels strongly impact neuromuscular function. Not only is ubiquitin depletion associated with motor neuron dysfunction (Anderson et al., 2005; P. C. Chen et al., 2009; Osaka et al., 2003), our studies of the TgUb and TgUb-High mice, which express moderate and high levels of ubiquitin, respectively, under the neuronal *Thy1.2* promoter, demonstrated that increased ubiquitin also impacts motor function. Measures of motor unit function, such as motor coordination, muscle development, and transcript abundance of the fetal γ -subunit of the muscle AChR, were improved in the TgUb mice compared to controls, but the opposite was true in the TgUb-High mice. In fact, levels of AChR- γ mRNA in the gastrocnemius muscles of the TgUb-High mice were similar to what is observed in the ax^J mice (P. C. Chen et al., 2011), and we have previously reported that TgUb-High mice develop motor endplate disease by 6-weeks-of-age (Hallengren et al., 2013).

Because ubiquitin levels impact motor function when wild type USP14 is present, these independent effects of ubiquitin may contribute to the differential effects of ubiquitin complementation in the ax^J and TgCA mice. The ax^J mice have a 60% reduction

in free ubiquitin and a 40% reduction in ubiquitin conjugates, so expression of *TgUb* restores free ubiquitin levels in the *ax^J* mice while causing only a slight elevation in ubiquitin conjugates compared to what is observed in wild type mice (P. C. Chen et al., 2011). Our studies of the *TgUb* mice indicate that a moderate increase in ubiquitin benefits many of the measures of motor function that are improved in the *ax^J,TgUb* mice compared to the *ax^J* mice. In contrast, expression of *TgUb* in the *TgCA* mice increased the levels of ubiquitin conjugates to nearly 2-fold what was observed in wild type mice. The reduced motor coordination, decreased muscle development, and increased transcription of AChR- γ observed in the *TgUb*-High mice demonstrated that this level of ubiquitin conjugates was associated with reduced motor function, even when wild type USP14 was present. Together, these findings may indicate that overexpression of ubiquitin partially masks the deficits in motor function in the *ax^J* mice without correcting the original mechanism of disease, while ubiquitin overexpression in the *TgCA* mice exaggerates the accumulation of ubiquitin conjugates caused by expression of USP14CA to cause profound functional deficits in the *TgCA*, *TgUb* mice.

Trimming of Proteasome-Independent Ubiquitin Chains by USP14

Expression of USP14CA caused an increase in K63-linked ubiquitin conjugates in the spinal cords of the *TgCA* mice, as did inhibition of USP14 in cultured cortical neurons. In contrast, inhibiting USP14 did not alter the abundance of K48-linked ubiquitin conjugates. Because K63-linked ubiquitin conjugates are primarily proteasome-independent and the levels of K48-linked ubiquitin conjugates are a reliable biomarker for proteasome function, these findings argue that the effects of expressing USP14CA in

the nervous system did not result from altered protein turnover by the proteasome but, instead, from aberrant proteasome-independent ubiquitin signaling. Our finding that the ubiquitin-dependent MLK3 kinase pathway was over-activated in the spinal cords of the TgCA mice supports this conclusion, especially because inhibition of JNK, which is downstream of MLK3, improved the neuromuscular phenotype caused by expression of USP14CA.

Ubiquitin chains linked through K63 are thought to be proteasome-independent because they are the only type of homotypic ubiquitin chain that does not accumulate following inhibition of the proteasome (Jacobson et al., 2009; Xu et al., 2009). Although K63-linked ubiquitin chains do act as a competent signal for proteasome-mediated degradation *in vitro* (Hofmann & Pickart, 2001; Kim et al., 2007; Peth, Uchiki, & Goldberg, 2010), the endosomal sorting complex required for transport-0 (ESCRT-0) proteins hepatocyte growth factor-regulated tyrosine kinase substrate (HRS) and signal transducing adaptor molecule (STAM) bind to K63-linked ubiquitin chains with high affinity *in vivo*, shuttling them towards the endosome and preventing interaction with the proteasome (Nathan, Tae Kim, Ting, Gygi, & Goldberg, 2013). A central remaining question, therefore, is how USP14, a proteasome-associated DUB, trims proteasome-independent ubiquitin chains.

Evidence for Disassembly of K63-Linked Ubiquitin Chains by Proteasome-Bound USP14

One possibility is that there are circumstances in which proteasome-bound USP14 has access to K63-linked chains, despite the tendency of ESCRT-0 to direct proteins modified by this type of ubiquitin chain to the endosome. It appears that another

proteasome-associated DUB, POH1, can disassemble K63-linked ubiquitin chains both *in vitro* (Cooper et al., 2009) and in the nucleus, where it regulates the accumulation of K63-linked chains on chromatin during the DNA double-strand break (DSB) response (Butler et al., 2012). POH1 antagonizes the actions of ring finger proteins 8 and 168 (RNF8/RNF168), which build K63-linked chains on the histones H2A and H2AX to recruit p53-binding protein (53BP1). Proteasome inhibition, which has been shown to inhibit POH1 (Verma et al., 2002), increases the accumulation of 53BP1 at sites of DNA damage, arguing that the POH1 performing this task is bound to the 26S proteasome (Butler et al., 2012). One explanation for these findings is that ESCRT-0 is primarily cytosolic (reviewed in Schuh & Audhya, 2014), and, as such, cannot sequester the K63-linked chains found in the nucleus.

On the other hand, proteasome-associated DUBs have also been reported to disassemble K63-linked chains outside of the nucleus. The neurotrophin receptor tropomyosin-related kinase A (TrkA) is modified by K63-linked ubiquitin chains and internalized upon binding of its ligand, nerve growth factor (NGF; Geetha, Jiang, & Wooten, 2005). TrkA is trafficked to the endosome following endocytosis, and either recycled to the plasma membrane or incorporated into the intraluminal vesicles (ILVs) of multivesicular bodies (MVBs) for lysosomal degradation (Jullien, Guili, Reichardt, & Rudkin, 2002). Consistent with this, the lysosome inhibitor methylamine blocks the degradation of TrkA (Geetha & Wooten, 2008; van Kerkhof et al., 2001). However, proteasome inhibition also prevents TrkA degradation (van Kerkhof et al., 2001) and leads to the accumulation of polyubiquitinated TrkA (Geetha & Wooten, 2008). In an elegant series of studies, Marie Wooten's lab showed that TrkA associates sequentially

with endosomal, proteasomal, and lysosomal markers following endocytosis, and that the removal of a K63-linked ubiquitin chain from TrkA by an unidentified proteasomal DUB is a prerequisite for its inclusion into ILVs and lysosomal degradation (Geetha & Wooten, 2008).

The degradation of a number of other lysosomal substrates, including the epidermal growth factor receptor (EGFR; Alwan, van Zoelen, & van Leeuwen, 2003; Longva et al., 2002; van Kerkhof et al., 2001) and the interleukin-2 receptor (IL-2R; Rocca, Lamaze, Subtil, & Dautry-Varsat, 2001; Yu & Malek, 2001), is also sensitive to proteasome inhibition and may employ proteasomal DUBs in a similar manner. These findings are not necessarily at odds with the report that ESCRT-0 prevents proteasomal degradation of proteins tagged with K63-linked ubiquitin chains (Nathan et al., 2013). ESCRT-0 is the initial complex in the ESCRT pathway and serves to recruit ubiquitinated cargo and concentrate it within the endosomal membrane (Schuh & Audhya, 2014). After ESCRT-0 has dissociated from the cargo, the proteasomal DUBs may have access to the K63-linked ubiquitin chains. Indeed, the proteasome subunit alpha type-7 (PSMA7), one of the α -subunits that make up the proteasome's catalytic core, directly interacts with Ras-related protein 7 (Rab7), a GTPase involved in the transition of cargo from the early to late endosome (Dong, Chen, Welford, & Wandinger-Ness, 2004), demonstrating that proteasomes associate with the endocytic sorting machinery. Therefore, ESCRT cargo that has already been incorporated into the endosomal membrane could be deubiquitinated by proteasome-associated DUBs without being subject to proteasome-mediated degradation.

Evidence for an Alternative Binding Partner of USP14

A second possibility is that non-proteasome associated USP14 trims K63-linked ubiquitin chains. In support of this option, only half of full-length USP14 fractionates with neuronal proteasomes and neurons express a splice variant of USP14 that is incapable of proteasome binding (Crimmins et al., 2006). The major argument against this line of reasoning is that USP14's ubiquitin hydrolase activity towards model DUB substrates has only been observed when it is associated with the proteasome (B. H. Lee et al., 2010; Leggett et al., 2002). According to structural studies, USP14 is auto-inhibited by two regulatory loops that prevent ubiquitin from entering its catalytic cleft, and proteasome binding causes these loops to translocate (Hu et al., 2005). Therefore, an alternative binding partner could cause a similar conformational change to activate USP14 off of the proteasome.

There is indirect evidence that UCH37, the other DUB that reversibly associates with the proteasome, may have an alternative activator. Similar to USP14, UCH37 is auto-inhibited by a c-terminal tail that obscures its catalytic domain (Jiao et al., 2014). UCH37 associates with the proteasome through RPN13, which causes the translocation of its c-terminal domain, allowing ubiquitin access to UCH37's catalytic cleft (Hamazaki et al., 2006; Jiao et al., 2014; Yao et al., 2006). Notably, although UCH37 has also been reported to associate with regulatory particle non-ATPase 10 (RPN10; Stone et al., 2004), this interaction is weak and does not activate UCH37's catalytic activity (Qiu et al., 2006). The finding that *Uch37*^{-/-} mice die *in utero* whereas *Rpn13*^{-/-} mice are viable (Al-Shami et al., 2010), therefore, suggests that UCH37 is active and has a critical role off of the proteasome. UCH37 has been shown to impact transforming growth factor beta

(TGF- β) signaling by acting in complex with Smad7 to counteract the ubiquitination of the type I TGF- β receptor by the ubiquitin ligase Smurf (Wicks et al., 2005), raising the possibility that Smad7 can stimulate UCH37's DUB activity.

Similarly, MLK3 is associated with the scaffolding protein JIP1 when it is ubiquitinated by the ubiquitin ligase TRAF6 (Humphrey et al., 2013), so USP14 may be recruited to this complex to regulate MLK3's ubiquitination status. At least three other DUBs—ubiquitin-specific protease 4 (USP4), cylindromatosis (CYLD), and A20 (also known as tumor necrosis factor alpha-induced protein 3; TNFAIP3)—have been reported to interact with TRAF6 to limit the activation of the TRAF-6 dependent NF- κ B pathway, either by DUBing TRAF6 itself, which reduces its activity, or by acting on TRAF6's substrates (Boone et al., 2004; W. Jin et al., 2008; Ning & Pagano, 2010; Shi & Kehrl, 2010; F. Zhou et al., 2012). Furthermore, both USP14 (Jung et al., 2013) and CYLD (Tauriello et al., 2010) remove K63-linked ubiquitin chains from Dvl2, demonstrating an overlap in substrates. Therefore, USP14 may be recruited to signaling complexes to antagonize the activity of the ubiquitin ligase TRAF6.

Conclusion

At the outset of this work, we knew that USP14 was a critical determinant of NMJ structure and function, but its precise role in ubiquitin signaling was not known. My studies have shifted the way we think about USP14 in the nervous system from a regulator of protein stability to a regulator of protein activity. Although this is a major paradigm shift, it is supported by *in vitro* work from others, demonstrating that USP14 alters the activity of Dvl2 within the Wnt signaling pathway (Jung et al., 2013). By

defining a new role for USP14 in the nervous system, my work has opened the door to exciting studies in the future, examining the mechanism by which pJNK regulates NMJ structure, the regulation of other kinase cascades by USP14, and the possibility that USP14 is activated off of the proteasome by an alternative binding partner.

LIST OF GENERAL REFERENCES

- Al-Shami, A., Jhaver, K. G., Vogel, P., Wilkins, C., Humphries, J., Davis, J. J., . . . Oravec, T. (2010). Regulators of the proteasome pathway, Uch37 and Rpn13, play distinct roles in mouse development. *PLoS One*, 5(10), e13654. doi: 10.1371/journal.pone.0013654
- Alwan, H. A., van Zoelen, E. J., & van Leeuwen, J. E. (2003). Ligand-induced lysosomal epidermal growth factor receptor (EGFR) degradation is preceded by proteasome-dependent EGFR de-ubiquitination. *J Biol Chem*, 278(37), 35781-35790. doi: 10.1074/jbc.M301326200
- Amerik, A. Y., Li, S. J., & Hochstrasser, M. (2000). Analysis of the deubiquitinating enzymes of the yeast *Saccharomyces cerevisiae*. *Biol Chem*, 381(9-10), 981-992. doi: 10.1515/bc.2000.121
- Anderson, C., Crimmins, S., Wilson, J. A., Korbel, G. A., Ploegh, H. L., & Wilson, S. M. (2005). Loss of Usp14 results in reduced levels of ubiquitin in ataxia mice. *J Neurochem*, 95(3), 724-731. doi: 10.1111/j.1471-4159.2005.03409.x
- Bennett, B. L., Sasaki, D. T., Murray, B. W., O'Leary, E. C., Sakata, S. T., Xu, W., . . . Anderson, D. W. (2001). SP600125, an anthrapyrazolone inhibitor of Jun N-terminal kinase. *Proc Natl Acad Sci U S A*, 98(24), 13681-13686. doi: 10.1073/pnas.251194298
- Bhandari, D., Robia, S. L., & Marchese, A. (2009). The E3 ubiquitin ligase atrophin interacting protein 4 binds directly to the chemokine receptor CXCR4 via a novel WW domain-mediated interaction. *Mol Biol Cell*, 20(5), 1324-1339. doi: 10.1091/mbc.E08-03-0308
- Bhattacharyya, B. J., Wilson, S. M., Jung, H., & Miller, R. J. (2011). Altered neurotransmitter release machinery in mice deficient for the deubiquitinating enzyme Usp14. *Am J Physiol Cell Physiol*, 302(4), C698-708.

- Bogoyevitch, M. A., & Kobe, B. (2006). Uses for JNK: the many and varied substrates of the c-Jun N-terminal kinases. *Microbiol Mol Biol Rev*, 70(4), 1061-1095. doi: 10.1128/mmbr.00025-06
- Boone, D. L., Turer, E. E., Lee, E. G., Ahmad, R. C., Wheeler, M. T., Tsui, C., . . . Ma, A. (2004). The ubiquitin-modifying enzyme A20 is required for termination of Toll-like receptor responses. *Nat Immunol*, 5(10), 1052-1060. doi: 10.1038/ni1110
- Butler, L. R., Densham, R. M., Jia, J., Garvin, A. J., Stone, H. R., Shah, V., . . . Morris, J. R. (2012). The proteasomal de-ubiquitinating enzyme POH1 promotes the double-strand DNA break response. *Embo J*, 31(19), 3918-3934. doi: 10.1038/emboj.2012.232
- Cane, S., Ponnappan, S., & Ponnappan, U. (2012). Altered regulation of CXCR4 expression during aging contributes to increased CXCL12-dependent chemotactic migration of CD4(+) T cells. *Aging Cell*, 11(4), 651-658. doi: 10.1111/j.1474-9726.2012.00830.x
- Chang, L., Jones, Y., Ellisman, M. H., Goldstein, L. S., & Karin, M. (2003). JNK1 is required for maintenance of neuronal microtubules and controls phosphorylation of microtubule-associated proteins. *Dev Cell*, 4(4), 521-533.
- Chen, P. C., Bhattacharyya, B. J., Hanna, J., Minkel, H., Wilson, J. A., Finley, D., . . . Wilson, S. M. (2011). Ubiquitin homeostasis is critical for synaptic development and function. *J Neurosci*, 31(48), 17505-17513.
- Chen, P. C., Qin, L. N., Li, X. M., Walters, B. J., Wilson, J. A., Mei, L., & Wilson, S. M. (2009). The proteasome-associated deubiquitinating enzyme Usp14 is essential for the maintenance of synaptic ubiquitin levels and the development of neuromuscular junctions. *J Neurosci*, 29(35), 10909-10919. doi: 10.1523/jneurosci.2635-09.2009
- Chen, Z. J., Parent, L., & Maniatis, T. (1996). Site-specific phosphorylation of I κ B α by a novel ubiquitination-dependent protein kinase activity. *Cell*, 84(6), 853-862.
- Chernova, T. A., Allen, K. D., Wesoloski, L. M., Shanks, J. R., Chernoff, Y. O., & Wilkinson, K. D. (2003). Pleiotropic effects of Ubp6 loss on drug sensitivities and yeast prion are due to depletion of the free ubiquitin pool. *J Biol Chem*, 278(52), 52102-52115. doi: 10.1074/jbc.M310283200

- Chiu, R. K., Brun, J., Ramaekers, C., Theys, J., Weng, L., Lambin, P., . . . Wouters, B. G. (2006). Lysine 63-polyubiquitination guards against translesion synthesis-induced mutations. *PLoS Genet*, 2(7), e116. doi: 10.1371/journal.pgen.0020116.eor
- Ciechanover, A., Elias, S., Heller, H., & Hershko, A. (1982). "Covalent affinity" purification of ubiquitin-activating enzyme. *J Biol Chem*, 257(5), 2537-2542.
- Ciechanover, A., Heller, H., Elias, S., Haas, A. L., & Hershko, A. (1980). ATP-dependent conjugation of reticulocyte proteins with the polypeptide required for protein degradation. *Proc Natl Acad Sci U S A*, 77(3), 1365-1368.
- Ciechanover, A., Heller, H., Katz-Etzion, R., & Hershko, A. (1981). Activation of the heat-stable polypeptide of the ATP-dependent proteolytic system. *Proc Natl Acad Sci U S A*, 78(2), 761-765.
- Ciechanover, A., Hod, Y., & Hershko, A. (1978). A heat-stable polypeptide component of an ATP-dependent proteolytic system from reticulocytes. *Biochem Biophys Res Commun*, 81(4), 1100-1105.
- Coffey, E. T. (2014). Nuclear and cytosolic JNK signalling in neurons. *Nat Rev Neurosci*, 15(5), 285-299. doi: 10.1038/nrn3729
- Collins, C. A., Wairkar, Y. P., Johnson, S. L., & DiAntonio, A. (2006). Highwire restrains synaptic growth by attenuating a MAP kinase signal. *Neuron*, 51(1), 57-69. doi: 10.1016/j.neuron.2006.05.026
- Consortium, I. H. G. S. (2004). Finishing the euchromatic sequence of the human genome. *Nature*, 431(7011), 931-945. doi: 10.1038/nature03001
- Cooper, E. M., Cutcliffe, C., Kristiansen, T. Z., Pandey, A., Pickart, C. M., & Cohen, R. E. (2009). K63-specific deubiquitination by two JAMM/MPN+ complexes: BRISC-associated Brcc36 and proteasomal Pih1. *Embo J*, 28(6), 621-631. doi: 10.1038/emboj.2009.27
- Costello, D. A., & Herron, C. E. (2004). The role of c-Jun N-terminal kinase in the A beta-mediated impairment of LTP and regulation of synaptic transmission in the hippocampus. *Neuropharmacology*, 46(5), 655-662. doi: 10.1016/j.neuropharm.2003.11.016

- Crimmins, S., Jin, Y., Wheeler, C., Huffman, A. K., Chapman, C., Dobrunz, L. E., . . . Wilson, S. M. (2006). Transgenic rescue of ataxia mice with neuronal-specific expression of ubiquitin-specific protease 14. *J Neurosci*, 26(44), 11423-11431.
- Crimmins, S., Sutovsky, M., Chen, P. C., Huffman, A., Wheeler, C., Swing, D. A., . . . Wilson, S. (2009). Transgenic rescue of ataxia mice reveals a male-specific sterility defect. *Dev Biol*, 325(1), 33-42. doi: 10.1016/j.ydbio.2008.09.021
- D'Amato, C. J., & Hicks, S. P. (1965). Neuropathologic alterations in the ataxia (paralytic) mouse. *Arch Pathol*, 80(6), 604-612.
- D'Arcy, P., Brnjic, S., Olofsson, M. H., Fryknas, M., Lindsten, K., De Cesare, M., . . . Linder, S. (2011). Inhibition of proteasome deubiquitinating activity as a new cancer therapy. *Nat Med*, 17(12), 1636-1640. doi: 10.1038/nm.2536
- Dale, J. M., & Garcia, M. L. (2012). Neurofilament Phosphorylation during Development and Disease: Which Came First, the Phosphorylation or the Accumulation? *J Amino Acids*, 2012, 382107. doi: 10.1155/2012/382107
- Dantuma, N. P., & Bott, L. C. (2014). The ubiquitin-proteasome system in neurodegenerative diseases: precipitating factor, yet part of the solution. *Front Mol Neurosci*, 7, 70. doi: 10.3389/fnmol.2014.00070
- Deng, L., Wang, C., Spencer, E., Yang, L., Braun, A., You, J., . . . Chen, Z. J. (2000). Activation of the IkappaB kinase complex by TRAF6 requires a dimeric ubiquitin-conjugating enzyme complex and a unique polyubiquitin chain. *Cell*, 103(2), 351-361.
- Desai, A., & Mitchison, T. J. (1997). Microtubule polymerization dynamics. *Annu Rev Cell Dev Biol*, 13, 83-117. doi: 10.1146/annurev.cellbio.13.1.83
- Deveraux, Q., Ustrell, V., Pickart, C., & Rechsteiner, M. (1994). A 26 S protease subunit that binds ubiquitin conjugates. *J Biol Chem*, 269(10), 7059-7061.
- Dong, J., Chen, W., Welford, A., & Wandinger-Ness, A. (2004). The proteasome alpha-subunit XAPC7 interacts specifically with Rab7 and late endosomes. *J Biol Chem*, 279(20), 21334-21342. doi: 10.1074/jbc.M401022200

- Drerup, C. M., & Nechiporuk, A. V. (2013). JNK-interacting protein 3 mediates the retrograde transport of activated c-Jun N-terminal kinase and lysosomes. *PLoS Genet*, 9(2), e1003303. doi: 10.1371/journal.pgen.1003303
- Edelmann, M. J., Nicholson, B., & Kessler, B. M. (2011). Pharmacological targets in the ubiquitin system offer new ways of treating cancer, neurodegenerative disorders and infectious diseases. *Expert Rev Mol Med*, 13, e35. doi: 10.1017/s1462399411002031
- Eletr, Z. M., Huang, D. T., Duda, D. M., Schulman, B. A., & Kuhlman, B. (2005). E2 conjugating enzymes must disengage from their E1 enzymes before E3-dependent ubiquitin and ubiquitin-like transfer. *Nat Struct Mol Biol*, 12(10), 933-934. doi: 10.1038/nsmb984
- Etter, P. D., Narayanan, R., Navratilova, Z., Patel, C., Bohmann, D., Jasper, H., & Ramaswami, M. (2005). Synaptic and genomic responses to JNK and AP-1 signaling in *Drosophila* neurons. *BMC Neurosci*, 6, 39. doi: 10.1186/1471-2202-6-39
- Feltrin, D., Fusco, L., Witte, H., Moretti, F., Martin, K., Letzelter, M., . . . Pertz, O. (2012). Growth cone MKK7 mRNA targeting regulates MAP1b-dependent microtubule bundling to control neurite elongation. *PLoS Biol*, 10(12), e1001439. doi: 10.1371/journal.pbio.1001439
- Fernyhough, P., Gallagher, A., Averill, S. A., Priestley, J. V., Hounsom, L., Patel, J., & Tomlinson, D. R. (1999). Aberrant neurofilament phosphorylation in sensory neurons of rats with diabetic neuropathy. *Diabetes*, 48(4), 881-889.
- Fiskus, W., Saba, N., Shen, M., Ghias, M., Liu, J., Gupta, S. D., . . . Bhalla, K. N. (2014). Auranofin induces lethal oxidative and endoplasmic reticulum stress and exerts potent preclinical activity against chronic lymphocytic leukemia. *Cancer Res*, 74(9), 2520-2532. doi: 10.1158/0008-5472.can-13-2033
- Geetha, T., Jiang, J., & Wooten, M. W. (2005). Lysine 63 polyubiquitination of the nerve growth factor receptor TrkA directs internalization and signaling. *Mol Cell*, 20(2), 301-312. doi: 10.1016/j.molcel.2005.09.014
- Geetha, T., & Wooten, M. W. (2008). TrkA receptor endolysosomal degradation is both ubiquitin and proteasome dependent. *Traffic*, 9(7), 1146-1156. doi: 10.1111/j.1600-0854.2008.00751.x

- Goldstein, G., Scheid, M., Hammerling, U., Schlesinger, D. H., Niall, H. D., & Boyse, E. A. (1975). Isolation of a polypeptide that has lymphocyte-differentiating properties and is probably represented universally in living cells. *Proc Natl Acad Sci U S A*, 72(1), 11-15.
- Gong, C. X., Wang, J. Z., Iqbal, K., & Grundke-Iqbal, I. (2003). Inhibition of protein phosphatase 2A induces phosphorylation and accumulation of neurofilaments in metabolically active rat brain slices. *Neurosci Lett*, 340(2), 107-110.
- Haas, A. L., Warms, J. V., Hershko, A., & Rose, I. A. (1982). Ubiquitin-activating enzyme. Mechanism and role in protein-ubiquitin conjugation. *J Biol Chem*, 257(5), 2543-2548.
- Hallengren, J., Chen, P. C., & Wilson, S. M. (2013). Neuronal ubiquitin homeostasis. *Cell Biochem Biophys*, 67(1), 67-73. doi: 10.1007/s12013-013-9634-4
- Hamazaki, J., Iemura, S., Natsume, T., Yashiroda, H., Tanaka, K., & Murata, S. (2006). A novel proteasome interacting protein recruits the deubiquitinating enzyme UCH37 to 26S proteasomes. *Embo J*, 25(19), 4524-4536. doi: 10.1038/sj.emboj.7601338
- Hanna, J., Hathaway, N. A., Tone, Y., Crosas, B., Elsasser, S., Kirkpatrick, D. S., . . . Finley, D. (2006). Deubiquitinating enzyme Ubp6 functions noncatalytically to delay proteasomal degradation. *Cell*, 127(1), 99-111. doi: 10.1016/j.cell.2006.07.038
- Hanna, J., Leggett, D. S., & Finley, D. (2003). Ubiquitin depletion as a key mediator of toxicity by translational inhibitors. *Mol Cell Biol*, 23(24), 9251-9261.
- Hanna, J., Meides, A., Zhang, D. P., & Finley, D. (2007). A ubiquitin stress response induces altered proteasome composition. *Cell*, 129(4), 747-759. doi: 10.1016/j.cell.2007.03.042
- Hershko, A., Ciechanover, A., Heller, H., Haas, A. L., & Rose, I. A. (1980). Proposed role of ATP in protein breakdown: conjugation of protein with multiple chains of the polypeptide of ATP-dependent proteolysis. *Proc Natl Acad Sci U S A*, 77(4), 1783-1786.

- Hershko, A., Heller, H., Elias, S., & Ciechanover, A. (1983). Components of ubiquitin-protein ligase system. Resolution, affinity purification, and role in protein breakdown. *J Biol Chem*, 258(13), 8206-8214.
- Hofmann, R. M., & Pickart, C. M. (2001). In vitro assembly and recognition of Lys-63 polyubiquitin chains. *J Biol Chem*, 276(30), 27936-27943. doi: 10.1074/jbc.M103378200
- Hu, M., Li, P., Song, L., Jeffrey, P. D., Chenova, T. A., Wilkinson, K. D., . . . Shi, Y. (2005). Structure and mechanisms of the proteasome-associated deubiquitinating enzyme USP14. *Embo J*, 24(21), 3747-3756. doi: 10.1038/sj.emboj.7600832
- Humphrey, R. K., Yu, S. M., Bellary, A., Gonuguntla, S., Yebra, M., & Jhala, U. S. (2013). Lysine 63-linked ubiquitination modulates mixed lineage kinase-3 interaction with JIP1 scaffold protein in cytokine-induced pancreatic beta cell death. *J Biol Chem*, 288(4), 2428-2440. doi: 10.1074/jbc.M112.425884
- Husnjak, K., Elsasser, S., Zhang, N., Chen, X., Randles, L., Shi, Y., . . . Dikic, I. (2008). Proteasome subunit Rpn13 is a novel ubiquitin receptor. *Nature*, 453(7194), 481-488. doi: 10.1038/nature06926
- Jacobson, A. D., Zhang, N. Y., Xu, P., Han, K. J., Noone, S., Peng, J., & Liu, C. W. (2009). The lysine 48 and lysine 63 ubiquitin conjugates are processed differently by the 26 s proteasome. *J Biol Chem*, 284(51), 35485-35494. doi: 10.1074/jbc.M109.052928
- Jensen, O. N. (2004). Modification-specific proteomics: characterization of post-translational modifications by mass spectrometry. *Curr Opin Chem Biol*, 8(1), 33-41. doi: 10.1016/j.cbpa.2003.12.009
- Jiao, L., Ouyang, S., Shaw, N., Song, G., Feng, Y., Niu, F., . . . Liu, Z. J. (2014). Mechanism of the Rpn13-induced activation of Uch37. *Protein Cell*, 5(8), 616-630. doi: 10.1007/s13238-014-0046-z
- Jin, W., Chang, M., Paul, E. M., Babu, G., Lee, A. J., Reiley, W., . . . Sun, S. C. (2008). Deubiquitinating enzyme CYLD negatively regulates RANK signaling and osteoclastogenesis in mice. *J Clin Invest*, 118(5), 1858-1866. doi: 10.1172/jci34257

- Jin, Y. N., Chen, P. C., Watson, J. A., Walters, B. J., Phillips, S. E., Green, K., . . . Wilson, S. M. (2012). Usp14 deficiency increases tau phosphorylation without altering tau degradation or causing tau-dependent deficits. *PLoS One*, 7(10), e47884. doi: 10.1371/journal.pone.0047884
- Jorgensen, J. P., Lauridsen, A. M., Kristensen, P., Dissing, K., Johnsen, A. H., Hendil, K. B., & Hartmann-Petersen, R. (2006). Adrm1, a putative cell adhesion regulating protein, is a novel proteasome-associated factor. *J Mol Biol*, 360(5), 1043-1052. doi: 10.1016/j.jmb.2006.06.011
- Jullien, J., Guili, V., Reichardt, L. F., & Rudkin, B. B. (2002). Molecular kinetics of nerve growth factor receptor trafficking and activation. *J Biol Chem*, 277(41), 38700-38708. doi: 10.1074/jbc.M202348200
- Jung, H., Kim, B. G., Han, W. H., Lee, J. H., Cho, J. Y., Park, W. S., . . . Jho, E. H. (2013). Deubiquitination of Dishevelled by Usp14 is required for Wnt signaling. *Oncogenesis*, 2, e64. doi: 10.1038/oncsis.2013.28
- Kaiser, S. E., Riley, B. E., Shaler, T. A., Trevino, R. S., Becker, C. H., Schulman, H., & Kopito, R. R. (2011). Protein standard absolute quantification (PSAQ) method for the measurement of cellular ubiquitin pools. *Nat Methods*, 8(8), 691-696. doi: 10.1038/nmeth.1649
- Kanayama, H. O., Tamura, T., Ugai, S., Kagawa, S., Tanahashi, N., Yoshimura, T., . . . Ichihara, A. (1992). Demonstration that a human 26S proteolytic complex consists of a proteasome and multiple associated protein components and hydrolyzes ATP and ubiquitin-ligated proteins by closely linked mechanisms. *Eur J Biochem*, 206(2), 567-578.
- Kim, H. T., Kim, K. P., Lledias, F., Kisselev, A. F., Scaglione, K. M., Skowrya, D., . . . Goldberg, A. L. (2007). Certain pairs of ubiquitin-conjugating enzymes (E2s) and ubiquitin-protein ligases (E3s) synthesize nondegradable forked ubiquitin chains containing all possible isopeptide linkages. *J Biol Chem*, 282(24), 17375-17386. doi: 10.1074/jbc.M609659200
- Klinedinst, S., Wang, X., Xiong, X., Haenfler, J. M., & Collins, C. A. (2013). Independent pathways downstream of the Wnd/DLK MAPKKK regulate synaptic structure, axonal transport, and injury signaling. *J Neurosci*, 33(31), 12764-12778. doi: 10.1523/jneurosci.5160-12.2013

- Komander, D. (2009). The emerging complexity of protein ubiquitination. *Biochem Soc Trans*, 37(Pt 5), 937-953. doi: 10.1042/bst0370937
- Komander, D., Reyes-Turcu, F., Licchesi, J. D., Odenwaelde, P., Wilkinson, K. D., & Barford, D. (2009). Molecular discrimination of structurally equivalent Lys 63-linked and linear polyubiquitin chains. *EMBO Rep*, 10(5), 466-473. doi: 10.1038/embor.2009.55
- Lam, Y. A., Xu, W., DeMartino, G. N., & Cohen, R. E. (1997). Editing of ubiquitin conjugates by an isopeptidase in the 26S proteasome. *Nature*, 385(6618), 737-740. doi: 10.1038/385737a0
- Langie, S. A., Knaapen, A. M., Ramaekers, C. H., Theys, J., Brun, J., Godschalk, R. W., . . . Chiu, R. K. (2007). Formation of lysine 63-linked poly-ubiquitin chains protects human lung cells against benzo[a]pyrene-diol-epoxide-induced mutagenicity. *DNA Repair (Amst)*, 6(6), 852-862. doi: 10.1016/j.dnarep.2007.02.012
- Lappe-Siefke, C., Loebrich, S., Hevers, W., Waidmann, O. B., Schweizer, M., Fehr, S., . . . Kneussel, M. (2009). The ataxia (axJ) mutation causes abnormal GABAA receptor turnover in mice. *PLoS Genet*, 5(9), e1000631.
- Lauwers, E., Jacob, C., & Andre, B. (2009). K63-linked ubiquitin chains as a specific signal for protein sorting into the multivesicular body pathway. *J Cell Biol*, 185(3), 493-502. doi: 10.1083/jcb.200810114
- Lee, B. H., Finley, D., & King, R. W. (2012). A High-Throughput Screening Method for Identification of Inhibitors of the Deubiquitinating Enzyme USP14. *Curr Protoc Chem Biol*, 4(4), 311-330. doi: 10.1002/9780470559277.ch120078
- Lee, B. H., Lee, M. J., Park, S., Oh, D. C., Elsasser, S., Chen, P. C., . . . Finley, D. (2010). Enhancement of proteasome activity by a small-molecule inhibitor of USP14. *Nature*, 467(7312), 179-184.
- Lee, M. J., Lee, B. H., Hanna, J., King, R. W., & Finley, D. (2011). Trimming of ubiquitin chains by proteasome-associated deubiquitinating enzymes. *Mol Cell Proteomics*, 10(5), R110.003871. doi: 10.1074/mcp.R110.003871

- Leggett, D. S., Hanna, J., Borodovsky, A., Crosas, B., Schmidt, M., Baker, R. T., . . . Finley, D. (2002). Multiple associated proteins regulate proteasome structure and function. *Mol Cell*, 10(3), 495-507.
- Lindwall, C., & Kanje, M. (2005). Retrograde axonal transport of JNK signaling molecules influence injury induced nuclear changes in p-c-Jun and ATF3 in adult rat sensory neurons. *Mol Cell Neurosci*, 29(2), 269-282. doi: 10.1016/j.mcn.2005.03.002
- Liu, N., Li, X., Huang, H., Zhao, C., Liao, S., Yang, C., . . . Liu, J. (2014). Clinically used antirheumatic agent auranofin is a proteasomal deubiquitinase inhibitor and inhibits tumor growth. *Oncotarget*, 5(14), 5453-5471.
- Longva, K. E., Blystad, F. D., Stang, E., Larsen, A. M., Johannessen, L. E., & Madhus, I. H. (2002). Ubiquitination and proteasomal activity is required for transport of the EGF receptor to inner membranes of multivesicular bodies. *J Cell Biol*, 156(5), 843-854. doi: 10.1083/jcb.200106056
- Lupas, A., Koster, A. J., & Baumeister, W. (1993). Structural features of 26S and 20S proteasomes. *Enzyme Protein*, 47(4-6), 252-273.
- Marchese, A., Raiborg, C., Santini, F., Keen, J. H., Stenmark, H., & Benovic, J. L. (2003). The E3 ubiquitin ligase AIP4 mediates ubiquitination and sorting of the G protein-coupled receptor CXCR4. *Dev Cell*, 5(5), 709-722.
- Mines, M. A., Goodwin, J. S., Limbird, L. E., Cui, F. F., & Fan, G. H. (2009). Deubiquitination of CXCR4 by USP14 is critical for both CXCL12-induced CXCR4 degradation and chemotaxis but not ERK activation. *J Biol Chem*, 284(9), 5742-5752. doi: 10.1074/jbc.M808507200
- Mirabelli, C. K., Johnson, R. K., Hill, D. T., Faucette, L. F., Girard, G. R., Kuo, G. Y., . . . Crooke, S. T. (1986). Correlation of the in vitro cytotoxic and in vivo antitumor activities of gold(I) coordination complexes. *J Med Chem*, 29(2), 218-223.
- Mirabelli, C. K., Johnson, R. K., Sung, C. M., Faucette, L., Muirhead, K., & Crooke, S. T. (1985). Evaluation of the in vivo antitumor activity and in vitro cytotoxic properties of auranofin, a coordinated gold compound, in murine tumor models. *Cancer Res*, 45(1), 32-39.

- Nathan, J. A., Tae Kim, H., Ting, L., Gygi, S. P., & Goldberg, A. L. (2013). Why do cellular proteins linked to K63-polyubiquitin chains not associate with proteasomes? *Embo J*, 32(4), 552-565. doi: 10.1038/emboj.2012.354
- Neidhart, S., Antonsson, B., Gillieron, C., Vilbois, F., Grenningloh, G., & Arkinstall, S. (2001). c-Jun N-terminal kinase-3 (JNK3)/stress-activated protein kinase-beta (SAPKbeta) binds and phosphorylates the neuronal microtubule regulator SCG10. *FEBS Lett*, 508(2), 259-264.
- Nickell, S., Beck, F., Scheres, S. H., Korinek, A., Forster, F., Lasker, K., . . . Baumeister, W. (2009). Insights into the molecular architecture of the 26S proteasome. *Proc Natl Acad Sci U S A*, 106(29), 11943-11947. doi: 10.1073/pnas.0905081106
- Ning, S., & Pagano, J. S. (2010). The A20 deubiquitinase activity negatively regulates LMP1 activation of IRF7. *J Virol*, 84(12), 6130-6138. doi: 10.1128/jvi.00364-10
- Osaka, H., Wang, Y. L., Takada, K., Takizawa, S., Setsuie, R., Li, H., . . . Wada, K. (2003). Ubiquitin carboxy-terminal hydrolase L1 binds to and stabilizes monoubiquitin in neuron. *Hum Mol Genet*, 12(16), 1945-1958.
- Pathare, G. R., Nagy, I., Bohn, S., Unverdorben, P., Hubert, A., Korner, R., . . . Bracher, A. (2012). The proteasomal subunit Rpn6 is a molecular clamp holding the core and regulatory subcomplexes together. *Proc Natl Acad Sci U S A*, 109(1), 149-154. doi: 10.1073/pnas.1117648108
- Peth, A., Besche, H. C., & Goldberg, A. L. (2009). Ubiquitinated proteins activate the proteasome by binding to Usp14/Ubp6, which causes 20S gate opening. *Mol Cell*, 36(5), 794-804.
- Peth, A., Kukushkin, N., Bosse, M., & Goldberg, A. L. (2013). Ubiquitinated proteins activate the proteasomal ATPases by binding to Usp14 or Uch37 homologs. *J Biol Chem*, 288(11), 7781-7790. doi: 10.1074/jbc.M112.441907
- Peth, A., Uchiki, T., & Goldberg, A. L. (2010). ATP-dependent steps in the binding of ubiquitin conjugates to the 26S proteasome that commit to degradation. *Mol Cell*, 40(4), 671-681. doi: 10.1016/j.molcel.2010.11.002
- Piotrowski, J., Beal, R., Hoffman, L., Wilkinson, K. D., Cohen, R. E., & Pickart, C. M. (1997). Inhibition of the 26 S proteasome by polyubiquitin chains synthesized to have defined lengths. *J Biol Chem*, 272(38), 23712-23721.

- Puhler, G., Weinkauff, S., Bachmann, L., Muller, S., Engel, A., Hegerl, R., & Baumeister, W. (1992). Subunit stoichiometry and three-dimensional arrangement in proteasomes from *Thermoplasma acidophilum*. *Embo J*, 11(4), 1607-1616.
- Qiu, X. B., Ouyang, S. Y., Li, C. J., Miao, S., Wang, L., & Goldberg, A. L. (2006). hRpn13/ADRM1/GP110 is a novel proteasome subunit that binds the deubiquitinating enzyme, UCH37. *Embo J*, 25(24), 5742-5753. doi: 10.1038/sj.emboj.7601450
- Qu, C., Li, W., Shao, Q., Dwyer, T., Huang, H., Yang, T., & Liu, G. (2013). c-Jun N-terminal kinase 1 (JNK1) is required for coordination of netrin signaling in axon guidance. *J Biol Chem*, 288(3), 1883-1895. doi: 10.1074/jbc.M112.417881
- Ristic, G., Tsou, W. L., & Todi, S. V. (2014). An optimal ubiquitin-proteasome pathway in the nervous system: the role of deubiquitinating enzymes. *Front Mol Neurosci*, 7, 72. doi: 10.3389/fnmol.2014.00072
- Rocca, A., Lamaze, C., Subtil, A., & Dautry-Varsat, A. (2001). Involvement of the ubiquitin/proteasome system in sorting of the interleukin 2 receptor beta chain to late endocytic compartments. *Mol Biol Cell*, 12(5), 1293-1301.
- Schmidt, M., & Finley, D. (2014). Regulation of proteasome activity in health and disease. *Biochim Biophys Acta*, 1843(1), 13-25. doi: 10.1016/j.bbamcr.2013.08.012
- Schuh, A. L., & Audhya, A. (2014). The ESCRT machinery: from the plasma membrane to endosomes and back again. *Crit Rev Biochem Mol Biol*, 49(3), 242-261. doi: 10.3109/10409238.2014.881777
- Seemuller, E., Lupas, A., Stock, D., Lowe, J., Huber, R., & Baumeister, W. (1995). Proteasome from *Thermoplasma acidophilum*: a threonine protease. *Science*, 268(5210), 579-582.
- Shafer, B., Onishi, K., Lo, C., Colakoglu, G., & Zou, Y. (2011). Vangl2 promotes Wnt/planar cell polarity-like signaling by antagonizing Dvl1-mediated feedback inhibition in growth cone guidance. *Dev Cell*, 20(2), 177-191. doi: 10.1016/j.devcel.2011.01.002

- Shi, C. S., & Kehrl, J. H. (2010). TRAF6 and A20 regulate lysine 63-linked ubiquitination of Beclin-1 to control TLR4-induced autophagy. *Sci Signal*, 3(123), ra42. doi: 10.1126/scisignal.2000751
- Shin, J. E., Cho, Y., Beirowski, B., Milbrandt, J., Cavalli, V., & DiAntonio, A. (2012). Dual leucine zipper kinase is required for retrograde injury signaling and axonal regeneration. *Neuron*, 74(6), 1015-1022. doi: 10.1016/j.neuron.2012.04.028
- Stone, M., Hartmann-Petersen, R., Seeger, M., Bech-Otschir, D., Wallace, M., & Gordon, C. (2004). Uch2/Uch37 is the major deubiquitinating enzyme associated with the 26S proteasome in fission yeast. *J Mol Biol*, 344(3), 697-706. doi: 10.1016/j.jmb.2004.09.057
- Sweatt, J. D. (2004). Mitogen-activated protein kinases in synaptic plasticity and memory. *Curr Opin Neurobiol*, 14(3), 311-317. doi: 10.1016/j.conb.2004.04.001
- Tanno, H., & Komada, M. (2013). The ubiquitin code and its decoding machinery in the endocytic pathway. *J Biochem*, 153(6), 497-504. doi: 10.1093/jb/mvt028
- Tararuk, T., Ostman, N., Li, W., Bjorkblom, B., Padzik, A., Zdrojewska, J., . . . Coffey, E. T. (2006). JNK1 phosphorylation of SCG10 determines microtubule dynamics and axodendritic length. *J Cell Biol*, 173(2), 265-277. doi: 10.1083/jcb.200511055
- Tatebayashi, Y., Planel, E., Chui, D. H., Sato, S., Miyasaka, T., Sahara, N., . . . Takashima, A. (2006). c-jun N-terminal kinase hyperphosphorylates R406W tau at the PHF-1 site during mitosis. *Faseb j*, 20(6), 762-764. doi: 10.1096/fj.05-4362fje
- Tauriello, D. V., Haegebarth, A., Kuper, I., Edelmann, M. J., Henraat, M., Canninga-van Dijk, M. R., . . . Maurice, M. M. (2010). Loss of the tumor suppressor CYLD enhances Wnt/beta-catenin signaling through K63-linked ubiquitination of Dvl. *Mol Cell*, 37(5), 607-619. doi: 10.1016/j.molcel.2010.01.035
- Tenno, T., Fujiwara, K., Tochio, H., Iwai, K., Morita, E. H., Hayashi, H., . . . Shirakawa, M. (2004). Structural basis for distinct roles of Lys63- and Lys48-linked polyubiquitin chains. *Genes Cells*, 9(10), 865-875. doi: 10.1111/j.1365-2443.2004.00780.x

- Thrower, J. S., Hoffman, L., Rechsteiner, M., & Pickart, C. M. (2000). Recognition of the polyubiquitin proteolytic signal. *Embo J*, 19(1), 94-102. doi: 10.1093/emboj/19.1.94
- Tian, Z., D'Arcy, P., Wang, X., Ray, A., Tai, Y. T., Hu, Y., . . . Anderson, K. C. (2014). A novel small molecule inhibitor of deubiquitylating enzyme USP14 and UCHL5 induces apoptosis in multiple myeloma and overcomes bortezomib resistance. *Blood*, 123(5), 706-716. doi: 10.1182/blood-2013-05-500033
- Todi, S. V., & Paulson, H. L. (2011). Balancing act: deubiquitinating enzymes in the nervous system. *Trends Neurosci*, 34(7), 370-382. doi: 10.1016/j.tins.2011.05.004
- Vaden, J. H., Bhattacharyya, B. J., Chen, P. C., Watson, J. A., Marshall, A. G., Phillips, S. E., . . . Wilson, S. M. (2015). Ubiquitin-specific protease 14 regulates c-Jun N-terminal kinase signaling at the neuromuscular junction. *Mol Neurodegener*, 10(1), 3. doi: 10.1186/1750-1326-10-3
- van Kerkhof, P., Alves dos Santos, C. M., Sachse, M., Klumperman, J., Bu, G., & Strous, G. J. (2001). Proteasome inhibitors block a late step in lysosomal transport of selected membrane but not soluble proteins. *Mol Biol Cell*, 12(8), 2556-2566.
- Varadan, R., Assfalg, M., Haririnia, A., Raasi, S., Pickart, C., & Fushman, D. (2004). Solution conformation of Lys63-linked di-ubiquitin chain provides clues to functional diversity of polyubiquitin signaling. *J Biol Chem*, 279(8), 7055-7063. doi: 10.1074/jbc.M309184200
- Verma, R., Aravind, L., Oania, R., McDonald, W. H., Yates, J. R., 3rd, Koonin, E. V., & Deshaies, R. J. (2002). Role of Rpn11 metalloprotease in deubiquitination and degradation by the 26S proteasome. *Science*, 298(5593), 611-615. doi: 10.1126/science.1075898
- Vilchez, D., Boyer, L., Morante, I., Lutz, M., Merkwirth, C., Joyce, D., . . . Dillin, A. (2012). Increased proteasome activity in human embryonic stem cells is regulated by PSMD11. *Nature*, 489(7415), 304-308. doi: 10.1038/nature11468
- Walters, B. J., Hallengren, J. J., Theile, C. S., Ploegh, H. L., Wilson, S. M., & Dobrunz, L. E. (2014). A catalytic independent function of the deubiquitinating enzyme USP14 regulates hippocampal synaptic short-term plasticity and vesicle number. *J Physiol*, 592(Pt 4), 571-586. doi: 10.1113/jphysiol.2013.266015

- Wang, C., Deng, L., Hong, M., Akkaraju, G. R., Inoue, J., & Chen, Z. J. (2001). TAK1 is a ubiquitin-dependent kinase of MKK and IKK. *Nature*, *412*(6844), 346-351. doi: 10.1038/35085597
- Westerlund, N., Zdrojewska, J., Padzik, A., Komulainen, E., Bjorkblom, B., Rannikko, E., . . . Coffey, E. T. (2011). Phosphorylation of SCG10/stathmin-2 determines multipolar stage exit and neuronal migration rate. *Nat Neurosci*, *14*(3), 305-313. doi: 10.1038/nn.2755
- Wicks, S. J., Haros, K., Maillard, M., Song, L., Cohen, R. E., Dijke, P. T., & Chantry, A. (2005). The deubiquitinating enzyme UCH37 interacts with Smads and regulates TGF-beta signalling. *Oncogene*, *24*(54), 8080-8084. doi: 10.1038/sj.onc.1208944
- Wilkinson, K. D., Urban, M. K., & Haas, A. L. (1980). Ubiquitin is the ATP-dependent proteolysis factor I of rabbit reticulocytes. *J Biol Chem*, *255*(16), 7529-7532.
- Wilson, S. M., Bhattacharyya, B., Rachel, R. A., Coppola, V., Tessarollo, L., Householder, D. B., . . . Jenkins, N. A. (2002). Synaptic defects in ataxia mice result from a mutation in Usp14, encoding a ubiquitin-specific protease. *Nat Genet*, *32*(3), 420-425.
- Xiong, X., Wang, X., Ewanek, R., Bhat, P., Diantonio, A., & Collins, C. A. (2010). Protein turnover of the Wallenda/DLK kinase regulates a retrograde response to axonal injury. *J Cell Biol*, *191*(1), 211-223. doi: 10.1083/jcb.201006039
- Xu, P., Duong, D. M., Seyfried, N. T., Cheng, D., Xie, Y., Robert, J., . . . Peng, J. (2009). Quantitative proteomics reveals the function of unconventional ubiquitin chains in proteasomal degradation. *Cell*, *137*(1), 133-145. doi: 10.1016/j.cell.2009.01.041
- Yan, J., & Jetten, A. M. (2008). RAP80 and RNF8, key players in the recruitment of repair proteins to DNA damage sites. *Cancer Lett*, *271*(2), 179-190. doi: 10.1016/j.canlet.2008.04.046
- Yang, G., Liu, Y., Yang, K., Liu, R., Zhu, S., Coquinco, A., . . . Cynader, M. (2012). Isoform-specific palmitoylation of JNK regulates axonal development. *Cell Death Differ*, *19*(4), 553-561. doi: 10.1038/cdd.2011.124
- Yang, W. L., Wang, J., Chan, C. H., Lee, S. W., Campos, A. D., Lamothe, B., . . . Lin, H. K. (2009). The E3 ligase TRAF6 regulates Akt ubiquitination and activation. *Science*, *325*(5944), 1134-1138. doi: 10.1126/science.1175065

- Yang, W. L., Wu, C. Y., Wu, J., & Lin, H. K. (2010). Regulation of Akt signaling activation by ubiquitination. *Cell Cycle*, 9(3), 487-497.
- Yao, T., & Cohen, R. E. (2002). A cryptic protease couples deubiquitination and degradation by the proteasome. *Nature*, 419(6905), 403-407. doi: 10.1038/nature01071
- Yao, T., Song, L., Xu, W., DeMartino, G. N., Florens, L., Swanson, S. K., . . . Cohen, R. E. (2006). Proteasome recruitment and activation of the Uch37 deubiquitinating enzyme by Adrm1. *Nat Cell Biol*, 8(9), 994-1002. doi: 10.1038/ncb1460
- Ying, Z., Wang, H., & Wang, G. (2013). The ubiquitin proteasome system as a potential target for the treatment of neurodegenerative diseases. *Curr Pharm Des*, 19(18), 3305-3314.
- Yoshimura, T., Kameyama, K., Takagi, T., Ikai, A., Tokunaga, F., Koide, T., . . . et al. (1993). Molecular characterization of the "26S" proteasome complex from rat liver. *J Struct Biol*, 111(3), 200-211.
- Yu, A., & Malek, T. R. (2001). The proteasome regulates receptor-mediated endocytosis of interleukin-2. *J Biol Chem*, 276(1), 381-385. doi: 10.1074/jbc.M007991200
- Zhou, A. Y., Shen, R. R., Kim, E., Lock, Y. J., Xu, M., Chen, Z. J., & Hahn, W. C. (2013). IKKepsilon-Mediated Tumorigenesis Requires K63-Linked Polyubiquitination by a cIAP1/cIAP2/TRAF2 E3 Ubiquitin Ligase Complex. *Cell Rep*. doi: 10.1016/j.celrep.2013.01.031
- Zhou, F., Zhang, X., van Dam, H., Ten Dijke, P., Huang, H., & Zhang, L. (2012). Ubiquitin-specific protease 4 mitigates Toll-like/interleukin-1 receptor signaling and regulates innate immune activation. *J Biol Chem*, 287(14), 11002-11010. doi: 10.1074/jbc.M111.328187

APPENDIX

INSTITUTIONAL ANIMAL CARE AND USE APPROVAL FORM



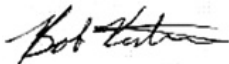
THE UNIVERSITY OF ALABAMA AT BIRMINGHAM

Institutional Animal Care and Use Committee (IACUC)

NOTICE OF APPROVAL

DATE: March 21, 2014

TO: SCOTT M WILSON, Ph.D.
SHEL-914
(205) 975-5573

FROM: 
Robert A. Kesterson, Ph.D., Chair
Institutional Animal Care and Use Committee (IACUC)

SUBJECT: Title: The Role of Usp14 in Regulating Neuronal Function-1
Sponsor: NIH
Animal Project_Number: 140409054

As of April 19, 2014 the animal use proposed in the above referenced application is approved. The University of Alabama at Birmingham Institutional Animal Care and Use Committee (IACUC) approves the use of the following species and number of animals:

Species	Use Category	Number In Category
Mice	A	345
Mice	B	15

Animal use must be renewed by April 18, 2015. Approval from the IACUC must be obtained before implementing any changes or modifications in the approved animal use.

Please keep this record for your files, and forward the attached letter to the appropriate granting agency.

Refer to Animal Protocol Number (APN) 140409054 when ordering animals or in any correspondence with the IACUC or Animal Resources Program (ARP) offices regarding this study. If you have concerns or questions regarding this notice, please call the IACUC office at (205) 934-7692.

Institutional Animal Care and Use Committee (IACUC)	Mailing Address:
CH19 Suite 403	CH19 Suite 403
933 19th Street South	1530 3rd Ave S
(205) 934-7692	Birmingham, AL 35294-0019
FAX (205) 934-1188	



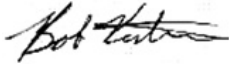
THE UNIVERSITY OF ALABAMA AT BIRMINGHAM

Institutional Animal Care and Use Committee (IACUC)

MEMORANDUM

DATE: March 21, 2014

TO: SCOTT M WILSON, Ph.D.
SHEL-914
(205) 975-5573

FROM: 
Robert A. Kesterson, Ph.D., Chair
Institutional Animal Care and Use Committee (IACUC)

SUBJECT: **NOTICE OF APPROVAL - Please forward this notice to the appropriate granting agency.**

The following application was renewed by the University of Alabama at Birmingham Institutional Animal Care and Use Committee (IACUC) on March 21, 2014.

Title: The Role of Usp14 in Regulating Neuronal Function-1
Sponsor: NIH

This institution has an Animal Welfare Assurance on file with the Office of Laboratory Animal Welfare (OLAW), is registered as a Research Facility with the USDA, and is accredited by the Association for Assessment and Accreditation of Laboratory Animal Care International (AAALAC).

Institutional Animal Care and Use Committee (IACUC)	Mailing Address:
CH19 Suite 403	CH19 Suite 403
933 19th Street South	1530 3rd Ave S
(205) 934-7692	Birmingham, AL 35294-0019
FAX (205) 934-1188	